Spring 2023

New Perspectives and Insights Into Direct Epoxidation of C_3H_6 Using O_2 and Ag Based Catalysts and Measurement of Active Ag Site Concentration of Promoted Ag Catalyst for C_2H_4 Epoxidation by H_2 Pulse Titration Over Oxygen Pre-covered Surface

Md Masudur Rahman

NEW PERSPECTIVES AND INSIGHTS INTO DIRECT EPOXIDATION OF C_3H_6 USING O_2 AND Ag BASED CATALYSTS AND MEASUREMENT OF ACTIVE Ag SITE CONCENTRATION OF PROMOTED Ag CATALYST FOR C_2H_4 EPOXIDATION BY H_2 PULSE TITRATION OVER OXYGEN PRE-COVERED SURFACE

By

Md Masudur Rahman

Bachelor of Science
Bangladesh University of Engineering and Technology, 2015

Submitted in Partial Fulfillment of the Requirements

For the Degree of Doctor of Philosophy in

Chemical Engineering

College of Engineering and Computing

University of South Carolina

2023

Accepted by:

John R. Monnier, Major Professor

John R. Regalbuto, Major Professor

Christopher T. Williams, Committee Member

Aaron K. Vannucci, Committee Member

Melissa A. Moss, Committee Member

Cheryl L. Addy, Interim Vice Provost and Dean of the Graduate School

DEDICATION

I dedicate this work to my mother, Halima Rahman, my father, Md Majibur Rahman, and my wife, Shafikunessa Prova, for their unconditional love, support, help, and dedication. I owe my success to my parents.

ACKNOWLEDGEMENTS

I want to thank Dr. John R. Monnier for providing me with the opportunity to work in his group. I am grateful to him for teaching me the science of catalysis and teaching me to be a better person. He allowed me to go to the Masjid every Friday for prayer without any question, I cannot express my gratitude toward him in words. Thank you, Dr. Monnier, for teaching me all the life lessons.

I want to thank Dr. John R. Regalbuto for always being kind to me. Without your recommendation, Dr. Monnier would not allow me in his group. Thanks for teaching me the fundamentals of heterogeneous catalysis.

I want to thank Dr. Christopher T. Williams and Dr. Aaron K. Vannucci for being my Ph.D. committee members. Your advice and guidance helped me throughout my Ph.D. career. Thanks to both of you for your precious time dedicated to teaching me.

I want to thank all the staff in the chemical engineering department, Marcia Rowen, Loretta Hardcastle, Vernon Dorrell, and Kachet DesChamps for their assistance throughout my graduate studies.

I want to thank Dr. Anne M. Gaffney and Dr. Michael B. Burkholder for all the support and guidance on the propylene epoxidation project. Thank you, Mike, for treating me like a brother.

I want to thank Dr. Donna Chen and Dr. Ralph White for teaching me surface science and mass transfer.

I want to especially thank Dr. Weijian Diao, Dr. John Meynard Tengco, Dr. Gregory Tate, Dr. Benjamin Thomas Egelske for all the support and for teaching me catalyst synthesis, reactor design, and catalyst characterization techniques. Graduate school would be more challenging without all of your help.

In addition, I want to thank all my colleagues, Dr. Yanjiao Yi, Dr. Fahim Bin Rahman, Dr. Wen Xiong, Dr. Anhua Dong, Dr. Leandro DeCastro, Md Fakhruddin Patwary, Alaba Ojo, Haiying Zhou, Kevin Enyekew. It was a pleasure to work with all of you.

ABSTRACT

Direct epoxidation of C_3H_6 using molecular O_2 and Ag catalysts to produce propylene oxide (PO) selectively is a long-sought goal in the field of heterogeneous catalysis. In the early 1990's Scientists at ARCO reported promising results of 58 – 59% selectivity to PO at 3.2% conversion of C_3H_6 over an unusual composition of 54.0 wt% Ag, 2.0 wt% K^+, 0.5 wt% Mo and balance $CaCO_3$. Feed additives of ethyl chloride (EtCl), nitric oxide (NO) and CO_2 were stated necessary to achieve the claimed high PO selectivities. The roles of relatively high levels of NO and EtCl (200 ppmv each) and 2.0 wt% K^+, and 0.5 wt% Mo were not explained, nor was the choice of $CaCO_3$, rather than the typically used α-alumina support. Ag supported on ZrO_2 promoted/modified with Mo and W has been reported to achieve high selectivity to PO 53% to 67% at moderated 2.0% to 12.0% conversion of C_3H_6 at a significantly high (400°C – 460°C) temperature compared to the temperature (240ºC – 280ºC) reported by ARCO for propylene epoxidation. For ethylene epoxidation to ethylene oxide and 1,3 butadiene epoxidation to 3,4-epoxy-1-butene (EpB) reported reaction temperature was 200ºC – 270ºC. Therefore, these results for propylene epoxidation to propylene oxide (PO) using Mo and W promoted 20 wt% Ag/ZrO_2 catalyst at high temperature (400 – 460°C) need to be confirmed with further investigation.

In this dissertation, a series of Ag catalysts supported on low surface area α-Al_2O_3, $CaCO_3$ and ZrO_2 was prepared and evaluated for direct epoxidation of C_3H_6 using molecular O_2. Active surface Ag site concentration was measured by H_2 pulse titration over

oxygen pre-covered surface. XRD analysis, SEM imaging with EDXS analysis, BET surface area and BJH pore size distribution analysis was performed to characterize all the catalysts. Isomerization of PO was studied over α-Al_2O_3, $CaCO_3$ and ZrO_2 supports to examine PO stability at a temperature range from 220ºC to 300ºC. Effects of promoters (K^+, Cs^+, MoO_3) and gas feed additives (EtCl, NO) were studied rationally for fundamental understanding. EtCl showed enhancement in PO selectivity by inhibiting the total oxidation of PO. However, over chlorination of the catalyst surface showed irreversible formation of AgCl and caused the loss in catalyst activity. A critical amount of NO (50 ppmv) was found to be required to achieve improvement in both activity and PO selectivity. Further increase in NO concentration at the feed > 50 ppmv showed only improvement in activity. K^+ showed resistance to AgCl formation when 50 ppmv EtCl was present at the feed. In the presence of EtCl, NO and promoted with K^+ both 12 wt% Ag/α-Al_2O_3 and 56 wt% Ag/$CaCO_3$ showed > 35.0% selectivity at a 4.0% – 6.0 % conversion of C_3H_6. The 20 wt% Ag – 4 wt% Mo/ZrO_2 catalyst at 460ºC showed the formation of acrolein as the selective product instead of PO as claimed in the literature. PO stability study at 360ºC showed PO was not stable at this high temperature. Catalytic evaluation for partial oxidation of C_3H_6 over a 4 wt% Ag/ZrO_2 catalyst at 460ºC showed Ag was not required for the formation of acrolein.

TABLE OF CONTENTS

LIST OF FIGURES

LIST OF TABLES

CHAPTER 1

NEW PERSPECTIVES AND INSIGHTS INTO DIRECT EPOXIDATION OF C_3H_6 USING O_2 AND Ag – BASED CATALYSTS[1]

[1] M.B. Burkholder, M.M. Rahman, A.C. Reber, A.M. Gaffney, B.F. Gupton, J.R. Monnier, New perspectives and insights into direct epoxidation of propylene using O_2 and silver-based catalysts, *Applied Catalysis A: General*, **650** (2023). (Co-first author)

1.1 ABSTRACT

A series of Ag-based catalysts were studied for direct epoxidation of propylene using molecular O_2 as the oxidant. Ag supported on $CaCO_3$ and α-Al_2O_3 were prepared as base materials to study. Different amounts of alkali earth metal promoter (K) and feed additives, ethyl chloride (EtCl) and nitric oxide (NO), were added to the catalyst and feed stream, respectively, to evaluate their effects on catalyst performance in terms of PO selectivity and propylene conversion. A conventional catalyst supported on α-Al_2O_3 performed similarly to the ARCO Ag (50 wt%) catalyst, supported on $CaCO_3$, at a much lower Ag loading (12 wt%). EtCl inhibited consecutive oxidation presumably by Cl deposition on Ag sites and NO increased activity possibly by Ag-catalyzed oxidation of NO to NO_x which was the selective oxidant. K^+ promoter loadings as high as 1.9 wt% were essential to stabilize both Cl and NO_x on the catalyst surface. PO Selectivities as high as 50% were obtained.

1.2 INTRODUCTION

Propylene oxide (PO) is a major chemical intermediate used to synthesize a variety of products including glycols, surfactants, pharmaceuticals, and plastics [3, 4]. Global production in 2020 was 11.2 million tons [5]. Despite the importance of this chemical, current synthesis methods rely on indirect and more expensive oxidants such as organic hydroperoxides rather than molecular oxygen (O_2), which is used in the cases of ethylene and 1,3-butadiene [3, 6-8]. Organic hydroperoxides, such as t-butyl hydroperoxide and 2-peroxy ethylbenzene, are typically used in coproduct synthesis routes where PO is produced as the minor product by weight. However, the economic viability of PO synthesis through these routes is dependent on the coproducts, such as t-butanol and styrene, markets. Thus, direct epoxidation by O_2 to synthesize PO remains an especially desirable goal for research and development. Many researchers have attempted to develop catalysts, typically Ag-based, for the selective epoxidation of propylene to PO. Ag catalysts are well known to selectively epoxidize ethylene and butadiene. However, extending Ag-based epoxidation catalysts to propylene results in a non-selective reaction to primarily form CO_2 and H_2O with PO selectivity limited to $< 2 – 5\%$ [4, 8]. The rationale is that removal of the allylic C-H groups on propylene is energetically more favorable than for the vinylic C-H bonds of ethylene. Nucleophilic H abstraction occurs more readily for propylene, leading to complete combustion products, rather than electrophilic addition of adsorbed O to the C=C bond to form PO [4, 9-11]. The bond dissociation energy of the allylic C-H bond in propylene is only 77 kcal/mol compared to vinylic C-H bond at 112 kcal/mol, so allylic C-H bond breaking is energetically preferred [12]. The H binding energy at propylene's allylic site is much lower than that of the other H binding energies on the vinylic carbons.

The H binding energies for propylene's vinylic carbons are similar to that of ethylene. As shown in Figure 1.1, the allylic C-H bond of propylene is 3.81 eV vs. 4.92 eV for the vinylic C-H bond of ethylene.

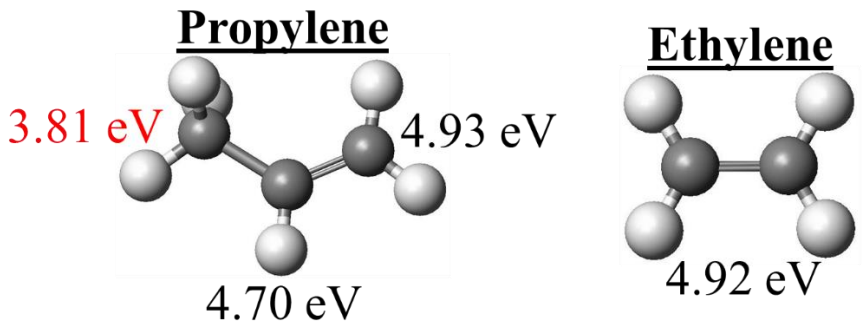

Figure 1.1: The hydrogen binding energies on propylene and ethylene. These binding energies were determined by the DFT calculations performed in this study. They may differ slightly from literature values.

Conventional EO catalysts contain relatively high weight loadings (15 – 25 wt%) of Ag supported on non-acidic α-Al_2O_3. Promoters such as alkali earth metals, especially Cs, and high-valent oxyanions (HVOAs), such as ReO_4^-, MoO_4^{2-}, WO_4^{2-}, and SO_4^{2-} are also added to improve selectivities from ~70% to 87 – 91% [13]. Promoter loadings are always < 1000 ppmw based on the metal (or S). Little has been written about the roles of the different promoters, but it is interesting to note that both a univalent, large cation (Cs^+) must be present along with the high valent oxyanions to achieve high EO selectivities. In a recent study, Monnier offered an explanation and mechanism to explain the roles of HVOAs and why Cs^+ must also be present to achieve high selectivities, especially when HVOAs are present [2]. The role of HVOAs is to increase the electrophilicity of adjacent Ag-O to favor addition to the e^- rich C=C double bond, rather than nucleophilic C-H bond breaking, but it also increases adsorption of the adsorbed EO precursor to hinder desorption of the epoxide. Addition of Cs^+ to Ag lowers the desorption energy of EO from the catalyst

surface due to its very high polarizability [2, 8, 14]. In essence, each type of promoter affects different steps in the formation of EO. These findings and understandings about the fundamental nature of EO catalysts may be helpful to understand and improve Ag-based catalysts for direct PO synthesis.

The most noteworthy success for Ag-catalyzed propylene epoxidation was achieved by Gaffney and coworkers at ARCO in the 1980's; they observed up to 60% PO selectivity [15-23] for an unusual composition of a Ag-based catalyst which also required surprising and high levels of gas feed additives. The optimal catalyst composition was much different from conventional EO catalysts that contained 15 – 25 wt% Ag supported on low surface area α-Al_2O_3. The ARCO catalyst was prepared by physically mixing (by ball-milling) essentially equal weights of $CaCO_3$ with a Ag salt to give a mixture of both components before the Ag was reduced to Ag^0. The 50 wt% Ag-50 wt% $CaCO_3$ was also promoted with 2 wt% K to give the final catalyst. This amount of K (20,000 ppmw) is much higher than the 100 – 500 ppmw levels of alkali metal salts that are used for EO catalysts. Further, to achieve PO selectivities higher than 50%, it was necessary to add up to 200 ppmv EtCl and 200 ppmv NO to the feed stream. The amount of EtCl that was required is much higher than the 1 – 4 ppmv EtCl added to EO feeds, and the only other NO feed additives were reported much earlier by Hayden [24, 25] and Notermann [26].

This study will investigate some of the critical differences between the ARCO type of catalyst and conventional EO Ag-based catalysts. Specifically, does $CaCO_3$ function only as a non-acidic support for Ag or is it also part of the catalyst system. The method of preparation of the 50% Ag – 50% $CaCO_3$ using ball-milling is much different than wet impregnation of a Ag salt on a low surface area α-Al_2O_3. We will compare performances

of both types of catalysts in this study. Another difference to investigate is why the ARCO catalyst requires 2 wt% K rather than much lower levels, in line with conventional EO catalysts. The addition of high levels of EtCl (200 ppmv) is clearly different from the 1 – 4 ppmv levels used for EO. In fact, prolonged exposure of EO catalysts would irreversibly poison Ag catalyst by the irreversible formation of bulk AgCl. Does this also occur with PO catalysts. Finally, one of the most intriguing observations is the role(s) of 50 – 200 ppmv NO feed additive for increasing PO performance. Which is more affected, the activity or selectivity. Is NO part of the oxygen cycle, along with O_2, as the selective oxidant, or do the free radical properties of NO change electronic structure of the Ag-O to make it more active and/or selective. Our goal is to offer a more complete understanding of this potentially-important reaction using a Ag-based catalyst and molecular oxygen.

1.3 EXPERIMENTAL METHODS

1.3.1 Catalyst preparation

The chemicals used to prepare the catalysts in this investigation were ethylene diamine (EN, $C_2H_8N_2$, Millipore-Sigma >99%), oxalic acid dihydrate (OA, $H_2C_2O_4{\cdot}2H_2O$, Oakwood Chemical >99%), silver (I) oxide (Ag_2O, Alfa Aesar >99%), calcium carbonate ($CaCO_3$, Oakwood Chemical >99%), alpha-alumina (α-Al_2O_3, Norpro-St. Gobain, SA5562), ethanolamine (C_2H_7NO, Oakwood Chemical >99.5%), diammonium molybdate ($(NH_4)_2MoO_4$, Fisher Scientific >99.99%), potassium nitrate (KNO_3, Oakwood Chemical >98%), cesium nitrate ($CsNO_3$, Sigma Aldrich ≥99%) and potassium acetate (KOAc, Alfa Aesar ≥99%). For certain cases, silver (I) oxalate ($Ag_2C_2O_4$) was used in place of Ag_2O and OA. Catalysts prepared will be designated here and elsewhere with the weight loading of Ag or promoters in parentheses, e.g. 56 wt% Ag on $CaCO_3$ is Ag(56)/$CaCO_3$. The gases

utilized in the reaction were propylene (99.5% purity, Airgas), molecular oxygen (O_2, 99.993% purity, Praxair), helium (He, 99.999% purity, Praxair), 1000 ppmv nitric oxide (NO) balance He gas mixture (Airgas), 500 ppmv ethyl chloride (EtCl) balance He gas mixture (Airgas).

The target Ag loadings were maintained at 56 wt% on the $CaCO_3$ catalyst support by slowly adding Ag_2O to an aqueous solution containing a 1.1:0.7:1 M ratio of EN:$H_2C_2O_4$:Ag. The solution was kept in an ice bath during these steps due to the exothermic nature of mixing. The order of addition of components was: 1) EN to water, 2) $H_2C_2O_4$ to that solution, and 3) Ag_2O when all the $H_2C_2O_4$ was dissolved. The solution was removed from the ice bath after all the Ag_2O was added and allowed to mix for another hour. The solution was returned to the ice bath when ethanolamine (0.4:1 M ratio to Ag) and molybdic acid (0.01:1 M ratio to Ag) was slowly added to the solution. The solution was removed from the ice bath after both components were completely incorporated into the solution.

$CaCO_3$ was added to a 20 mL alumina ball mill with a single alumina ball (d = 0.5 in). The Ag containing solution was then added directly to the ball mill and sealed with Viton gaskets and placed into a high-energy ball-mill mixer (SPEX SamplePrep 8000M Mill). The vessel and sample were then mixed for 10 mins at ~1060 lateral cycles per minute with 5.7 cm back-and-forth and 2.5 cm side-to-side oscillatory movements. After milling, the highly viscous sample was collected into a quartz evaporating dish. and the evaporating dish was placed into a convection oven at 110°C to dry for 2 h. The dried sample was collected from the dish and loaded into a ½" quartz tube held in place by glass wool. The quartz tube and calcined at 300°C in 100 cm^3/min for 4 h. After calcining, the

sample was ground again by mortar and pestle, and stored in an amber bottle until ready for addition of promoter salts in a second step or reaction. This sample is referred to as unpromoted Ag(56)/$CaCO_3$ catalyst.

The base Ag (12)/α-Al_2O_3 catalyst was prepared as described by Diao [2]. $CsNO_3$ solution was added during $Ag_2C_2O_4$ addition to prepare Cs promoted Ag (12)/α-Al_2O_3 samples. The Ag (12)/α-Al_2O_3 catalyst was the reference material to the $CaCO_3$ supported catalysts. The K promoter for this catalyst was added in the same manner as the $CaCO_3$ catalysts in a second step after calcination.

Promoters for the ARCO type catalysts were done in a second step after calcination of the unpromoted Ag(56)/$CaCO_3$ catalyst. Specifically, the proper amount of KNO_3 or $(NH_4)_2MoO_4$ was dissolved in a round-bottom rotary evaporation flask. After dissolution of the 10% excess liquid relative to incipient wetness, the ARCO type catalyst was added, and the H_2O was removed by rotary evaporation at 60°C. The flask was then placed into a convection oven at 110°C for 2 h to dry the sample more fully. After grinding the catalyst was placed in a vial for further use.

1.3.2 Catalyst characterization

Scanning electron microscopy (SEM) micrographs were collected using a Zeiss Gemini 500 SEM. For EDS analysis, electrons were collected using a secondary electron detector; the incident electron beam energy was set to 5.0 keV. Crystalline structures were examined by X-ray diffraction (XRD) using a Rigaku Miniflex-II system equipped with a scintillation counter detector. XRD patterns were recorded from 20 – 80° 2θ using a Cu-Kα radiation source (λ = 1.5406 Å) operated at 30 mA and 15 kV. Chemisorption measurements were conducted using a Micromeritics Autochem II 2920 automated

chemisorption analyzer and active Ag site concentrations for unpromoted samples were determined by H_2 pulse titration of O-precovered Ag sites using the method developed by Vannice [27]; a Ag:H_2 = 1:1 stoichiometry was used to determine the number of active Ag sites, since the pulsed H_2 reacted with Ag-O to form H_2O and a vacant Ag site; silver does not undergo dissociative chemisorption of H_2 at 170℃. Sample pretreatment for chemisorption was conducted by reduction at 280℃ for 2 h flowing H_2 and then cooling to 170℃ in flowing He. The sample was then exposed to a gas stream of 10% O_2/He for 30 mins before purging with flowing Ar; after baseline stabilization, the sample was pulsed with 10% H_2/balance Ar, also at 170℃. The surface areas of these materials were determined from a BET (Brunauer-Emmett-Teller) method at a relative pressure (P/P_0) in the 0.05 – 1.0 range using a Micromeritics ASAP 2020 Plus instrument. Kr gas was used for the determination of the surface area for both supports.

1.3.3 Temperature programmed reaction (TPRxn)

Temperature programmed reaction (TPRxn) was performed using a residual gas analyzer (RGA)/mass spectrometer. The sample was first calcined at 280°C to remove excess EN from the catalyst then reduced with H_2 at 280°C for 2 h. After purging the sample was cooled down to 140°C in a flowing Ar stream. Afterward, a stream of 5 vol.% O_2, 500 ppmv NO balance was introduced to the feed stream and the reactor outlet was analyzed by an RGA.

1.3.4 Catalyst evaluation

A continuous flow, fixed bed system with a 316 stainless steel reactor of 0.38 in. ID, 0.5 in. OD was used to evaluate catalyst performance and PO isomerization trends. A feed stream of 17% C_3H_6, 9% O_2, 50 – 200 ppmv NO and EtCl, with balance He was used

for catalyst evaluation. This was considered standard reaction conditions unless otherwise stated in the results. PO isomerization studies were conducted with a feed stream of 1 – 5% PO, 9% O_2, 0 – 50 ppmv EtCl, 200 ppmv NO, and balance He. For both isomerization and catalyst evaluations, a total flow rate of 60 (STP) cm^3/min (SCCM) was used. Sample masses of either 4.0 g or 2.0 g were loaded into the reactor for catalytic performance and PO isomerization studies, respectively. Catalyst evaluations were conducted at 30 psig total pressure at temperatures between 220℃ and 250℃. Evaluation times were typically 50 – 200 h on-line. The PO isomerization study was conducted at 1 atm total pressure at temperature between 220℃ and 270℃. In all cases, catalysts were pretreated in an atmosphere of 20% H_2/He at 1 atm pressure and 280℃ for 2 h before conducting any experiments. The outlet stream from the reactor was analyzed in-line with a HP 5890 Series II gas chromatograph containing two Poraplot Q columns equipped with a thermal conductivity detector (TCD) and flame ionization detector (FID). TCD was used for quantitative analysis of O_2, CO_2 and H_2O and FID was used for analyzing propylene, PO, propionaldehyde, acetone and acrolein, if present.

1.3.5 Computation methods

Theoretical studies used in first-principles density functional theory, and have been carried out using the Amsterdam Density functional (ADF) set of codes [28]. The GGA-PBE exchange correlation functional were used, as proposed by Perdew, Burke, and Ernzehof (PBE) [29]. The TZ2P basis set with a large frozen electron core was used in the computations. In all cases, the local geometrical minimum for each minimum for each structure was obtained by using quasi-Newton method without any symmetrical restriction. The zero-order regular approximation (ZORA) was used to include scalar-relativistic effect

[30]. This level of theory has been found to accurately model the reactivity of silver clusters and catalysts [31, 32].

1.4 RESULTS AND DISCUSSION

1.4.1 Comparison of $CaCO_3$ and α-Al_2O_3 as catalyst supports

ARCO used $CaCO_3$ as "support" material, although the $CaCO_3$ was added to a Ag oxalate solution and was then ball milled to achieve homogeneity in the slurry of catalyst precursor. With this method, the Ag concentration of the final composition was approximately 50 wt%. Alternatively, the traditional method of incipient wetness of an ethylenediamine stabilized solution of Ag oxalate to a non-acidic, low surface α-Al_2O_3 support was used to prepare a 12 wt% Ag catalyst. The use of $CaCO_3$, a relatively non-porous material, made the mixing process important and challenging due to the viscosity of the slurry. Ball milling was found to effectively mix the viscous paste following the procedure outlined in the patents [15-23]. For comparison, several samples supported on $CaCO_3$ were prepared using the conventional impregnation procedure used for the α-Al_2O_3 samples in this study. The impregnated, supported $CaCO_3$ catalysts were inferior, both in measured H_2 uptake (Ag surface site concentrations) and catalytic activity, relative to the catalysts prepared by milling. This is likely due to the lower pore volume of $CaCO_3$, which was ~ 0.2 cc/g, relative to 0.45 cc/g for the α-Al_2O_3 support. Thus, for $CaCO_3$, effective ball milling of the catalyst components was critical to ensure the best performance possible, as observed by ARCO [15-23]. Thus, the milling technique was followed for all prepared catalysts supported on $CaCO_3$. The catalysts supported on α-Al_2O_3 were prepared following the conventional impregnation method described above and described earlier [2]. SEM images and particle size analysis for both base catalysts, Ag(56)/$CaCO_3$ and

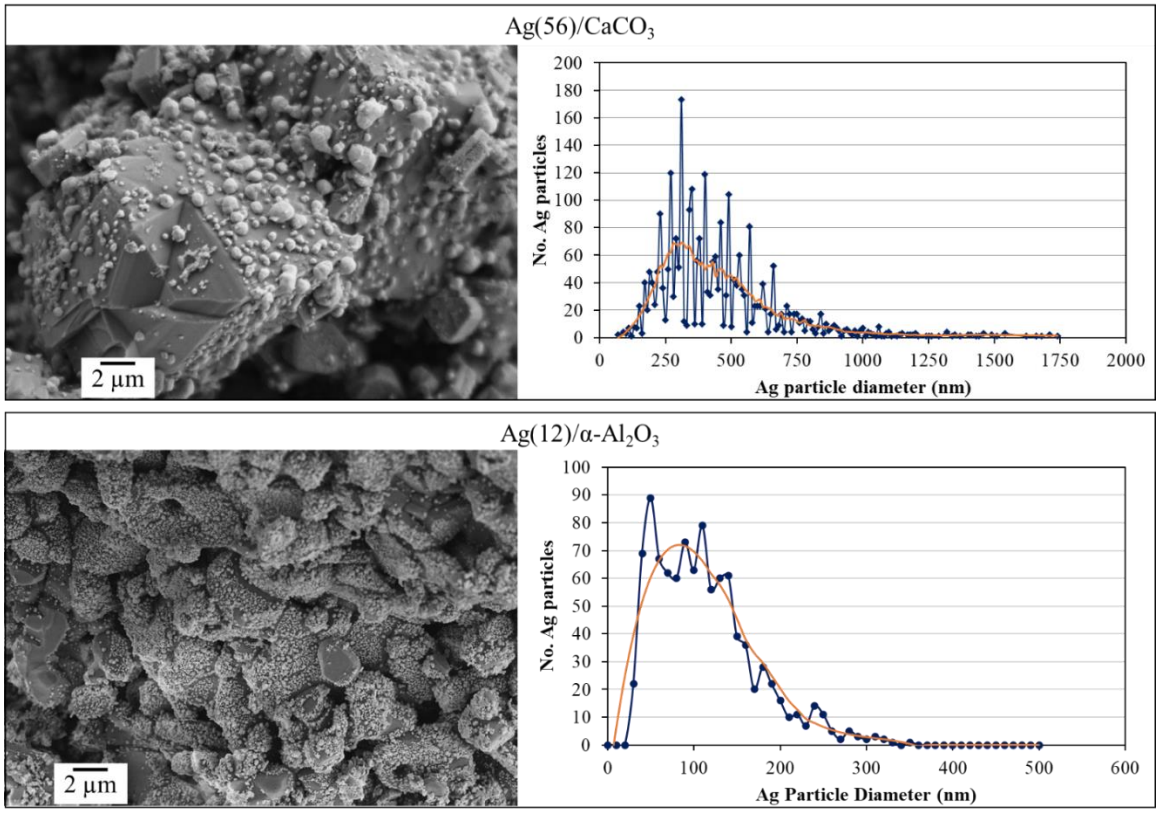

Figure 1.2: SEM and particle size histogram of unpromoted Ag(56)/$CaCO_3$ (above) and Ag(12)/α-Al_2O_3 (below) catalyst. Analysis of the particle sizes gives surface average particle sizes of 465 and 172 nm for $CaCO_3$ and α-Al_2O_3, respectively. 1973 and 1000 particles were counted for the Ag(56)/$CaCO_3$ and Ag(12)/α-Al_2O_3, respectively. Magnification for both SEM images are 3.9 KX at a working distance of 5.9 mm.

Ag(12)/α-Al_2O_3, are shown in Figure 1.2 The images show that the Ag particles on α-Al_2O_3 are smaller and more evenly distributed on the surface than for the $CaCO_3$ support; note the difference in scales of the x-axis. The histograms also indicate a narrower distribution of Ag particle sizes for α-Al_2O_3 The impact of the larger Ag particle sizes for the ARCO-type catalysts are shown in the pulse Ag chemisorption curves in Figure 1.3 and Table 1. The results show that even though the amount of Ag in the ARCO-type catalyst is 4.7 larger than for the α-Al_2O_3 sample, the concentration of active Ag sites is only 1.4 times larger, suggesting substantial Ag site losses due to larger Ag particles with lower Ag surface atom concentrations/total Ag atom concentrations and very likely some of the Ag particles

buried in the $CaCO_3$ slurry during preparation. One would not select the ball mill approach for more efficient use of the Ag component.

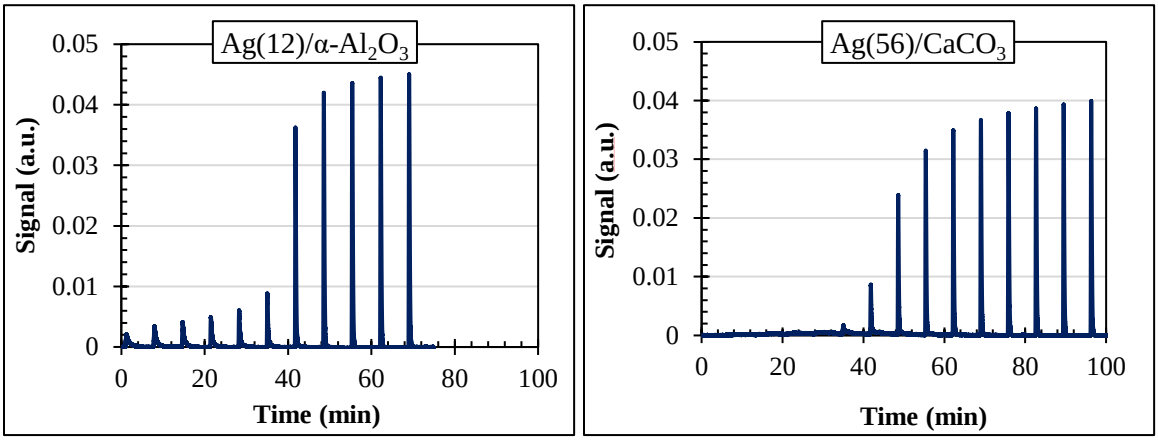

Figure 1.3: H_2 uptake values for conventional (left) and ARCO (right) catalysts. 2.0 g of catalysts were used for each experiment.

Table 1.1: Comparison of number of active Ag sites on unpromoted Ag(12)/α-Al_2O_3 and Ag(56)/$CaCO_3$ samples calculated by H_2 pulse titration.

Sample	H_2 uptake (μmol/g cat STP)	Active Sites (# Ag site/g cat) $\times 10^{18}$	Ag particle size (nm)*
Ag(56)/$CaCO_3$	5.42 ± 0.05	3.26 ± 0.03	1040
Ag(12)/α-Al_2O_3	3.83 ± 0.18	2.31 ± 0.11	340

*Calculated from the Ag site concentration data in chemisorption measurements.

1.4.2 Reactivity of PO over catalyst supports

A second primary reason for selection of $CaCO_3$ is the basicity of the surface, which should suppress the acid-catalyzed ring opening of PO to form isomerization products of PO which typically lead to combustion to CO_2/H_2O. Activities of $CaCO_3$ and α-Al_2O_3 for PO isomerization were determined by flowing a PO-containing gas stream at reaction conditions over each support. The gas stream also contained 10% O_2 to duplicate actual reaction conditions more closely; results are shown in Figure 1.4. Also included in Figure 1.4 are the reactivity trends of the supported Ag catalysts for the 4 – 5% PO, 10% O_2, and balance He feed stream. The supports alone showed little reactivity; O_2 conversion

remained less than 3% for α-Al_2O_3 and less than 1% for $CaCO_3$ at all three temperatures. Conversion of PO was higher for α-Al_2O_3 than $CaCO_3$ at 270°C, 15.8% vs 8.4%, respectively. However, for normal reaction conditions of 225 – 250°C, both support performed similarly. Interestingly, no CO_2 or H_2O was formed but only the structural isomerization products propionaldehyde > acetone > acrolein, (although acrolein is an oxidation product) and small amounts of acetaldehyde were observed. Acetaldehyde was likely produced from the cracking of propionaldehyde.

Most of the PO was converted to propionaldehyde (EtCHO), although some acetaldehyde (CH_3CHO) was observed at 245°C and 270°C, but not in significant quantities. Acrolein formation was only observed at 270°C. The $CaCO_3$ support was substantially different than the α-Al_2O_3 support. In general, increased temperature produced more acetone relative to propionaldehyde. However, a significant amount of acetaldehyde was produced at 245°C and 270°C, reducing the relative amount of

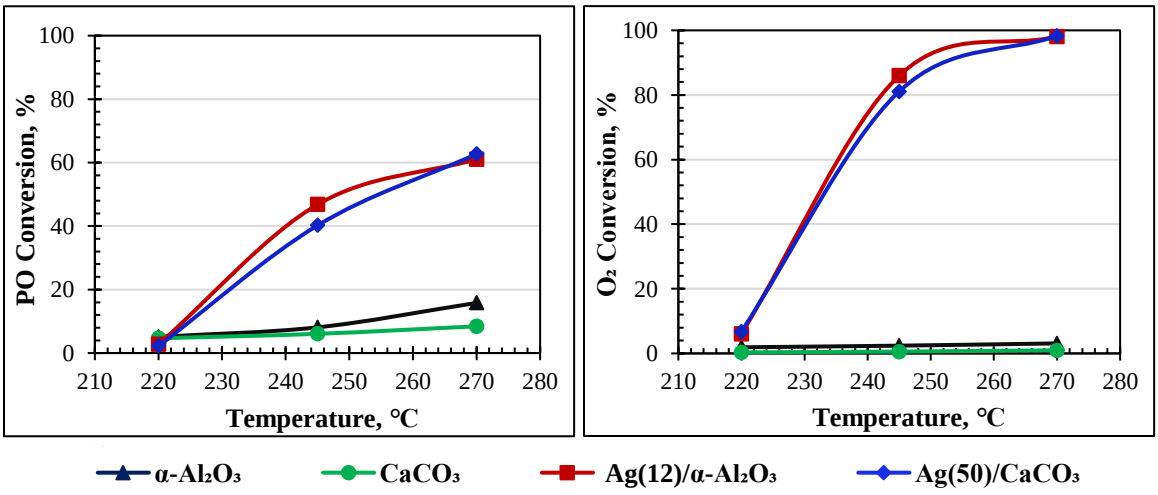

Figure 1.4: PO conversion (left) and O_2 conversion (right) vs. temperature. Conditions: 4 – 5% PO, 8 – 10% O_2, balance He, 1 atm pressure, GHSV = 1200 – 2000 h^{-1}, sample weight: 2.0 g.

propionaldehyde being produced. Acrolein was observed only at 270°C, the same as for the α-Al_2O_3 support. The change in product distribution indicates that C=O hydrogenolysis of propionaldehyde to form acetone and C-C hydrogenolysis to form CH_3CHO as well as oxidation to form acrolein are energetically more demanding reaction pathways then hydroisomerization of PO to form propionaldehyde. The results are summarized in Table 1.2 below.

Table 1.2: Product distribution pertaining to temperature.

Support	**Temperature (°C)**	**CH_3CHO (%)**	**EtCHO (%)**	**Acetone (%)**	**Acrolein (%)**
α-Al_2O_3	220	0.0	89.6	10.4	0.0
	245	1.0	89.6	9.4	0.0
	270	0.5	88.7	9.2	1.6
$CaCO_3$	220	0.0	95.5	4.5	0.0
	245	13.5	76.9	9.6	0.0
	270	11.5	74.4	12.2	1.9

DFT computations were performed to better understand the reactive nature of the C-H bonds present in both PO and its structural isomers. Figure 1.5 shows the binding energies of the C-H bonds for each molecule and Table 1.3 lists both the relative stability and H-binding energy of the C-H bond at the position α to the C-O bond. Acrolein is not included since it is an oxidation product.

The relative stability was calculated, following the methods outlined in section 1.4 and the values are relative to the total electronic energy of PO, where the more negative values indicate a molecule which is more energetically stable than PO. This means it would be thermodynamically favorable for PO to isomerize into propionaldehyde and acetone if PO did not desorb from the catalyst surface quickly enough. The hydrogen binding energies

of PO were higher than the allylic H of the propylene feed (3.81 eV) and isomerization product.

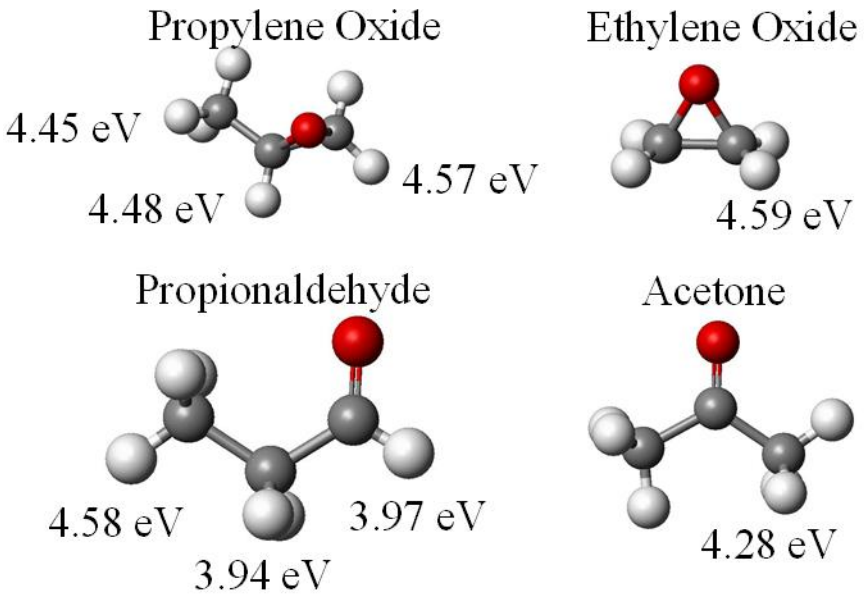

Figure 1.5: H-binding energy for the C-H bonds for PO, EO, and PO isomers.

Table 1.3: Relative stability and C-H binding energy in the α-position to C-O bond for PO, EO, and PO isomers.

Molecule	Relative Stability (eV)	H-Binding Energy (eV)
Acetone	-1.16	4.28
Propionaldehyde	-0.89	3.94
Propylene Oxide	**0.00**	**4.45**
Ethylene Oxide	**0.00**	**4.59**

Propionaldehyde is more reactive than acetone, suggesting that PO could isomerize to propionaldehyde and then combust to CO_2/H_2O, in much the same way that acetaldehyde is considered to be the reactive isomer formed from EO that undergoes combustion. This supports the idea that PO is capable of isomerization and that the presence of the hydrogen poaching Ag will likely cause the isomerized products to undergo consecutive combustion at typical operating temperatures of 250°C. The weaker C-H binding energy at the

α-position relative to the vinylic C – H of EO suggests that higher levels of EtCl may be required for high selectivity to PO.

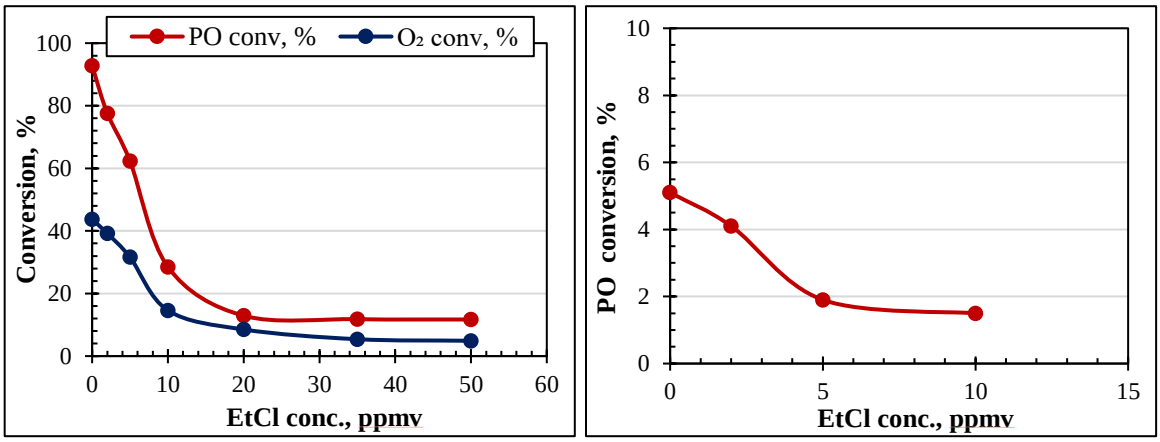

Figure 1.6: Reactivity of PO in presence of 9% O_2 (left) and for PO isomerization in absence of O_2 (right) vs. EtCl concentration. Reaction conditions, feed stream: 1% PO, 200 ppmv NO, EtCl as stated, and balance He; pressure: 1 atm; temperature: 250°C; GHSV = 1000 h^{-1}, sample weight; 2.0 g. Catalyst was Ag(56)/$CaCO_3$.

Finally, addition of Ag to both supports to form the working catalysts resulted in Ag-catalyzed combustion to CO_2/H_2O as shown in Figure 1.4. At 245°C more than 80% of the PO underwent combustion and at 270°C complete combustion had occurred. Since this was an Ag-catalyzed process, there was no effect of the catalyst support except on isomerization of PO to form more reactive intermediates. These results do not mean the same reactivity of PO will occur during reaction, since ethyl chloride (EtCl) will be present in the feed. However, the higher reactivity of PO relative to EO may require higher EtCl levels during reaction. PO isomerization activity as a function of ppm EtCl co-feed for the ARCO Ag(56)/$CaCO_3$ was determined and the results are shown in Figure 1.6. When O_2 was present in the feed, Ag-catalyzed combustion to CO_2/ H_2O occurred until ≥ 20 ppmv EtCl was present in the feed. In the absence of O_2 low levels of propionaldehyde and acetone isomers were formed until ≥ 5 ppmv EtCl was added to the feed. Regardless of whether O_2 was present, the levels of EtCl were much higher than the 1 – 3 ppmv levels

required for Ag-catalyzed formation of EO [33]. The effect of EtCl levels will be discussed below in section 1.4.2 with catalyst performance.

1.4.3 Effects of gas phase feed additives

Chloride species have been used as reaction modifiers to improve both activity and selectivity for other epoxidation processes, specifically, the EO and EpB processes [2, 12, 34]. Chloride can be added during the catalyst synthesis in the form of a promoter salt, such as KCl or CsCl, or by addition to the gas phase as organic chlorides during reaction. The most common method has been gas phase addition of EtCl for direct epoxidation reactions with molecular oxygen over Ag catalysts [7, 12, 34-37]. The addition of Cl^- to propylene epoxidation also increased PO selectivity [12, 15-23], and inhibited PO combustion and isomerization as shown above in Figure 1.6. However, excess Cl^- typically causes catalyst poisoning by irreversible AgCl formation [31]. Considering that the levels of EtCl used by ARCO in their process was at least one order of magnitude higher for PO compared to the amount typically used for EO, AgCl formation was a concern. The results in Figure 1.6 above also indicated that a minimum of 20 ppmv EtCl was needed to suppress PO combustion over Ag catalysts. To determine the effects of EtCl over the extended range discussed by ARCO, catalyst performance was evaluated from 20 – 100 ppmv EtCl and the results shown in Figure 1.7. Note that the catalyst was of the ARCO type and that it was promoted with 1.9 wt% K and included 200 ppmv NO in the feed stream, as taught by ARCO. The effects of K and NO will be discussed at a later point in this discussion.

Selectivity to PO with 20 ppmv EtCl increased slowly from 2% to 25% during the first 70 hours on-line and then more quickly as EtCl was increased in steps to 100 ppmv. However, improvements in PO selectivity were more marginal when EtCl was changed

from 50 to 70 to 100 ppmv. The EtCl effect was reversible; when EtCl was lowered back to 50 ppmv, the EO selectivity was the same as the initial exposure to 50 ppmv. Similar results have been reported by Hermans for an ARCO type of composition that contained 56 wt% Ag supported on $CaCO_3$ [38]. The authors found that addition of EtCl resulted in

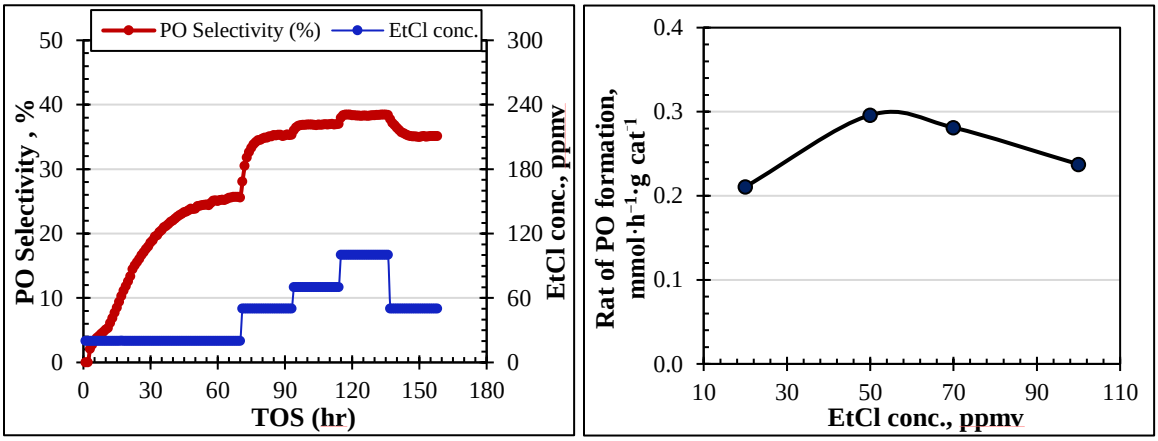

Figure 1.7: PO selectivity (left) and rate of PO formation (right) vs. EtCl concentration. EtCl concentration was varied between 20 – 100 ppmv, feedstream composition: 17% C_3H_6, 9% O_2, diluent He + variable ppmv EtCl + 200 ppmv NO; pressure: 30 psig; temperature: 250°C, sample weight: 4.0 g. Catalyst was Ag(56)-K(1.9)/$CaCO_3$.

the increase of PO selectivity from 4.5 to 20% when 210 ppmv EtCl was added to the feed; their EtCl effect was also reversible. Unfortunately, Hermans did not report the effects of EtCl concentrations other than at 210 ppmv or for reaction times longer than 24 h. Our results suggest that optimal effects on PO selectivity were obtained at ~ 100 ppmv EtCl. The selectivity-enhancing effect of surface Cl can be attributed to either Cl poisoning of inherently non-selective Ag sites or changes in the e^- density on adjacent Ag sites to increase electrophilicity of O adsorbed at these sites [12, 34]. The volcano shape relationship between rate of PO formation and EtCl concentration in Figure 1.7 demonstrates the balance between Cl^- promotion and poisoning, achieving an optimum at 50 ppmv EtCl feed. The Cl^- promotion for PO likely follows the same mechanism as EO

promotion; Cl^- deposition on the Ag surface promotes epoxide formation through modification of the electron density on adsorbed O to favor electrophilic oxygen [34, 36]. Additionally, the Cl^- promotion also inhibited the consecutive combustion pathway as shown in Figure 1.6, which contributed to the improvements in PO selectivity as EtCl levels in the feed increased from 20 – 100 ppmv. Because the EtCl concentration was optimal at 50 ppmv, this level was used for all subsequent evaluations.

In order to determine whether bulk AgCl was formed during extended reaction times at higher levels of EtCl in the feed, a series of K promoted catalysts were analyzed by XRD after reaction times from approximately 40 – 130 h on-line; the patterns are shown in Figure 1.8. Not unexpectedly, the XRD peaks at $2\theta = 27.8$ and 32.2° indicate that some AgCl was formed during reaction. Very little AgCl was formed for the catalysts containing K^+, suggesting the presence of K^+ may be to suppress formation of AgCl. More discussion of the K effect on catalyst performance is discussed at a later point.

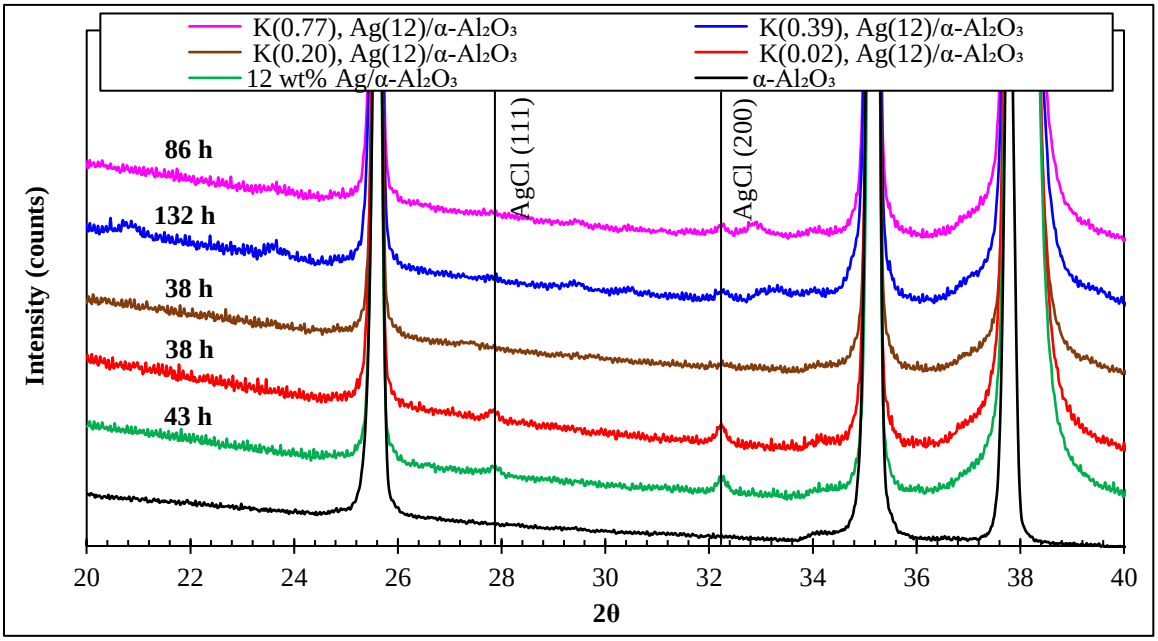

Figure 1.8: XRD patterns after reaction for specified hours on-line. Concentration of EtCl in feed was 50 ppmv in all cases and wt% K promoter shown in legend. Feed stream composition: 17% C_3H_6, 9% O_2, diluent He + 200 ppmv NO; pressure: 30 psig; temperature: 250°C. Ag(111) peak is off-scale at $2\theta = 38.1°$.

In addition to higher levels of EtCl in the feed stream relative to the EO process, ARCO and Hermans added NO at levels between 0 – 200 ppmv to increase the rate and selectivity of PO formation [12, 15-23]. NO is not a common gas-phase additive and is typically not added to epoxidation gas streams; however, Hayden [24, 25, 39] and Notermann [26] claimed higher EO and PO selectivity, respectively, when NO was added to the feed. Hayden added 20 ppmv of methyl nitrate (CH_3NO_2) to a feed stream containing 43% C_2H_4, 8% O_2, 5.2 ppmv organic chlorides, and balance N_2 diluent and reported EO selectivity as high as 85 – 87% at 30% O_2 conversion. The selectivity to EO in the absence of CH_3NO_2 was not reported, but EO selectivity for that generation of catalyst were typically 78 – 82%. Thus, there was a boost in EO selectivities when CH_3NO_2 was added. Unfortunately, in these patents Hayden gave no information on catalyst performance for other CH_3NO_2 levels. Notermann [26] used a catalyst containing 17.7% Ag promoted with KNO_3 (0.38% K basis) for propylene epoxidation with a feed containing 9.9% C_3H_6, 7.8% O_2, 200 ppmv each of EtCl and NO, and balance N_2 and CH_4. The catalyst was run for 22.5 h to form PO at 47.3% selectivity. Neither Hayden nor Notermann specified whether NO, NO_2, N_2O_3, or N_2O_4 was the active and selective oxidant; both stated that K, existing as KNO_3, was also critical for selectivity enhancement.

The results in Figure 1.9 summarize the effects of variable feed concentrations of NO for PO synthesis. The catalyst was a K-promoted Ag/$CaCO_3$ catalyst. NO was required to produce PO at higher rates; adding 50 ppmv of NO to the feed increased the rate of PO formation from <0.02 mmol/hr-g cat to 0.12 mmol/hr-g cat. Higher levels of NO had smaller, but still positive, effects on activity. Removal of NO from the feed caused a reversible and rapid decrease in activity for PO formation. Above 50 ppmv however, NO

primarily affected only catalyst activity; PO selectivity remained relatively constant at ~30% throughout the experiment. During the first 90 hours on-line propylene conversion slowly increased, which may have been due to addition of both EtCl and NO to the feed.

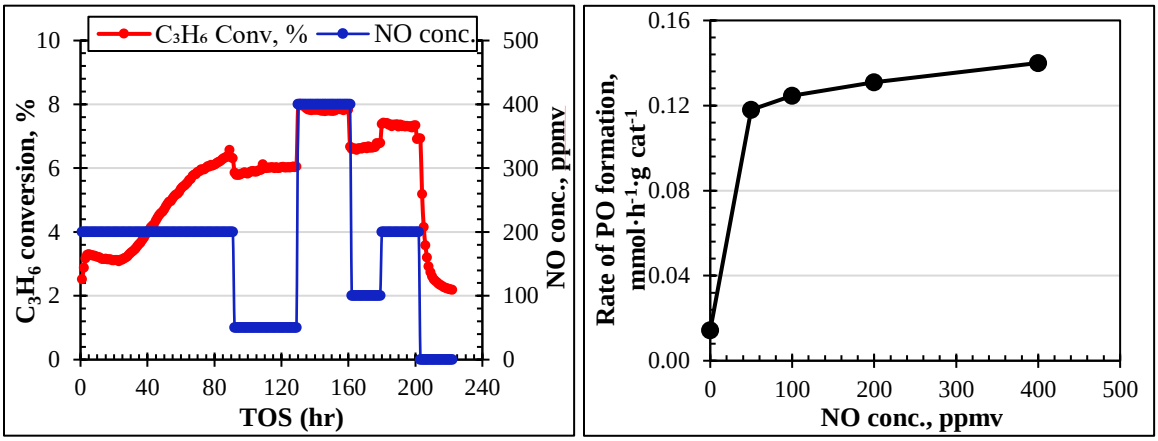

Figure 1.9: Propylene conversion (left) and rate of PO formation (right) as a function of NO concentration. NO concentrations were varied between 0 – 400 ppmv, Feed stream composition: 17% C_3H_6, 9% O_2, diluent He + 50 ppmv EtCl; pressure: 30 psig; temperature: 250°C, sample weight: 4.0 g. Catalyst was Ag(53)-K(1.9)/$CaCO_3$.

Since 200 ppmv NO gave approximately the same results as 400 ppmv, all subsequent work was conducted using 200 ppmv NO as the standard feed concentration and EtCl was maintained at 50 ppmv.

Identification and specific role(s) of NO_x for epoxidation of C_3H_6 have not been determined. In fact, almost all the limited mention of NO_x has been in patents, where, not surprisingly, no discussion has taken place. Generally, there is a belief that NO_x participates in the epoxidation process, perhaps as the source of selective oxygen in the PO molecule. If this is the case, then a reactive N species containing more than one O would be required, since loss of O from NO to form ½ N_2 would not likely be oxidized back to the NO state at reaction conditions. Notermann [26] stated that the NO_3 species existing in a stable form as KNO_3 was the preferred promoter; NO_3 was stable only in the anionic state when

electrostatically bound to a cation, such as K^+, possibly explaining why K loadings are so high for PO catalysts. ARCO claimed that 1.9 wt% K (added as KNO_3) was the optimal loading of promoter. Of course, if reduction of NO_3 to NO_2 was a one-time event, the promoter effect would be over after all the NO_3 was consumed. Rather, it is more likely that the redox couple involves NO since it is what is added to the feed and the active, oxidized form of NO is NO_2 or NO_3. Vannice [40] used DRIFTS to study adsorption of NO on $Ag/\alpha\text{-}Al_2O_3$ catalysts and found that adsorbed NO was rapidly oxidized to form NO_2 and NO_3 species; NO_3 was only stable as an anion, so a cation had to be present (Cs, in his case). Both NO_2 and NO_3 were selective oxidants, and both NO and NO_2 were easily oxidized to anionic NO_3. Thus, NO was the gateway to the NO_2/NO_3 pair which could function as selective oxidants for reaction of C_3H_6 and O to form PO; regeneration was affected by reaction of adsorbed NO and NO_2 with Ag-O (formed by dissociative adsorption of O_2 on Ag). Since the NO_x cycle to selectively form PO kinetically competes with the conventional O_2 cycle to form Ag-O as the non-selective oxidant observed PO selectivity in the 40 – 50% range.

To determine optimum promoter loadings of KNO_3, several different K promoter loadings were prepared using both $Ag(56)/CaCO_3$ and $Ag(12)/\alpha\text{-}Al_2O_3$ base catalysts and the results are shown in Figure 1.10. The K^+ showed maximum promoter effect at approximately 0.5 wt% K (5000 ppmw). Higher levels had no effect on PO selectivity, and in the case of the conventional $Ag(12)/\alpha\text{-}Al_2O_3$ catalyst activity declined when K loading was increased to 0.77 wt%, indicating K^+ poisoning of the Ag surface. The ARCO type catalyst did not show the same decline in activity, either because of the much higher Ag

loading or interaction of K^+ with the $CaCO_3$ component. Regardless, both types of Ag catalyst showed maximum effect was reached at 0.5 wt% K.

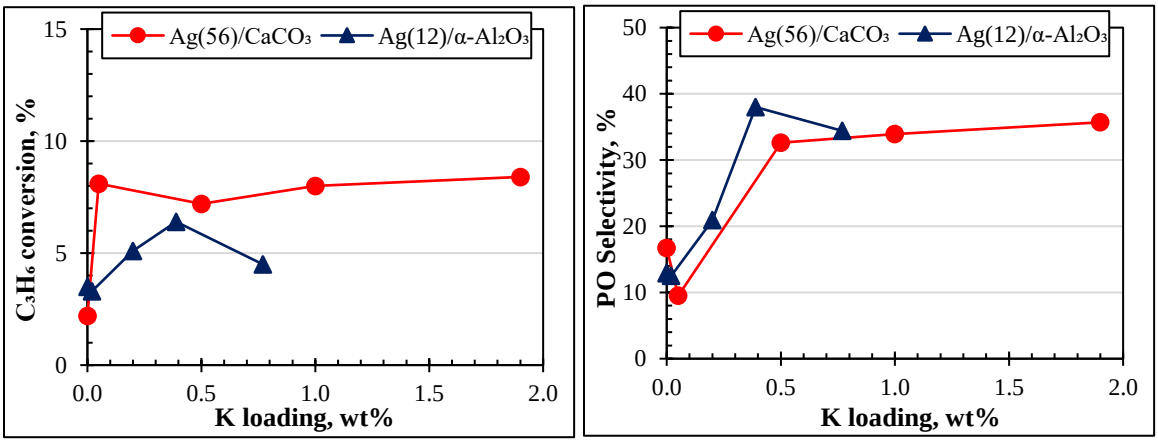

Figure 1.10: Propylene conversion (left) and PO selectivity (right) vs. K promoter loading for both conventional EO and ARCO type catalysts. Feed stream composition: 17% C_3H_6, 9% O_2, diluent He + 50 ppmv EtCl + 200 ppmv NO; pressure: 30 psig; temperature: 250°C, sample weight loadings were 4.0 g and 2.0 g for Ag(56)/$CaCO_3$ and Ag(12)/α-Al_2O_3, respectively. Catalysts were on-line for 50 h before data were taken. The K promoter salt was KNO_3.

In order to determine whether the NO_3^- species was necessary for the promoter effect of K^+, two 0.4 wt% K^+ promoted catalysts were prepared using potassium acetate (KOAc) and KNO_3 as the K sources and the results are shown in Figure 1.11. The base catalyst was Ag(12)/α-Al_2O_3. With only minor differences occurring in the first 15 – 20 h on-line, activities and PO selectivity were very similar, clearly showing KNO_3 was not required and that positive NO_x effects were derived from NO added to the feed. This conclusion is not surprising considering that only 6.2×10^{19} NO_3/g cat were present on the catalyst which would be consumed after a short time on-line. Using the data in Figure 1.12, for an average of 5% conversion of 17 vol.% C_3H_6 and 2.0 g catalyst at a total flow of 60 SCCM, all NO_3 would be consumed in ~9 minutes; the data in Figure 1.11 show catalysts were stable for 67 h on-line. Thus, K^+ was the active promoter species for the reaction.

While there were minor differences in the startup and break-in periods of the catalysts, both materials achieved similar steady state operations for both PO selectivity and propylene conversion. This indicated K^+ was the active promoter species for the reaction and that the anion did not participate in the reaction in a significant manner at these conditions. Direct PO synthesis did require catalysts containing the K^+ cation' however, the fundamental function of this promoter has still to be determined.

Effects of Cs^+ addition was studied to compare with K^+ since it is used as an alkali metal promoter for ethylene epoxidation. Cs promoters were tested over the range of 0 – 5000 ppmw on 12 wt% Ag/α-Al_2O_3 catalyst. Unlike the case for K^+, a modest promoter

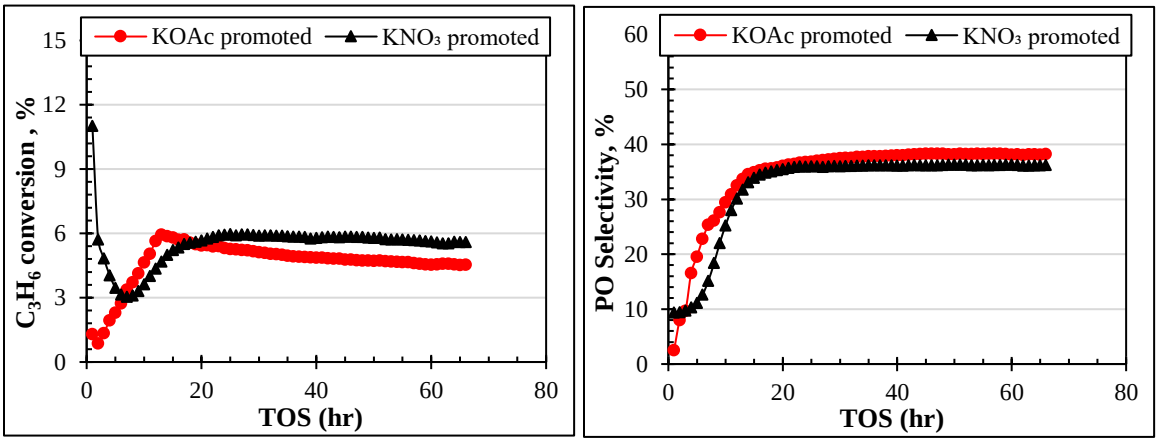

Figure 1.11: Propylene conversion (left) and PO selectivity (right) vs. time on-line for catalysts promoted with KOAc and KNO_3 salts. Feed stream composition: 17% C_3H_6, 9% O_2, diluent He + 50 ppmv EtCl + 200 ppmv NO; pressure: 30 psig; temperature: 250°C, sample weight: 2.0 g. Catalysts were Ag(12)-K(0.40)/α-Al_2O_3 from KNO_3, and Ag(12)-K(0.40)/α-Al_2O_3 from KOAc.

effect on activity, but not PO selectivity (still remained at < 10%), was observed for 350 ppmw, much lower than the amount of K^+ used for PO, particularly when the atomic weights of Cs and K are taken into account. indicates that K^+ promotion works in a different way for propylene epoxidation than Cs^+ promotion does for ethylene epoxidation.

A final difference between the mechanisms of propylene, ethylene and butadiene epoxidations is the reaction mechanism, and in particular, epoxide combustion. It is well known that both gas phase ethylene oxide and epoxybutene both undergo combustion,

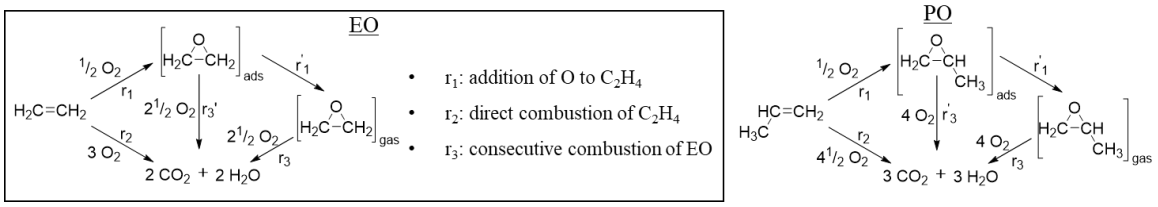

Figure 1.12: EO reaction network depicting parallel-consecutive scheme for non-selectivity and the proposed PO reaction network following a similar scheme [2].

indicative of consecutive combustion of the desired product [2, 7, 8, 12]. Since ethylene and butadiene can also directly undergo combustion, the mechanism for the reaction network is shown as parallel and consecutive pathways for combustion as shown in Figure 1.12.

This mechanistic scheme indicates that the rate of consecutive combustion of gas phase EO (reaction r_3) should increase as the concentration of EO increases. This correlation does not exist for PO formation; that is, increased concentrations of PO do not increase the rate of combustion. The results in Figure 1.13 show the expected results for both EO and epoxybutene [2, 7]. Even when the catalysts have been optimized for the highest selectivity using promoters there is still a decrease in epoxide selectivity with increasing epoxide concentrations. The negative slopes of the trendlines indicate the sensitivity of selectivity with epoxide concentrations, while the y-intercept values at 0.0% epoxide represent the loss in selectivity from direct combustion of C_2H_4 and C_4H_6. These values are shown in Table 3. This is not the case for C_3H_6 epoxidation: selectivities actually increase for the more non-selective catalysts with higher PO concentrations, suggesting major differences in the mechanism for PO formation.

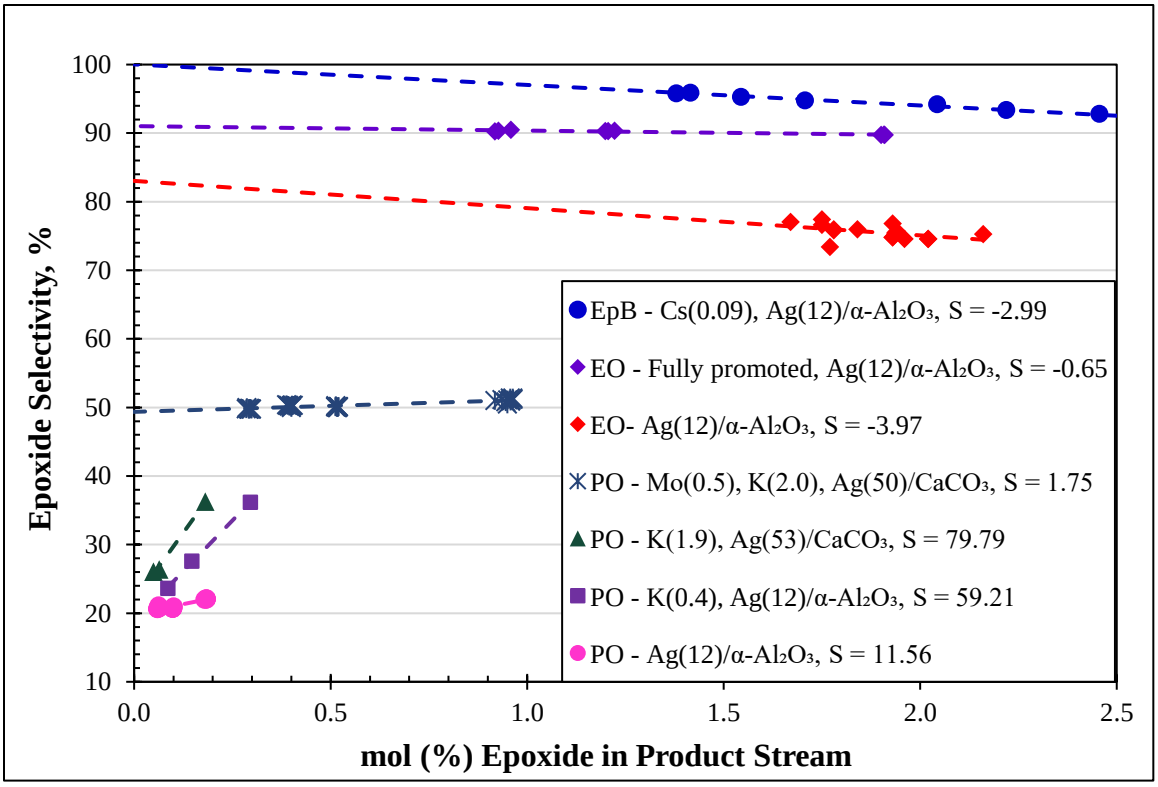

Figure 1.13: Epoxide selectivity vs. mol (%) epoxide formed for EpB, EO, and PO. S indicates slope of the fitted lines.

Table 1.4: y-intercept values for different epoxide reactions from Figure 13.

Epoxide reaction and catalyst	y-intercept value
EpB - Ag(12)-Cs(0.09)/α-Al_2O_3	100.0
EO - Fully promoted, Ag(12)/α-Al_2O_3	91.0
EO- Ag(12)/α-Al_2O_3	83.0
PO - Ag(50)-K(1.9)-Mo(0.8)/$CaCO_3$	49.4
PO - Ag(53)-K(1.9)/$CaCO_3$	21.8
PO - Ag(12)-K(0.4)/α-Al_2O_3	18.7
PO - Ag(12)/α-Al_2O_3	19.9

We showed earlier in Figure 1.6 that a gas stream containing 1% PO, 9% O_2 and no EtCl co-feed underwent > 92% conversion to CO_2/H_2O when passed over a Ag(56)/$CaCO_3$ catalyst, so PO is easily combusted in the presence of O_2 and a Ag catalyst. The addition

of > 20 ppmv EtCl was required to suppress PO combustion to acceptable levels. This observation can perhaps explain why higher concentrations of PO do not undergo more combustion to CO_2/H_2O if EtCl levels are sufficiently high enough but does not offer a satisfactory explanation why PO selectivity actually increases at higher concentrations of PO. The biggest difference between the conditions in Figure 1.6 and Figure 1.13 is that C_3H_6 is in the feed and that PO is being produced. Not shown in Figure 13 is that higher levels of CO_2 are also necessarily being formed during reaction and that higher concentrations of CO_2 are also being produced; the stoichiometric factor for combustion is one molecule of C_3H_6 or PO generates three molecules of CO_2. The ARCO patents [15-23] claimed that CO_2 was required in the gas feed to reach the highest selectivity, which is consistent with PO selectivity improving at higher PO levels. If we refer to Figure 1.13, 50% selectivity for the fully promoted catalyst gives a molar CO_2/PO ratio of 3/1, while for a selectivity of 30%, the ratio is 7/1.

Hermans also observed higher PO selectivity to PO at higher conversions of C_3H_6 [38]. In a detailed kinetic study, he found that the rate of CO_2 formation was inhibited more than PO formation when CO_2 was added to the feed; addition of 5% CO_2 increased the selectivity to PO from 26% to 39% compared to the case of no CO_2 addition. Hermans concluded that CO_2 adsorbed on surface Ag-O sites that were inherently non-selective for PO formation yet remained active for CO_2 formation as a product. Since we are operating at $\leq$ 50% PO selectivity, we are subject to this unusual CO_2 effect. It would be very interesting to see if the slope of the line relating PO selectivity to PO concentration exhibited a negative slope at higher selectivity values. For a selectivity of 80% PO, the molar ratio of CO_2/PO is 0.75, much different than 7/1 at 30% selectivity. It would be of

obvious interest and potential benefit to conduct additional studies where controlled amounts of CO_2 are added to the feed. However, because CO_2 is a kinetic inhibitor, not only to CO_2, but to PO, a balance between PO selectivity and rates of formation would need to be considered.

1.4.4 Temperature programmed reaction (TPRxn)

A 12 wt% Ag, 0.4 wt% K^+ (KNO_3)/α-Al_2O_3 sample was used for the TPRxn study using an RGA/mass spectrometer. The result of this study was summarized in Figure 1.14.

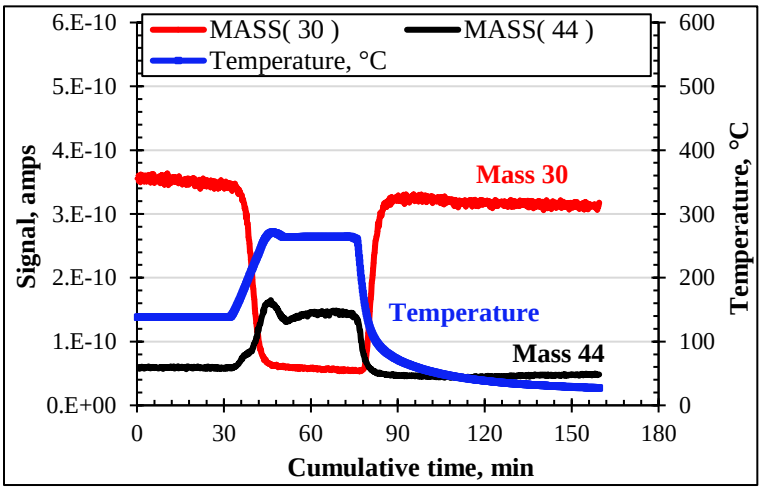

Figure 1.14: Temperature programmed reaction (TPRxn) study on 12 wt% Ag, 0.4 wt% K^+ (KNO_3)/α-Al_2O_3 sample. Feed: 5 vol.% O_2, 500 ppmv NO balance He, Pressure: 1 atm.

The main purpose of this study was to observe the conversion of NO at reaction conditions. It was found that at temperature >170°C, Mass 30 (NO) signal started to decrease and at the same time, Mass 44 signal (N_2O) started to increase. From this result, it could be concluded that NO was disproportionated to N_2O at reaction conditions. K. A. Bethke and H. H. Kung reported the formation of N_2O over a 6 wt% Ag/Al_2O_3 catalyst [41] which agreed with the result of this study. The signal for Mass 46 (NO_2) was also monitored and found 100 times lower than Mass 44 signal. However, the bass signal for NO_2 is Mass 30 which coincides with a base signal of NO. Therefore, it was not possible to separate NO

and NO_2 during the experiment and possible formation of NO_2 could not be discarded. At the end of the experiment, the temperature was lowered to room temperature and found when temperature dropped below 170°C the Mass 30 signal increased and Mass 44 signal disappeared indicating the NO was then converted to N_2O.

From the above study it could be possible that N_2O was providing the active oxygen for epoxidation of C_3H_6 as earlier we found NO was responsible for improving activity. Therefore, N_2O was added to the feed stream to study its effects on PO selectivity and C_3H_6 conversion. The results were summarized in Table 1.5.

Table 1.5: Effects of adding N_2O to the feed stream on PO selectivity and C_3H_6 conversion on 12 wt% Ag, 0.4 wt% $K^+(KNO_3)/\alpha$-Al_2O_3 catalyst at 250°C temperature and 30 psig pressure, GHSV: 1400 hr^{-1}.

Experiment No.	**Feed composition**	**PO Selectivity (%)**	**C_3H_6 conversion (%)**
1	9% O_2, 17% C_3H_6, 200 ppmv NO, 50 ppmv EtCl and balance He	36.5	6.9
2	9% O_2, **9% N_2O**, 17% C_3H_6, 50 ppmv EtCl, and balance He	8.1	2.4
3	9% O_2, **9% N_2O**, 17% C_3H_6, and balance He	4.8	4.1
4	**9% N_2O**, 17% C_3H_6, and balance He	0.0	0.04
5	9% O_2, **9% N_2O**, 17% C_3H_6, 200 ppmv NO, 50 ppmv EtCl and balance He	33.3	4.3
6	9% O_2, 17% C_3H_6, 200 ppmv NO, 50 ppmv EtCl and balance He	33.7	4.8

In Table 1.5 feed composition was varied to understand the effects of N_2O on a 12 wt% Ag, 0.4 wt% $K^+(KNO_3)/\alpha$-Al_2O_3 catalyst. At first, a standard feed stream was introduced to the catalyst to check the reproducibility of the system. It was found the performance was similar to the earlier run at 250°C temperature and 30 psig pressure, in presence of 200 ppmv NO and 50 ppmv EtCl. In the second experiment, 200 ppmv NO

was taken off from the feed and 9 vol.% N_2O was added. As a result, selectivity to PO and C_3H_6 conversion dropped significantly. In the third stage when 50 ppmv EtCl level was taken off from the feed C_3H_6 conversion increased from 2.4% to 4.1% as expected however PO selectivity remained low <10%. At the fourth stage when the feed stream consisted only of 9 vol.% N_2O and 17 vol.% C_3H_6 the C_3H_6 conversion was decreased to 0%. Therefore, it can be concluded that the previous hypothesis of N_2O could be supplying active oxygen during the reaction is incorrect. It is possible that NO disproportionated to N_2O during the reaction but N_2O does not provide selective oxygen to produce PO. In stage 5 it was found when N_2O was added along with oxygen, NO and EtCl the selectivity to PO increased to 33.3% at 4.3% conversion of C_3H_6 indicating N_2O is not the critical component in this reaction.

1.4.5 Variable post-catalytic volume study

Figure 1.13 shows for both ARCO type and traditional 12 wt% Ag/Al_2O_3 catalysts promoted with K^+ and in presence of 50 ppmv EtCl, 200 ppmv NO in the feed had positive correlation with mol (%) PO formed and PO selectivity. With the increase in mol (%) PO formed PO selectivity was found to be increased. For ethylene and 1,3 butadiene epoxidations opposite trend was reported, with an increase in mol (%) product selectivity decreased. Figure 1.13 was generated by varying flow rates only keeping other parameters constant. At a lower flow rate, the system showed higher selectivity to PO. Therefore, it was hypothesized that the free radical mechanism could be present in assisting formation of PO. To test the hypothesis quartz reactors with variable post catalytic volumes (15, 30, 60 cm^3) were used. Having a large post catalytic volume should increase free radical activity as the residence time was high. To achieve zero post catalytic volume after the

catalyst bed the void space was filled with glass wool. The results of this study were summarized in Table 1.6.

Table 1.6: Summary of variable post catalytic volume study using a12 wt% Ag, 0.4 wt% $K^+(KNO_3)/\alpha$-Al_2O_3 catalyst at 250°C temperature and 30 psig pressure, GHSV: 1400 hr^{-1}.

S.N.	Post catalyst bed volume, cm^3	PO Selectivity, %	C_3H_6 conversion, %	Flow direction
1	0	37.9	5.3	Downward
2	8	36.0	5.1	Downward
3	15	34.1	4.4	Downward
4	60	38.7	4.8	Downward
5	9	35.6	4.3	Upward
6	60	33.3	4.7	Upward

The results show no significant changes in performance on using variable post catalytic volume reactor setup in terms of PO selectivity and C_3H_6 conversion. The change in feed flow direction from downward to upward was made to (shown in Figure 1.15) ensure the presumably formed free radicals on catalyst surface avoid contact with catalyst bed support made of glass wool/quart after leaving catalyst bed. If the formed free radicals come into contact with catalyst bed it might lose energy. However, in this study, the existence of free radical activities was found to be absent. In the presence of free radical activities higher post catalytic volume should show higher activity or more selective formation of PO.

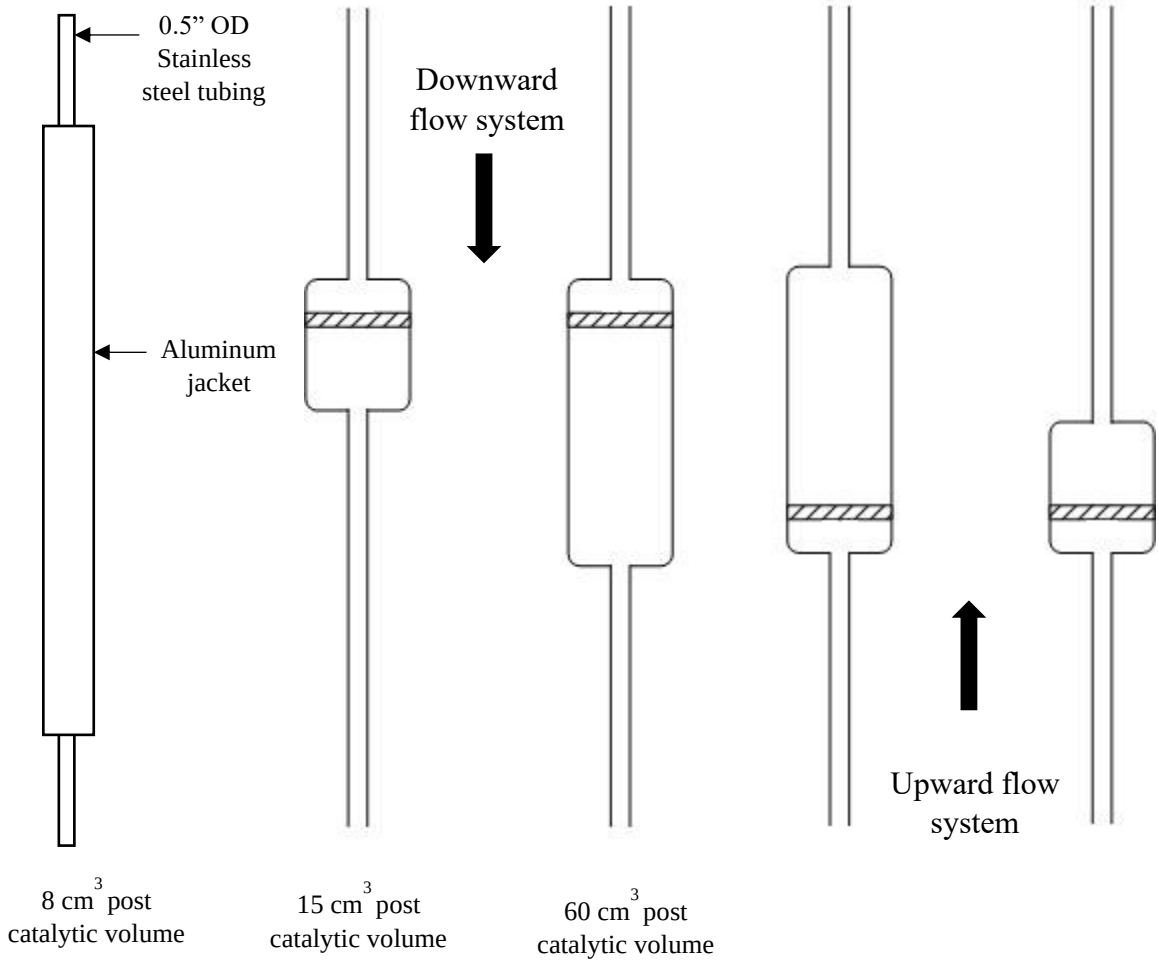

Figure 1.15: Schematic diagram of variable post catalytic volume quartz reactors and upward and downward flow setup.

1.5 CONCLUSION

A series of Ag supported catalysts supported on $CaCO_3$ (ARCO catalyst) and α-Al_2O_3 (conventional EO catalyst) have been prepared and evaluated for both propylene epoxidation and PO isomerization and combustion. Results have shown there are essentially no differences between the two supports. The non-acidic nature of both supports meant isomerization and combustion of PO was relatively inhibited; thus, $CaCO_3$ offered no advantage over a traditional, low surface area α-Al_2O_3 used for ethylene and butadiene epoxidation. However, the Ag weight loadings for Ag-$CaCO_3$ were 50 – 55 wt%, compared to 12% for the α-Al_2O_3 catalyst, yet contained only 40% more Ag surface sites based on selective chemisorption methods. The difference was due to larger Ag particles as determined by SEM measurements for the ARCO type catalyst and the likelihood of Ag particle occlusion by $CaCO_3$. These catalysts were prepared by ball milling $CaCO_3$ and the Ag metal precursor which would obviously lead to some Ag occlusion by $CaCO_3$.

The ARCO catalysts also required addition of high levels of both ethyl chloride (EtCl) and nitric oxide (NO) to improve PO selectivities from 10% to 50%. While 1-5 ppm EtCl is used for EO processes, 20 – 200 ppmv EtCl was required for higher selectivity. From PO isomerization studies a minimum of 20 ppm EtCl was required to suppress combustion of PO. We found that 50 ppmv EtCl gave an optimum performance with no apparent fouling due to bulk AgCl formation. In fact, post-reaction XRD analysis showed that one of or perhaps the main role of the very high levels of K^+ promoter 2 wt% K (20,000 ppmw) was to suppress formation of AgCl, perhaps by stabilizing and maintaining Cl at the Ag surface by forming K-Cl electrostatic pairs where Cl could be effective and not form bulk AgCl. The unusually high levels of K indicate a role more than simply

non-selective Ag site blocking as claimed by some for the role of Cs (300 – 800 ppmw) in EO catalysts. The role of NO provides a different function in promoting catalyst performance for PO formation. Concentrations of NO as high as 200 ppmv gave increased PO formation rates at constant selectivities for all NO concentrations. Our results combined with oxidation potentials of the NOx manifold indicate that a redox cycle starting from NO adsorbed on Ag sites which is oxidized by dissociatively adsorbed oxygen on an adjacent Ag site to form NO_2 and/or NO_3. Thus, NO is the gateway to the NO_2/NO_3 pair which could function as selective oxidants for reaction of C_3H_6 and O to form PO.

Overall, we have corroborated the results observed by ARCO scientists, but for the first time have offered a detailed investigation of the importance, or lack thereof, of the catalyst support, the need for high levels of the gas phase promoters ethyl chloride and NO, and possibly the unusually high levels of K^+ promoter. We have observed PO selectivities as high as 50%, with indications that we should be able to tune the catalyst composition and reaction conditions to achieve substantially higher selectivities.

CHAPTER 2

MEASUREMENT OF ACTIVE Ag SITE CONCENTRATION OF PROMOTED ETHYLENE OXIDE CATALYST BY H_2 PULSE TITRTATION OVER OXYGEN PRE-COVERED SURFACE[2]

[2]Md Masudur Rahman, Benjamin T. Egelske, John R. Monnier, to be submitted to *Journal of Catalysis*. (First author).

2.1 ABSTRACT

A series of 12 wt% Ag/α-Al_2O_3 catalysts promoted with 350 – 1000 ppmw Cs; 350 ppmw Cs, 250 ppmw Re and fully promoted with 350 ppmw Cs, 250 ppmw Re, x ppmw Mo and y ppmw S were prepared and performed H_2 pulse titration at 170ºC over oxygen pre-covered surface to measure active surface Ag site concentration. *In situ* XRD analysis was performed over an unpromoted 12 wt% Ag/α-Al_2O_3 catalyst at temperatures 280ºC and 170ºC at oxidation environment using a feed stream of Air or 10 vol.% O_2/He and reduction environment using a feed stream of 20 vol.% H_2/He to confirm Ag^0 metallic state or to check the formation of bulk Ag_2O. With the increased amount of promoter loading, active surface Ag site concentration was found to decrease linearly, indifferent to the nature of the promoters. Temperature programmed reduction (TPR) over 3 wt% Cs/α-Al_2O_3, 3 wt% Re/α-Al_2O_3 and 4 wt% Mo/α-Al_2O_3 showed H_2 uptake at > 250ºC confirming promoters reduction at 170ºC might not likely to occur. The thermodynamic calculation also corroborated the experimental findings indicating promoter reduction at 170ºC was unfavorable. The fractional coverage of Cs promoter on active surface Ag sites was calculated from the H_2 uptake value. All these catalyst performances were evaluated by direct epoxidation of ethylene to form ethylene oxide (EO) without adding ethyl chloride (EtCl) to the feed and turnover frequency (TOF) values were calculated.

2.2 INTRODUCTION

In the field of heterogeneous catalysis, Ag catalyst has significant importance in light olefin epoxidation reaction. One of the successful examples is the direct epoxidation of ethylene (C_2H_4) to selectively produce ethylene oxide (EO) (C_2H_4O) [42-44]. Supported Ag catalysts are also successfully used for partial oxidation of methanol (CH_3OH) to produce formaldehyde (HCHO) [45], epoxidation of 1,3 butadiene to produce 3,4 epoxy-1-butene (EpB) [14, 46, 47]. Besides these industrial applications, scientists tried supported Ag catalysts to produce propylene oxide (C_3H_6O) by the direct epoxidation of propylene (C_3H_6) using molecular oxygen (O_2) [48-54]. For EO production the newest generation catalysts contain alkali metals (Li, Cs) and high valent oxyanions (HVOA) of Mo, W, Cr, Ti, Hf, Zr, V, Ta, Nb, S, P and B [55-59] as a promoter package to reach EO selectivity to ~ 92% [60]. The use of this promoter package overcrowded the catalyst surface covering the active surface Ag sites. Therefore, a high temperature is required to achieve the required space-time yield compared to the older generation of EO catalysts. However, high temperature has adverse effects on catalyst life span and selectivity. To combat this problem, catalyst manufacturers are overloading Ag (27 – 33 wt% compare to 12 – 20 wt%) on their EO catalyst [59]. The main goal is to increase active Ag sites and achieve the required space-time yield at a lower reaction temperature. EO catalyst manufacturers use X-ray photoelectron spectroscopy (XPS) to measure the fraction of surface Ag coverage that might not be directly related to catalyst activity. The implication of the correct characterization method is necessary for the efficient use of Ag. In addition, an accurate measurement of turnover frequency (TOF) is needed to compare catalyst performance. The current characterization methods are XRD analysis, SEM/STEM/TEM

imaging, XPS analysis and oxygen chemisorption. These characterization methods failed to accurately measure active surface Ag site concentration. Oxygen chemisorption showed irreproducible results, the main reason might be due to the formation of subsurface oxygen [61]. Particle size calculated by XRD analysis gives inaccurate active surface Ag site concentration due to agglomeration of different sizes of Ag particles that may act as a single active Ag site, and it also disregards the presence of wide size distribution of Ag particles. SEM/STEM/TEM imaging also shows misleading results as the measurement of active surface Ag sites by imaging does not consider the promoter effects.

Vannice [61] developed a method to measure active surface Ag sites by H_2 titration over mono atomically chemisorbed oxygen on Ag surface. Vannice used Ag on η-Al_2O_3, TiO_2, SiO_2 and α-Al_2O_3 support. First, oxygen was mono atomically chemisorbed on the Ag surface at an elevated temperature of 170°C (443 K) as dissociative chemisorption of oxygen was a temperature activated process [62]. Later, the mono atomically chemisorbed oxygen was titrated by molecular H_2 at 170°C to measure the accurate number of surface Ag sites.

$$Ag_s + \frac{1}{2} O_2 \rightarrow Ag_s - O \qquad (2.1)$$

$$Ag_s - O + H_{2\,(g)} \rightarrow Ag_s + H_2O_{(ad)} \qquad (2.2)$$

According to equations 2.1 and 2.2 a stoichiometry ratio of 1:1 for Ag_s:H_2 was used to determine the number of active surface Ag sites. The H_2 titration method doubles the sensitivity compared to the oxygen chemisorption result, hence, providing better accuracy in measuring surface Ag sites [61].

However, Vannice only used unpromoted supported Ag catalysts in his study. The addition of different types of promoters (alkali earth metals or HVOA) might change Ag site concentration due to promoter coverage.

The promoter package used in the supported catalyst for EO production may be oxidized during oxygen chemisorption and may be reduced during H_2 pulse titration. Therefore, it is essential to determine whether the H_2 is reacting only with the monatomic oxygen chemisorbed on Ag sites rather than the oxygen from oxidized promoters. In this manuscript, a detailed study of the Ag/α-Al_2O_3 catalyst promoted with Cs, Re and Mo was performed. Temperature programmed reduction (TPR) study on Cs, Mo, and Re (3 – 4 wt% loading) supported on α-Al_2O_3 was performed to demonstrate the lack of H_2 uptake at 170°C on these materials. H_2 titration was also performed to examine H_2 uptake on Cs, Mo, and Re (3 – 4 wt% loading) supported on α-Al_2O_3 sample. *In situ* XRD analysis on unpromoted Ag/α-Al_2O_3 was performed at 170ºC and 280º temperatures in both oxidation and reduction environments replicating the chemisorption method to confirm the oxidation state of Ag. The theoretical calculation was performed to calculate the thermodynamic probability of the promoter reduction at 170°C. The characterized catalysts were evaluated for ethylene epoxidation reaction to form EO at a given reaction condition to measure turnover frequency (TOF) number.

2.3 EXPERIMENTAL METHODS

2.3.1 Catalyst synthesis

The unpromoted catalyst was prepared using the incipient wetness (5% excess solution) method described by Diao [33]. Silver oxalate ($Ag_2C_2O_4$) was used as an Ag precursor. $Ag_2C_2O_4$ was mixed with a calculated amount of deionized water (DI) and ethylenediamine (EN) solution to give a 3:1 molar ratio of EN to Ag. An ice bath was used for mixing to avoid Ag precipitation in the solution. After dissolving all the $Ag_2C_2O_4$ to the DI water + EN solution α-Al_2O_3 support rings (SA5562, 8 mm rings, BET surface area = 0.73 m^2/g determined by Kr adsorption, pore volume = 0.32 cm^3/g) were added. 20 g α-Al_2O_3 rings were added with calculated impregnation solution in a 50 ml fluted flask and allowed to tumble under vacuum at 60°C. The tumbling stopped when rings started to tumble freely. The impregnated rings were later fast calcined at 260°C for 6 min by flowing 100 L/min air to convert $Ag_2C_2O_4$ to metallic Ag^o. For Cs, Mo, S and Re promoted samples, solutions of $CsNO_3$, $(NH_4)_2MoO_4$, $(NH_4)_2SO_4$ and NH_4ReO_4 precursors, respectively were prepared individually. During DI water and EN mixing step calculated amount of these promoter solutions was added, resulting in Cs only, Cs and Re, and Cs, Re, Mo and S promoted Ag/α-Al_2O_3 catalyst. For different weight loading (3 – 4 wt%) of Cs, Mo and Re only samples, solutions of these individual metal precursors were used to perform incipient wet impregnation with 5% excess solution. Later they were dried and fast calcined in a similar method to the actual Ag/α-Al_2O_3 catalyst to preserve uniformity of sample preparation. After catalyst preparation, the rings were crushed and sieved to 20 – 40 mesh size (850 – 425 μm) to perform characterization by H_2 pulse titration on oxygen pre-covered Ag and ethylene epoxidation reaction. Powdered samples were used for XRD analysis.

2.3.2 *In situ* XRD analysis

A Rigaku SmartLab SE II XRD instrument was used for the XRD analysis, with a CuKα source (tube operational power = 2.2 kW) and equipped with a high speed 1D silicon strip detector (D/teX Ultra 250, Rigaku, Tokyo, JP) and an *in situ* cell (Reactor X, Rigaku, Tokyo, JP). Gas flows into the *in situ* cell was controlled by mass flow controllers (Brooks 5850e, Brooks Instrument, Hatfield, PA, USA). The gases used were He (Airgas, UHP), Air (Airgas, Zero Grade), and H_2 (Airgas, UHP). The sample was loaded into a quartz sample holder (sample indent dimensions: 13 × 20 × 0.4 mm, total volume 0.104 cm^3) and placed in the *in situ* cell. The sample was heated using controlled infrared heating from below the sample stage. The *in situ* chamber was purged with He gas at 100 sccm for 15 min before proceeding with the analysis.

2.3.3 H_2 pulse titration on Oxygen pre-covered Ag

Micromeritics Autochem 2920, equipped with a thermal conductivity detector (TCD) was used to perform H_2 pulse titration on O_2 pre-covered Ag catalyst. 2.0 g of 20 – 40 mesh size sample (850 – 425 μm) were weighted and loaded into an *ex situ* horizontal furnace to calcine the sample for 4 h at 280°C by flowing air. The *ex situ* pretreatment was performed to remove excess EN. Excess EN could partially cover the surface resulting in lower and irreproducible H_2 uptake. Desorbed EN from the sample might also condense in the equipment outlet line and create a line blockage.

After *ex situ* pretreatment, each sample was loaded into the Autochem 2920 instrument sample tube and reduced to 280°C for 2 h by flowing H_2 stream *in situ*. Then purged with inert gas (Ar) and cooled down to 170°C by flowing Ar. A stream of 10 vol.% O_2/He was introduced to the sample for 30 min to perform dissociative adsorption

of O_2 on Ag. Later the sample holder chamber was purged by flowing Ar. A stream of 10 vol.% of H_2/Ar was introduced from the instrument loop at a time interval of 4 min to perform pulse titration at 170°C. H_2O was formed during the titration process. H_2O has the same thermal conductivity (26.1 $mWm^{-1}K^{-1}$ at 400 K [63]) as the carrier gas Ar (22.4 $mWm^{-1}K^{-1}$ at 400 K [64]). As a result, H_2O was transparent to the TCD and only H_2 was detected. The recorded H_2 uptake was later converted into the number of active Ag sites using a stoichiometry ratio of 1:1 for Ag_s:H_2. For each sample, the titration process was repeated 3 times to confirm reproducibility.

2.3.4 Temperature programmed reduction

A Micromeritics Autocehm 2920 equipped with a thermal conductivity detector (TCD) was used to perform the temperature programmed reduction (TPR) experiments. All samples were sieved to 20 – 40 mesh size (850 – 425 μm) and loaded into an *ex situ* horizontal furnace to calcine the sample for 4 h at 280°C by flowing air. Then 2.0 g of sample was weighed and loaded into Autochem sample holder. The sample was then reduced to 280°C by flowing H_2 for 2 h. Later the sample chamber was purged by flowing Ar and cooled down to 170°C. 10 vol.% O_2/He was fed to the sample chamber to perform dissociative adsorption of O_2. After the sample was cooled down to 50°C by flowing Ar. A stream of 10% H_2/Ar was introduced to the sample chamber and TCD was started to record H_2 signal after achieving a stable baseline the sample temperature was increased to 500°C at a 10°C/min ramp rate and consumption of H_2 was monitored.

2.3.5 Catalyst performance evaluation

Six continuous flow, fixed bed systems with a 316 stainless steel reactor of 0.19 in. ID, 0.25 in. OD was used to evaluate catalyst performance. 6 parallel reactors were

connected through a common feed system and analyzed by a common GC for better accuracy. A feed stream of 25 vol.% C_2H_4, 8 vol.% O_2 balance CH_4 was used for catalyst evaluation. The temperature varied between 190°C to 210°C, and pressure was kept constant at 250 psig. Flow rates varied between 75 to 150 standard cm^3 per min (SCCM). This was considered standard reaction conditions unless otherwise stated in the results. The sample mass of 2.0 g sieved to 20 – 40 mesh size (850 – 425 μm) was loaded into the reactor for catalytic performance evaluation. Evaluation times were typically 50 – 200 h online. In all cases, catalysts were pretreated in a stream of 12% vol. O_2/CH_4 at 1 atm pressure, 260°C temperature for 12 to 18 h. The outlet stream from the reactor was analyzed in line with an HP 7890 Series II gas chromatograph containing two Poraplot Q columns equipped with a thermal conductivity detector (TCD) and flame ionization detector (FID). TCD was used for quantitative analysis of O_2, CO_2, and H_2O. If present, the FID was used to analyze C_2H_4, ethylene oxide (EO), and acetaldehyde.

2.4 RESULTS AND DISCUSSION

2.4.1 *In situ* XRD analysis

To accurately measure surface Ag site concentration from experimentally measured H_2 uptake values, Ag needed to be in Ag^0 state rather than $Ag^{\delta+}$ state. At the time of

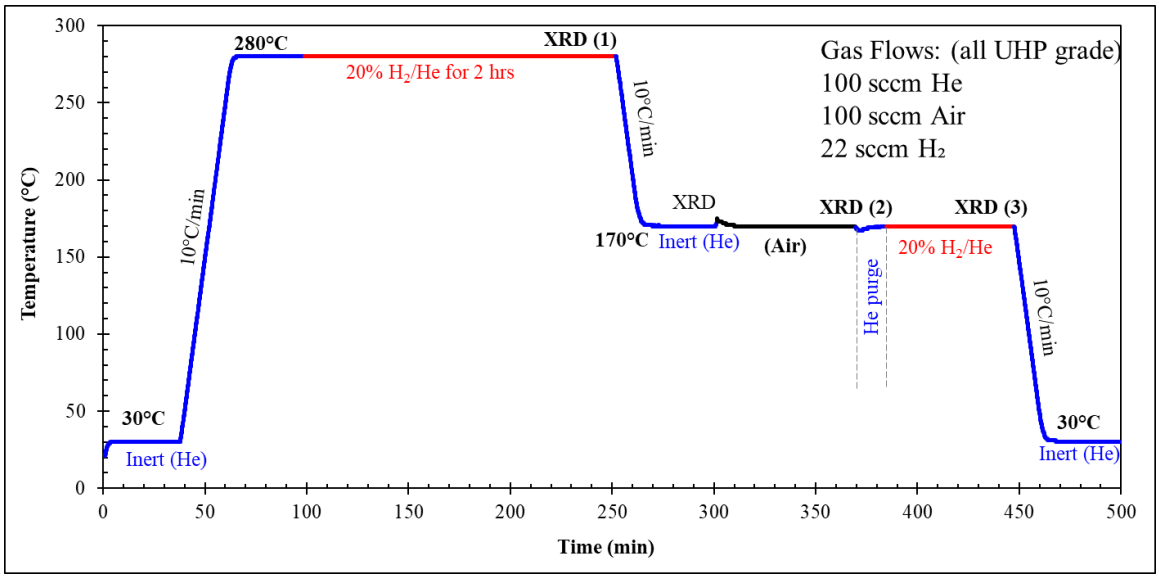

Figure 2.1: Temperature profile for in situ XRD analysis with ramp rate and gas feed stream.

pretreatment at 280°C to remove excess ethylene diamine (EN) and H_2 pulse titration, the supported Ag catalyst encountered Air and 10 vol.% O_2/He, respectively. If Ag changed to $Ag^{\delta+}$ state, the stoichiometry ratio of 1:1 for Ag_s:H_2 should not be accurate for calculating surface Ag site concentration. Figure 2.1 showed the temperature profile and different gas feeds where *in situ* XRD analysis was performed. XRD (1) analysis was performed after treating the sample at 280°C in Air for 1 h and consequently reducing it to 280°C for 2 h by flowing 20 vol.% H_2/He. XRD (2) was taken after cooling down to 170°C in an inert He stream and introducing Air to the feed stream for 30 min to imitate the dissociative O_2 adsorption step at the time of the actual pulse chemisorption experiment. XRD (3) was performed again after reduction imitating the H_2 pulse titration step. All three XRD

analysis results were summarized in Figure 2.2. The results show no evidence of the formation of bulk Ag_2O. Only peaks of metallic Ag (111), Ag (200), Ag (220) and Ag (311) at 2θ values of 38.12º, 44.30º, 64.44º and 77.40º were observed, respectively (PDF# 03-065-2871). The XRD analysis confirmed the presence of metallic Ag^0 state and discarded the formation of bulk Ag_2O.

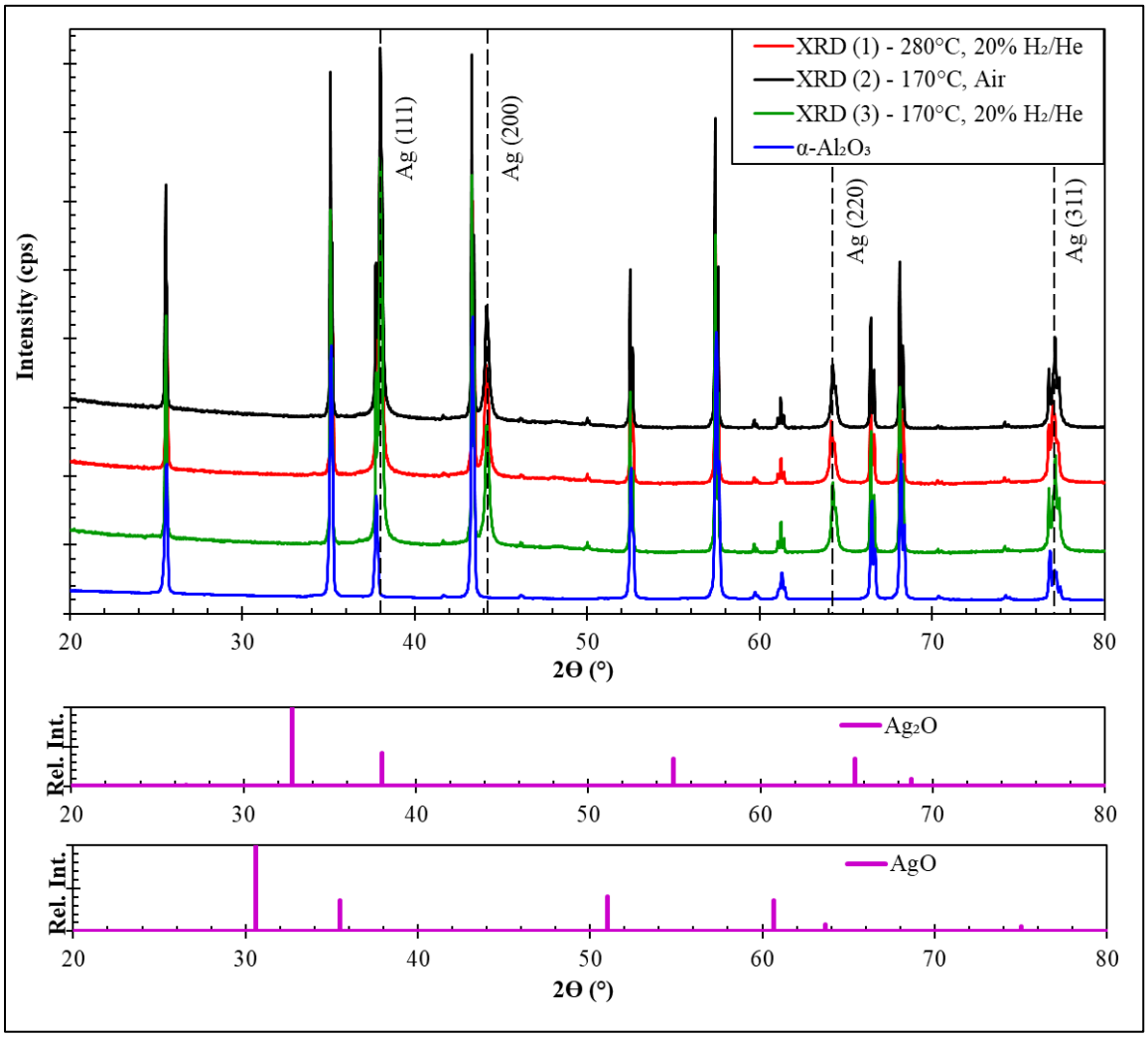

Figure 2.2: In situ XRD analysis of a 12 wt% Ag/α-Al_2O_3 sample. Ag (111), Ag (200), Ag (220) and Ag (311) at 2θ value of 38.12°, 44.30°, 64.44°, 77.40° were shown respectively.

2.4.2 H_2 pulse titration over oxygen pre-covered unpromoted and promote Ag catalyst

H_2 pulse titration over oxygen pre-covered 12 wt% Ag/α-Al_2O_3 sample was performed three times from a single batch and repeated three times for each sample to check reproducibility in total of 9 times. The results were summarized in Table 2.1. The result showed only a trivial variation in H_2 uptake value of ± 0.004 cm^3/g catalyst STP over 9 pulse titration experiments. The result confirmed the reproducibility of the experimental data with a trivial error bar.

Table 2.1: Chemisorption summary of a 12 wt% Ag/α-Al_2O_3 sample.

Sample	H_2 uptake, cm^3/g cat STP	Active Ag site concentration/g cat
12 wt% Ag/α-Al_2O_3	0.086 ± 0.004	$2.3 \pm 0.11 \times 10^{18}$

A typical H_2 pulse titration over oxygen pre-covered 12 wt% Ag/α-Al_2O_3 sample was shown in Figure 2.3. H_2 pulses were introduced after 4 min intervals. In the first 5 H_2 pulses, almost all the H_2 reacted with adsorbed O (atomic O_2) on Ag. Then, gradually, the H_2 pulse signal started to increase. Finally, the titration process stopped after no further H_2 uptake was recorded.

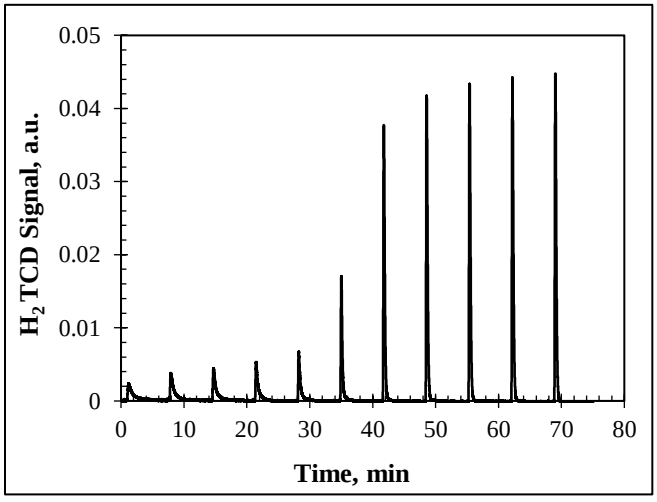

Figure 2.3: A typical H_2 pulse titration on O pre-covered surface Ag over an unpromoted 12 wt% Ag/α-Al_2O_3 sample.

Cs, Re, and Mo promoters were considered to study the promoter effects as they were used in the newest generation of ethylene epoxidation reaction along with Li, S, W [58, 59]. A series of Cs only promoted (350 to 1000 ppmw) on 12 wt% Ag/α-Al_2O_3 sample were made and performed H_2 pulse titration over oxygen pre-covered surface. Vannice argued during the rapid titration process that H_2 did not react with subsurface O_2, only atomic oxygen adsorbed on the surface Ag sits participated in the reaction with the H_2 [61]. The results were summarized in Table 2.2.

Table 2.2: H_2 pulse titration summary of Cs promoted 12 wt% Ag/α-Al_2O_3 samples.

Cs loading on 12 wt% Ag/α-Al_2O_3, ppmw	**H_2 uptake, cm^3/g cat STP**	**Active Ag sites concentration/ g cat, × 10^{18}**	**Theoretical Cs coverage, $\theta_{Cs(theoretical)}$**	**Experimental Cs coverage calculated from chemisorption, $\theta_{Cs(expt'l)}$**	**Calculated system coverage, $\theta_{Cs(system)}$**
0	0.086	2.3	x	x	x
350	0.074	2.0	0.69	0.14	0.17
800	0.054	1.5	1.57	0.32	0.40
1000	0.049	1.3	1.97	0.40	0.50

$\theta_{Cs(theoretical)}$, $\theta_{Cs(expt'l)}$, and $\theta_{Cs(system)}$ values were calculated using Eqn 2.3, 2.4, and 2.5, respectively.

$$\boldsymbol{\theta_{theoretical} = \frac{\#Cs\ atoms\ added}{\#\ Ag\ surface\ sites\ from\ chemisorption}} \quad (2.3)$$

$$\boldsymbol{\theta_{expt'l} = 1 - \frac{(\#\ sites\ of\ promoted\ catalyst)}{\#_{Ag\ surf\ sites\ \ from\ chemisorption}}} \quad (2.4)$$

$$\boldsymbol{\theta_{system} = \frac{\#Cs\ atoms\ added}{\#\ surface\ sites\ of\ Ag + \#sites\ of\ support}} \quad (2.5)$$

Here, # Cs atoms added represented the number of Cs atoms present calculated from nominal Cs loading on 12 wt% Ag/α-Al_2O_3 sample.

surface sites of Ag represented the number of Ag sites calculated from the chemisorption of an unpromoted 12 wt% Ag/α-Al_2O_3 sample.

sites of support represented the number of sites of the α-Al_2O_3 support calculated from BET surface area measurement using Kr as an adsorbent.

J.R. Anderson [65] reported 1 m^2/g surface area of a sample contained $1.24 \times 10^{19}/g$ surface sites and was irrelevant to the nature of the sites. From that value, the total number of surface sites for α-Al_2O_3 support (BET surface area = 0.73 m^2/g) was calculated $9.1 \times 10^{18}/g$.

Table 2.2 showed that from the chemisorption value, it was possible to calculate the fractional coverage of Cs promoter on active Ag sites and on the support. With increased loading of Cs, the Ag site concentration decreased linearly. Vannice also reported similar findings. Vannice *et al.* performed static oxygen chemisorption on 12 wt% Ag/α-Al_2O_3 promoted with 400 ppmw and 1200 ppmw Cs equivalent to 3.0 μmol and 9.0 μmol of Cs and reported oxygen uptake of 3.5 μmol and 2.7 μmol O_2/g cat, respectively [66]. However, the authors argued that this difference in uptake was insignificant as the unpromoted sample gave lower O_2 uptake of 3.0 μmol O_2/g cat. In this study, H_2 pulse titration was used instead of O_2 chemisorption therefore, the sensitivity was doubled. On a 1000 ppmw Cs loading (7.52 μmol of Cs) on 12 wt% Ag/α-Al_2O_3 catalyst showed 43% of the active Ag sites were lost due to Cs covering. The result indicated Cs was well dispersed on the Ag surface. A linear relationship was found when H_2 uptake vs Cs loading values was plotted. The 12 wt% Ag/α-Al_2O_3 catalyst promoted with Cs, Re, Cs and Re both, also showed similar behavior. With the increased μmole of promoter loading,

the H_2 uptake dropped linearly, indicating the effect was indifferent to the nature of the promoters. Details were shown in Figure 2.4

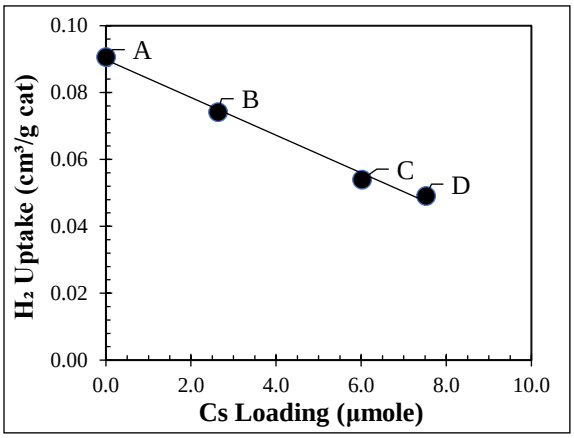

(A)

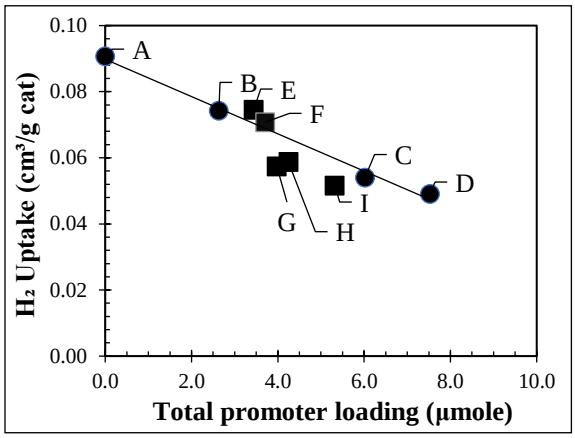

(B)

Sample	Promoter loading, µmole			H_2 uptake, µmole/g cat STP	Ag site concentration/g cat.
	Cs	Re	Total		
A	-	-	-	3.84	2.31×10^{18}
B	2.63	-	2.63	3.30	2.00×10^{18}
C	6.02	-	6.02	2.41	1.45×10^{18}
D	7.52	-	7.52	2.19	1.32×10^{18}
E	2.63	0.81	3.44	3.33	2.00×10^{18}
F	2.63	1.07	3.7	3.17	1.91×10^{18}
G	2.63	1.34	3.97	2.54	1.53×10^{18}
H	2.63	1.61	4.24	2.63	1.59×10^{18}
I	2.63	2.69	5.32	2.32	1.40×10^{18}

(C)

Figure 2.4: (A) H_2 uptake vs. Cs loading plot, (B) H_2 uptake vs total promoter loading plot, (C) Loading of different promoters with surface active Ag site concentration on 12 wt% Ag/α-Al_2O_3 catalyst shown in plot (A) and (B). [1]

2.4.3 Temperature programmed reduction (TPR) study

In H_2 pulse titration, a feed stream of 10 vol.% O_2/He was introduced to the sample chamber to perform dissociative adsorption of O_2 on Ag at 170°C. During the process, oxidation of promoters might occur i.e. Cs_2O, Re_2O_7/ReO_3, MoO_2/MoO_3. During H_2 titration reduction, these promoters might significantly increase H_2 uptake upon reduction leading to inaccurate measurement of the active Ag site concentration. TPR study was performed to examine the reduction of these promoters. 3 wt% Cs, 3 wt% Re and 4 wt% Mo on α-Al_2O_3 were made and performed TPR. The results were shown in Figure 2.5.

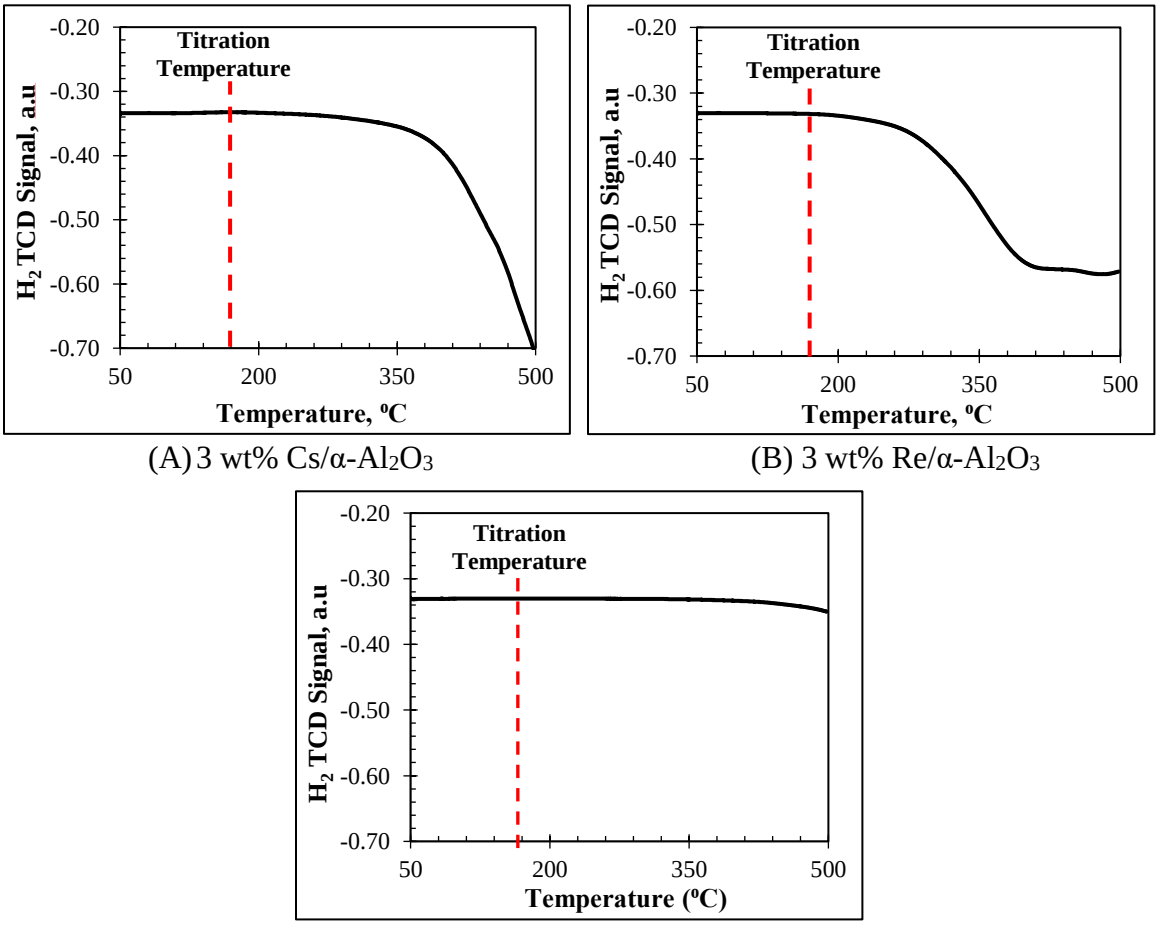

(A) 3 wt% Cs/α-Al_2O_3 (B) 3 wt% Re/α-Al_2O_3

(C) 4 wt% Mo/α-Al_2O_3

Figure 2.5: Plot (A), (B) and (C) show temperature programmed reduction of 3 wt% Cs/ α-Al_2O_3, 3 wt% Re/α-Al_2O_3 and 4 wt% Mo/α-Al_2O_3 sample respectively. [1]

Figure 2.5 showed at very high loading (3 – 4 wt%) of Cs, Re and Mo on α-Al_2O_3 support H_2 consumption started at > 250°C. H_2 pulse titration was performed at 170°C. The results confirmed that promoters at 30000 to 40000 ppmw loading do not show H_2 consumption at 170°C. Therefore, it might be concluded that these promoters should not be reduced during H_2 pulse titration at 170°C. Actual H_2 pulse titration with the same procedure was performed on these samples to corroborate the previous statement. The results were shown in Figure 2.6.

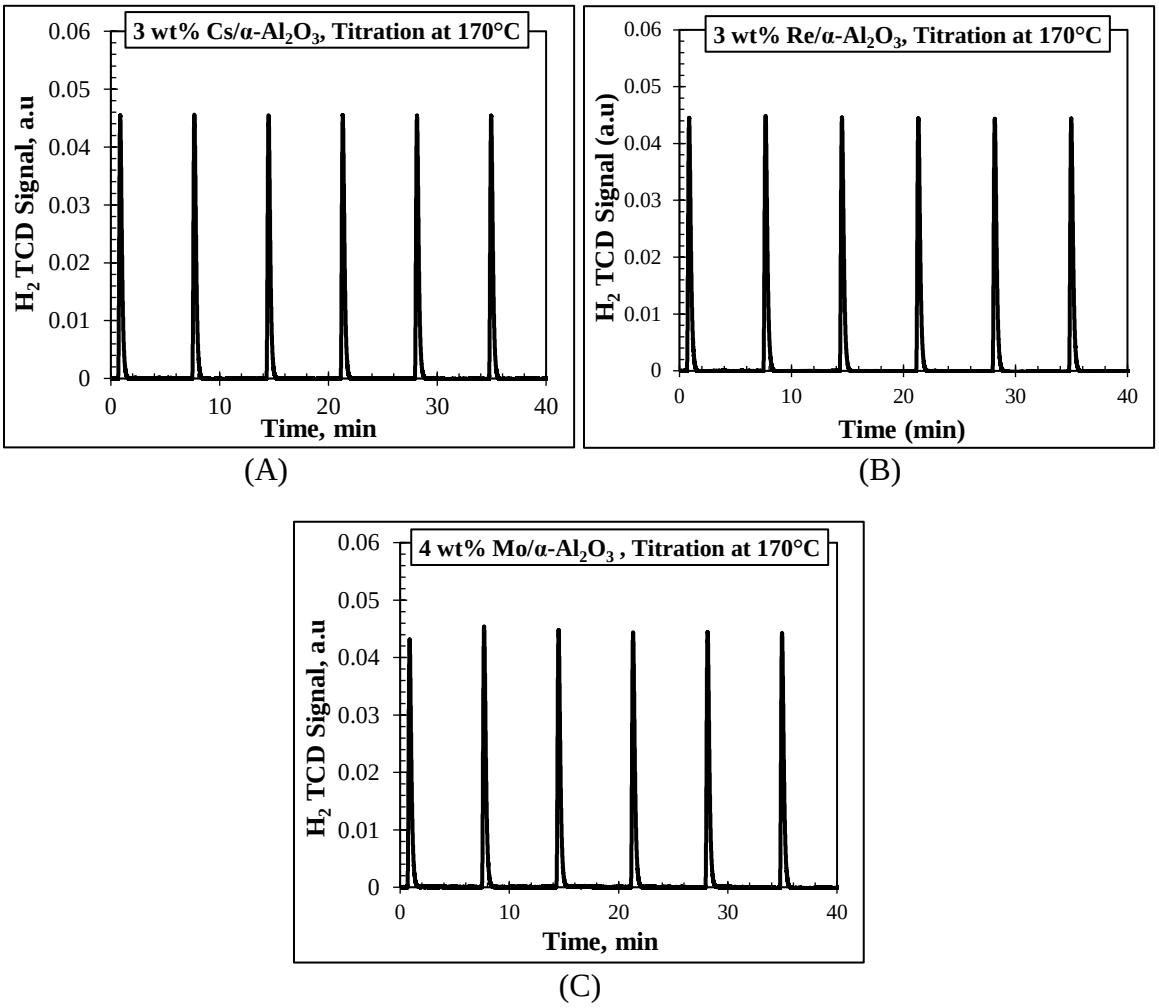

Figure 2.6: Plote (A), (B) and (C) show H_2 pulse titration of 3 wt% Cs/α-Al_2O_3, 3 wt% Re/α-Al_2O_3 and 4 wt% Mo/α-Al_2O_3 sample respectively [1].

Figure 2.6 showed that 3 wt% Cs/α-Al_2O_3, 3 wt% Re/α-Al_2O_3 and 4 wt% Mo/α-Al_2O_3 samples did not show any H_2 uptake during H_2 pulse titration at 170°C. These results were in agreement with the previous TPR results. Therefore, for further examination of promoter reduction at 170°C computational study was performed using density function theory (DFT), purbaix diagram and free energy.

Table 2.3: Calculated ΔG_f value to measure the spontaneity of Ag and promoter reduction.

Reaction	Method	Phase	Temp, (ºC)	pH	V_{cell}, V	ΔG_f, kJ/mole	Ref
$Ag_2O + ½ H_2 + e^- \rightarrow 2Ag^o + OH^-$	P	L	25	13	1.24	-120	[67]
$Ag_2O \rightarrow 2Ag^o + ½ O_2$	FE	S	170		n/a	-3	[68]
$Ag_2O + H_2 \rightarrow 2Ag^o + H_2O$	DFT	S	170			-224	[69]
$CsOH + 1/2H_2 \rightarrow Cs^o + H_2O$	EC	L	25	7	- 3.22	+ 311	[70]
$CsOH + 1/2H_2 \rightarrow Cs^o + H_2O$	DFT	S	170			+171	[69]
$Cs_2O + H_2 \rightarrow 2Cs^o + H_2O$	DFT	S	170			+23	[69]
$ReO_4^- + H_2 \rightarrow ReO_3 + H_2O$	P	L	25	0	+0.30	-58	[71]
			25	1	+0.24	-46	
			25	2.5	-0.08 (est)	+15	
$MoO_4^{2-} + H_2 + 2OH^- \rightarrow MoO_2 + 4OH^-$	P	L	25	10	+0.15	-28	[72]

*** P: Porbaix, FE: Free Energy, EC: Electro Chemistry, DFT: Density Function Theory
** L: Liquid, S: Solid

Table 2.3 summarized the reduction probability of Ag and other promoters by calculating ΔG_f value. Negative (-) ΔG_f values represent the reaction should occur spontaneously and thermodynamically favorable and positive value (+) ΔG_f indicated the reaction was thermodynamically unfavorable or nonspontaneous. A high negative ΔG_f value indicated the reduction of Ag_2O to Ag^o was thermodynamically favorable and very likely to occur both at 25ºC and 170ºC temperature. Reduction of $Cs^{\delta+}$ showed a positive (+) ΔG_f value indicating the reduction of $Cs^{\delta+}$ to Cs^o was thermodynamically unfavorable and should not like to occur at titration temperature (170ºC). ΔG_f value calculated for Re and Mo promoter reduction also showed positive value implying thermodynamically the

reduction was unfavorable. These calculated results corroborated the previous experimental findings. The experimental and theoretical calculations both confirmed that at titration temperature 170ºC the promoters should not reduce. Therefore, the H_2 uptake value measured during pulse H_2 titration only came from titration of adsorbed O on surface Ag sites.

2.4.4 Catalyst Evaluation

A 12 wt% Ag/α-Al_2O_3, 350 ppmw Cs promoted 12 wt% Ag/α-Al_2O_3, 350 ppmw Cs and 250 ppmw Re promoted 12 wt% Ag/α-Al_2O_3 and 350 ppmw Cs, 250 ppmw Re, x ppmw Mo and y ppmw S promoted (Fully promoted) 12 wt% Ag/α-Al_2O_3 sample were evaluated to measure catalytic performance by direct epoxidation of ethylene to form ethylene oxide (EO) using a standard feed at 190ºC to 210ºC temperature at 250 psig pressure using 50 – 150 sccm total flow rate. The reaction was started at 190ºC and temperature was increased in a 10ºC increment to reach 210ºC. The EO selectivity ranged from 62 to 72%. Ethyl chloride (EtCl) was not added to the feed stream to avoid its effects on active surface Ag sites. In the beginning, all reactor flow rate was maintained at 75 sccm. At 200ºC the unpromoted 12 wt% Ag/α-Al_2O_3 showed high activity (C_2H_4 conversion 9.4%). To lower the activity of the unpromoted 12 wt% Ag/α-Al_2O_3 catalyst and match with the promoted 12 wt% Ag/α-Al_2O_3 catalysts flow rates were adjusted as shown in Figure 2.7 (D). The reaction results were summarized in Figure 2.7. As expected, the unpromoted 12 wt% Ag/α-Al_2O_3 catalyst showed maximum activity and lowest selectivity among the four catalysts tested. The Fully promoted 12 wt% Ag/α-Al_2O_3 catalysts with 350 ppmw Cs, 250 ppmw Re, x ppmw Mo and y ppmw S showed the lowest activity and highest selectivity.

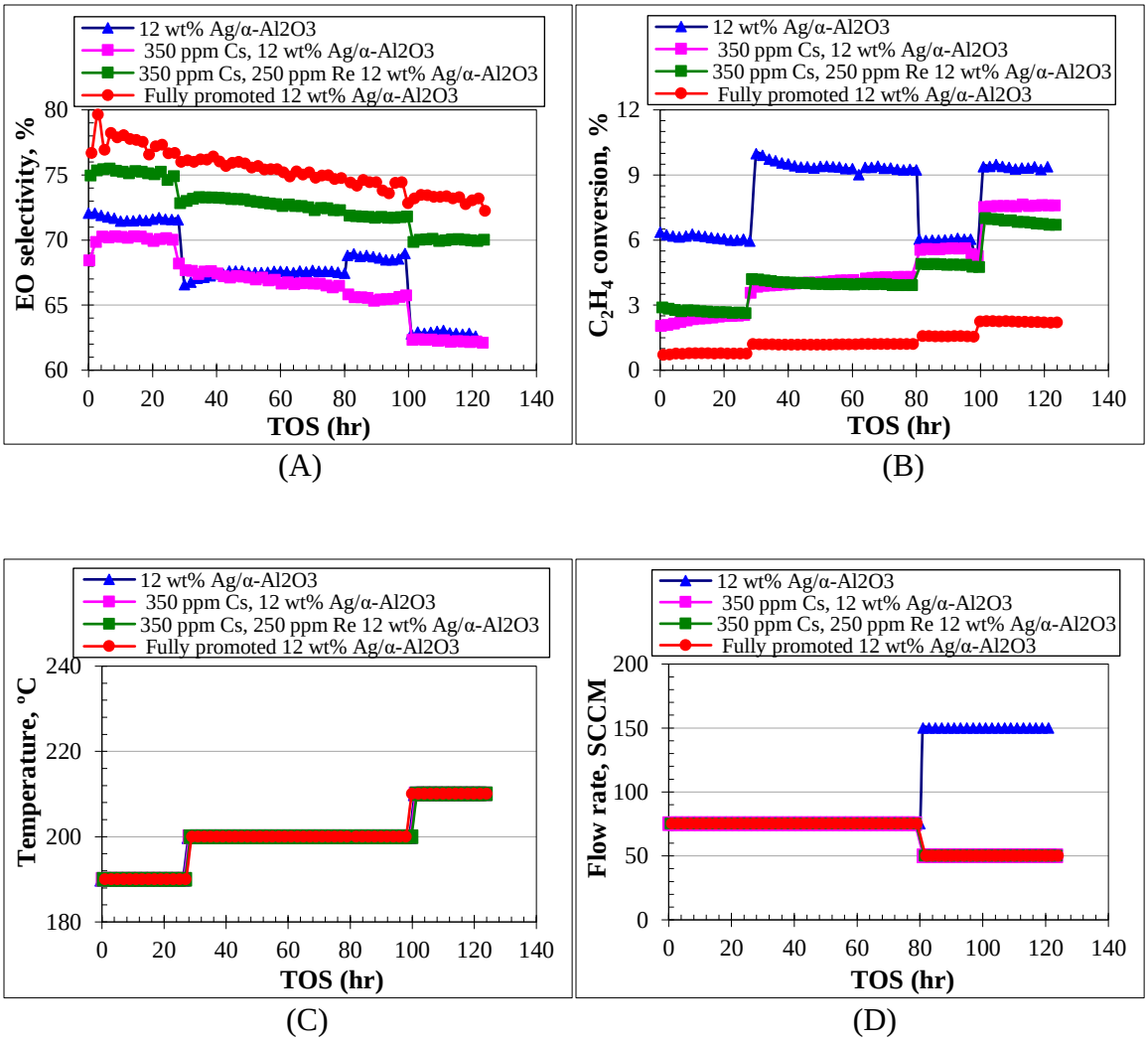

Figure 2.7: (A) EO selectivity vs time on stream (TOS); (B) C_2H_4 conversion vs TOS; (C) Temperature vs TOS; (D) Flow rate vs TOS plot for 12 wt% Ag/α-Al_2O_3, 350 ppmw Cs 12 wt% Ag/α-Al_2O_3, 350 ppmw Cs 250 ppmw Re 12 wt% Ag/α-Al_2O_3, 350 ppmw Cs 250 ppmw Re x ppmw Mo y ppmw S 12 wt% Ag/α-Al_2O_3 catalyst. Feed: 25 vol.% C_2H_4, 8 vol.% O_2 balance CH_4, Pressure: 250 psig.

Turnover frequency (TOF) was calculated for each of the four catalysts from chemisorption and reaction data. The results were summarized in Table 2.4. The reported TOF values were calculated at 210ºC temperature, constant reaction feed gas composition and pressure for all four catalysts at differential conversion. The unpromoted 12 wt% Ag/α-Al_2O_3 showed a higher TOF value for both C_2H_4 conversion and EO formation compared to the promoted 12 wt% Ag/α-Al_2O_3 catalysts. It might be due to promoter redistribution under

reaction conditions. Monnier [73] showed that Cs promoter was mobile on 12 wt% Ag/α-Al_2O_3 catalysts in his butadiene epoxidation study. Therefore, during pretreatment and at reaction conditions the promoters became well dispersed covering more active surface Ag sites.

Table 2.4: Catalyst performance results and calculated TOF values.

Catalyst	**Ag site conc/g cat.**	**Flow rate, sccm**	**C_2H_4 conv, %**	**Select to EO, %**	**TOF, (C_2H_4 conv) s^{-1}**	**TOF, (EO formed) s^{-1}**
12 wt% Ag/α-Al_2O_3	2.42×10^{18}	150	9.3	62.7	0.65	0.41
12 wt% Ag, 350 ppmw Cs/α-Al_2O_3	2.01×10^{18}	50	7.6	62.3	0.21	0.13
12 wt% Ag, 350 ppmw Cs, 250 ppmw Re/α-Al_2O_3	1.54×10^{18}	50	6.7	70.1	0.25	0.17
12 wt% Ag, 350 ppmw Cs, 250 ppmw Re, x ppmw Mo, y ppmw S/α-Al_2O_3	9.67×10^{17}	50	2.2	74.2	0.13	0.09

The fully promoted catalyst with Cs, Re, Mo and S on 12 wt% Ag/α-Al_2O_3 showed the highest selectivity and lowest activity (C_2H_4 conversion) and the unpromoted 12 wt% Ag/α-Al_2O_3 showed the lowest selectivity and highest activity among the four catalysts. The catalyst performance results for direct epoxidation of ethylene to ethylene oxide showed in agreement with the measured active surface Ag site concentration by H_2 pulse titration on oxygen pre-covered surface (chemisorption). The unpromoted 12 wt% Ag/α-Al_2O_3 catalyst has the highest active site concentration and showed the highest activity and the fully promoted 12 wt% Ag/α-Al_2O_3 has the lowest active Ag site concentration and showed the lowest activity.

2.5 CONCLUSION

A series of unpromoted 12 wt% Ag/α-Al_2O_3 and Cs, Re promoted (250 – 1000 ppmw) on 12 wt% Ag/α-Al_2O_3 were prepared and performed H_2 pulse titration on oxygen pre-covered surface (chemisorption). *In situ* XRD analysis was performed at 280°C and 170°C temperatures under oxidizing and reducing environment on 12 wt% Ag/α-Al_2O_3 to examine bulk Ag_2O formation. The *in situ* XRD analysis result showed absence of bulk Ag_2O formation. H_2 pulse titration on oxygen pre-covered surface was performed 9 times on the same batch of 12 wt% Ag/α-Al_2O_3 sample to examine experimental reproducibility. The H_2 uptake amount varied only $\pm$ 0.004 cm^3/g cat STP over the 9 pulse H_2 titration. The small deviation in H_2 uptake confirmed the reproducibility of the experimental results. For 350 – 1000 ppmw Cs promoted on 12 wt% Ag/α-Al_2O_3 catalyst, active site concentration was measured by chemisorption. From the H_2 uptake value, fractional coverage of Cs on active surface Ag sites and α-Al_2O_3 support was calculated. It was found that increased μmole of Cs loading, decreased active surface Ag site concentration linearly. It was also found regardless of the nature of the promoters, with increased μmole loading of promoters, the number of active surface Ag site concentration decreased linearly.

To check the reducibility of Cs, Re and Mo at titration temperature (170°C), temperature programmed reduction (TPR) on very high loading of promoters on α-Al_2O_3 support was performed. 3 wt% Cs/α-Al_2O_3, 3 wt% Re/α-Al_2O_3 and 4 wt% Mo/α-Al_2O_3 were made and performed TPR. Thermodynamic calculations were performed to corroborate experimental results. TPR experiments showed H_2 consumption started at > 250°C temperature. Thermodynamical calculation showed a positive (+) ΔG_f value on the reduction of Cs, Re and Mo at 170°C temperature. Therefore, both experimental results

and calculated thermodynamic value showed Cs, Re and Mo were not reducible at titration temperature. H_2 pulse titration on oxygen pre-covered surface of 3 wt% Cs/α-Al_2O_3, 3 wt% Re/α-Al_2O_3 and 4 wt% Mo/α-Al_2O_3 samples showed lack of H_2 uptake. The absence of H_2 uptake also corroborated the earlier TPR results and thermodynamic calculation that Cs, Re and Mo promoters were not reducible at 170°C.

The unpromoted 12 wt% Ag/α-Al_2O_3, 350 ppmw Cs promoted 12 wt% Ag/α-Al_2O_3, 350 ppmw Cs, 250 ppmw Re promoted 12 wt% Ag/α-Al_2O_3 and fully promoted with Cs, Re, Mo and S on 12 wt% Ag/α-Al_2O_3 catalysts performance were evaluated by direct epoxidation of ethylene to EO reaction. TOF values were calculated for C_2H_4 conversion and EO formation from reaction evaluation data and active surface Ag site concentration values measured by H_2 pulse titration on oxygen pre-covered surface for all four catalysts. The unpromoted 12 wt% Ag/α-Al_2O_3 catalyst containing the most active surface Ag site concentration showed the most activity in terms of C_2H_4 conversion. The fully promoted catalyst which has the least active surface Ag site concentration showed the least activity.

Overall, an accurate method has been developed to measure active surface Ag site concentration on promoted Ag supported catalyst for ethylene epoxidation reaction to produce ethylene oxide by H_2 pulse titration on oxygen pre-covered surface. This method has better accuracy compared to the current characterization methods available. Utilizing this method, it should be possible for EO catalyst manufacturers to predict catalyst activity without performing catalytical performance evaluation.

CHAPTER 3

AN INVESTIGATION OF 4 wt% Mo PROMOTED 20 wt% Ag/ZrO_2 CATALYST FOR SELECTIVE FORMATION OF PROPYLENE OXIDE BY DIRECT EPOXIDATION OF C_3H_6

3.1 ABSTRACT

Direct epoxidation of propylene with molecular O_2 to produce propylene oxide (PO) was investigated over 4 wt% Mo promoted 20 wt% Ag/ZrO_2 catalyst. Active surface Ag site concentration of the unpromoted and promoted catalysts was measured by H_2 pulse titration on oxygen pre-covered surface. The catalysts were characterized by ICP AES, N_2 physisorption, XRD analysis, SEM imaging with energy dispersed X-ray spectroscopy (EDXS). A feed stream of 17.0 vol.% C_3H_6, 9.0 vol.% O_2 and balance He was fed with a total flow rate of 60 standard cm^3/min (SCCM) over a 0.3 g, 20 wt% Ag – 4 wt% Mo/ZrO_2 catalyst at 1 atm pressure, 460°C temperature and 55.3% selectivity to acrolein at 8.5% conversion of C_3H_6 was found. Selective formation of acrolein as partial oxidation of propylene was found instead of PO as claimed in the literature. The PO stability experiment showed all the PO converted into CO_2/H_2O, propionaldehyde (EtCHO), acrolein, acetaldehyde (CH_3COH) and acetone even at 360°C temperature when a stream of 5.0 vol.% PO and 10.0 vol.% O_2 balance He was fed over a 20 wt% Ag – 4 wt% Mo/ZrO_2 catalyst. A 4 wt% Mo/ZrO_2 catalyst also showed formation of acrolein at 8.0% conversion of C_3H_6 without the presence of Ag. Fast deactivation over 15 h time on stream due to coke formation was noticed over the 4 wt% Mo/ZrO_2 catalyst during catalyst evaluation.

3.2 INTRODUCTION

Direct epoxidation of propylene to produce propylene oxide (PO) using molecular oxygen has been one of the most desired and challenging chemical reactions in the field of heterogeneous catalysis. Ag catalyst supported on α-Al_2O_3 has successfully been used for the epoxidation of ethylene to produce ethylene oxide (EO) with molecular oxygen [59, 74-76]. However, unlike ethylene, the presence of an allylic C – H bond in propylene made the selective formation of PO significantly more difficult. The allylic C – H bond dissociation energy present in propylene (77 kcal/mol) is lower than the vinylic C – H bond (112 kcal/mol) present in ethylene [77]. Therefore, the abstraction of the hydrogen from the allylic C – H bond by adsorbed oxygen on an active Ag site is preferable, leading to the complete oxidation of propylene. In the late 90's scientists at ARCO reported promising results on direct epoxidation of propylene using high Ag loading (50 – 56%) supported on $CaCO_3$ using molecular oxygen. ARCO claimed to achieve 58 – 64% selectivity to PO at propylene conversion of 1.5 – 3.2 % [48, 50-54, 78] over a 2.0 wt% K^+ promoted and either Mo, Re, or W co-promoted 50 – 56 wt% Ag/$CaCO_3$ catalyst. 50 – 200 ppmv EtCl and NO each along with 10.0 – 25.0 vol.% CO_2 was necessary at the feed stream to achieve the claimed selectivity reported by ARCO. In ARCO patents temperature ranging from 232°C to 260°C was reported for propylene epoxidation in a total pressure of 14 to 30 psig [52, 78]. Ag supported on ZrO_2 promoted/modified with Mo and W has been reported to achieve high selectivity to PO 53% to 67% at moderated 2.0% to 12.0% conversion of propylene at a significantly high (400°C – 460°C) temperature [79-85] compared to the temperature stated by ARCO for propylene epoxidation [49, 50, 86]. For ethylene epoxidation to ethylene oxide and 1,3 butadiene epoxidation to 3,4-epoxy-1-butene (EpB)

reported reaction temperature was 200ºC – 270ºC [14, 58, 59, 76, 87]. Therefore, these results for propylene epoxidation to propylene oxide (PO) using Mo and W promoted 20 wt% Ag/ZrO_2 catalyst at high temperature (400 – 460°C) needs to be confirmed with further investigation.

In this study unpromoted 20 wt% Ag/ZrO_2, 20 wt% Ag – 4 wt% Mo/ZrO_2, and 4 wt% Mo/ZrO_2 catalysts were prepared and evaluated for propylene epoxidation reaction using molecular oxygen. The catalysts were characterized by ICP-AES, N_2 physisorption, H_2 pulse titration over oxygen pre-covered surface, XRD analysis and SEM imaging with EDXS analysis. PO isomerization was studied over α-Al_2O_3, $CaCO_3$, and ZrO_2 support to examine PO stability from 220°C to 300°C temperature range. PO was added to the feed stream along with 10 vol.% O_2 balance He at 360ºC over 20 wt% Ag – 4 wt% Mo/ZrO_2 catalyst to study the extent PO conversion.

3.3 EXPERIMENTAL METHOD

3.3.1 Catalyst preparation

20 wt% Ag/ZrO_2 and 20 wt% Ag – 4 wt% Mo/ZrO_2 catalysts were prepared by the slurry method [84, 88]. 1.2 ml of ethylene diamine ($C_2H_8N_2$, Millipore – Sigma >99%) was added to 6.0 ml distilled water in an ice bath and stirred well. 1.83 g of $Ag_2C_2O_4$ was added slowly to dissolve completely to obtain a clear solution. For 4 wt% Mo loading, 0.53 g of ammonium molybdate($(NH_4)MoO_4$, Fisher Scientific >99.99%) was added to the solution. After dissolving all the components, 5.0 g of zirconium oxide (ZrO_2, Millipore Sigma, >99%) was slowly added to the solution to form a slurry. The slurry was then dried in a vacuum chamber at 70°C for 4 h to make it nearly waterless. The solid was then dried at 120°C in a convection oven for 1 day. The resultant solid was then ground and calcined at

460℃ for 3 h to obtain the catalyst. To prepare the 4 wt% Mo/ZrO_2 catalyst all the steps followed mentioned previously except the addition of $Ag_2C_2O_4$. The gases utilized in the reaction were propylene (99.5% purity, Airgas), molecular oxygen (O_2, 99.993% purity, Praxair), Helium (He, 99.999% purity, Praxair).

3.3.2 Catalyst characterization

The metal content of the catalysts was determined by ICP-AES (PerkinElmer, AAnalyst 400) analysis. Scanning electron microscopy (SEM) was performed using a Zeiss Gemini 500 SEM. For EDS analysis, electrons were collected using a secondary electron detector; the incident electron beam energy was set to 5.0 keV. Crystalline structures were examined by X-ray diffraction (XRD) using a Rigaku Miniflex-II system equipped with a scintillation counter detector. XRD patterns were recorded from 20 – 80° 2θ using a Cu-Kα radiation source (λ = 1.5406 Å) operated at 30 mA and 15 kV. Chemisorption measurement was conducted using a Micromeritics Autochem II 2920 automated chemisorption analyzer and active surface Ag site concentration for unpromoted and promoted 20 wt% Ag/ZrO_2 samples was determined by H_2 pulse titration of oxygen pre-covered surface using the method developed by Vannice [27]; A $Ag:H_2$ = 1:1 stoichiometry was used to determine the number of active surface Ag site concentration since the pulsed H_2 reacted with Ag – O to form H_2O and a vacant Ag site; silver did not undergo dissociative chemisorption of H_2 at 170℃. Sample pretreatment for chemisorption was conducted by reduction at 280℃ for 2 h flowing H_2 and then cooling to 170℃ in flowing He. The sample was then exposed to a gas stream of 10 vol.% O_2/He for 30 mins before purging with flowing Ar; after baseline stabilization, the sample was pulsed with 10 vol.% H_2/Ar, also at 170℃. The surface areas of these materials were determined from

a BET (Brunauer-Emmett-Teller) method at a relative pressure (P/P_0) in the 0.05 – 1.0 range using a Micromeritics ASAP 2020 Plus instrument. N_2 gas was used for the determination of the surface area and pore size distribution for support and catalyst.

3.3.3 Catalyst evaluation

A continuous flow, fixed bed system with a 316 stainless steel reactor of 0.18 in. ID, 0.25 in. OD was used to evaluate catalyst performance and PO isomerization. A feed stream of 17.0 vol.% C_3H_6, 9.0 vol.% O_2 with balance He was used for catalyst evaluation. Unless otherwise stated this feed composition was stated as a standard feed in the results. PO isomerization studies were conducted in a feed stream of 5.0 vol.% PO, 10 vol.% O_2, and balance He. For both isomerization and catalyst evaluations, a total flow rate of 60 (STP) cm^3/min (SCCM) was used. A sample mass of 0.3 g was loaded into the reactor for catalytic performance evaluation and 2.0 g for PO isomerization studies. Catalyst evaluation was conducted at 1 atm pressure at 320ºC – 460°C temperature. Evaluation times were typically 50 – 100 h on-line. The PO isomerization study was conducted at 1 atm total pressure and a temperature between 220°C to 300°C. In all cases, catalysts were pretreated in an atmosphere of 20% H_2/He at 1 atm pressure and 280°C for 2 h before conducting any experiments. The outlet stream from the reactor was analyzed in line with a HP 5890 Series II gas chromatograph containing two Poraplot Q columns equipped with a thermal conductivity detector (TCD) and flame ionization detector (FID). TCD was used for quantitative analysis of O_2, CO_2 and H_2O and FID was used for analyzing propylene, PO, propionaldehyde, acetone and acrolein, if present.

3.4 RESULTS AND DISCUSSION

3.4.1 Catalyst characterization

The physical properties and metal content of the materials were listed in Table 3.1. The measured BET surface area of ZrO_2 was in line with the ZrO_2 support surface area reported in the literature [82-84, 88]. With the addition of Ag and Mo to the ZrO_2 support BET surface area decreased by 30 – 32%. For ethylene, 1,3 butadiene epoxidation reaction lower surface area support (0.3 – 2.0 m^2/g) was preferred [43, 59, 89].

Table 3.1: Physical properties and measured metal content of ZrO_2, Mo/ZrO_2, Ag/ZrO_2, and $Ag\text{-}Mo/ZrO_2$ catalysts.

Sample	Ag content (wt%)	Mo content (wt%)	Surface area (m^2/g)	Pore Volume (cm^3/g)
ZrO_2	0	0	21.9	0.12
4 wt% Mo/ZrO_2	0	3.9	17.0	0.11
20 wt% Ag/ZrO_2	19.3	0	14.0	0.10
20 wt% Ag – 4 wt% Mo/ZrO_2	18.8	3.7	15.7	0.09

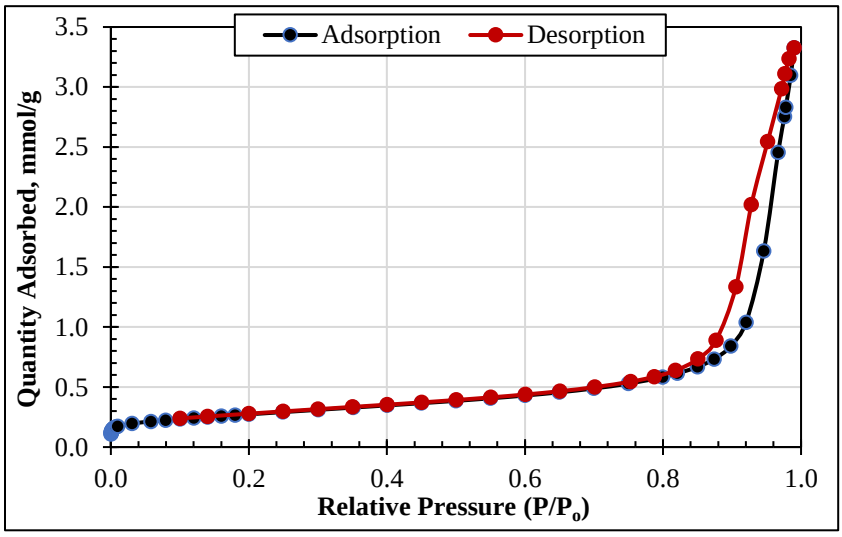

Figure 3.1: Physisorption isotherm plot of ZrO_2 support using N_2 as an adsorbent.

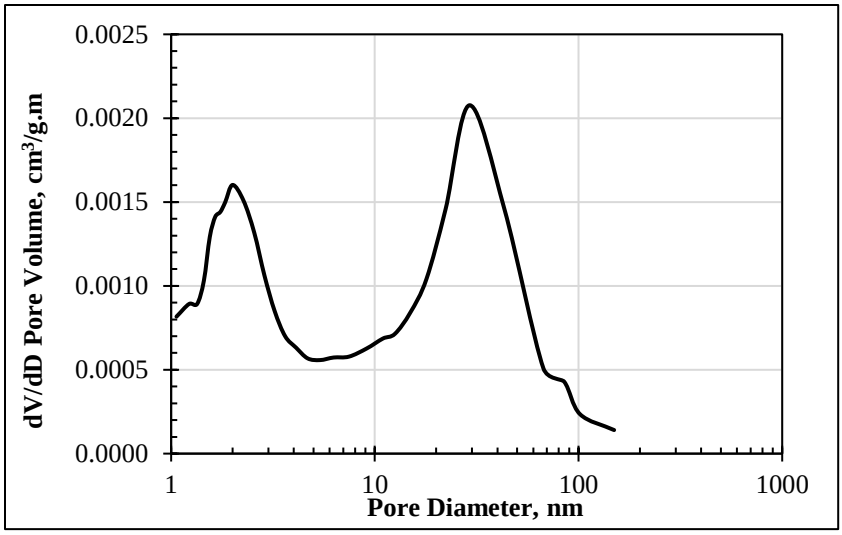

Figure 3.2: BJH pore size distribution plot for ZrO_2 support.

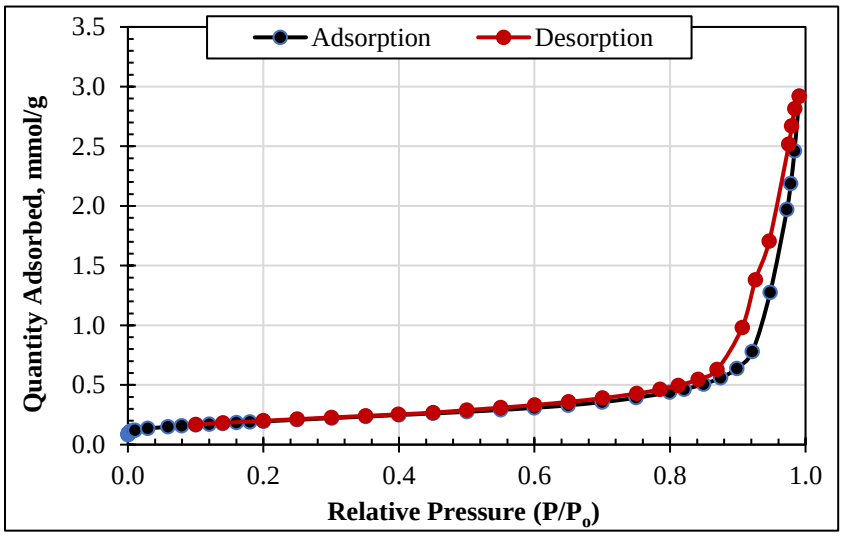

Figure 3.3: Physisorption isotherm plot of 20 wt% Ag – 4 wt% Mo/ZrO_2 support using N_2 as an adsorbent.

Figure 3.1, 3.3 and Figure 3.3, 3.4 showed physisorption isotherms and BJH (Barrett, Joyner and Halenda) pore size distribution of ZrO_2 support and 20 wt% Ag – 4 wt% Mo/ZrO_2 catalyst, respectively. The BJH pore size distribution of ZrO_2 support showed the presence of two types of pore sizes 2 nm and 29 nm. In the 20 wt% Ag – 4 wt% Mo/ZrO_2 catalyst volume fraction covered by 29 nm, pores were found to be less compared to the

ZrO_2 support. 20 wt% Ag – 4 wt% Mo/ZrO_2 catalyst showed the appearance of 7.5 nm pore size might be due to the fill up of 29 nm size pores with Ag and MoO_3. The adsorption isotherms also showed a higher quantity of N_2 adsorbed in ZrO_2 support compared to 20 wt% Ag – 4 wt% Mo/ZrO_2 catalyst as expected due to pore filling by Ag and MoO_3.

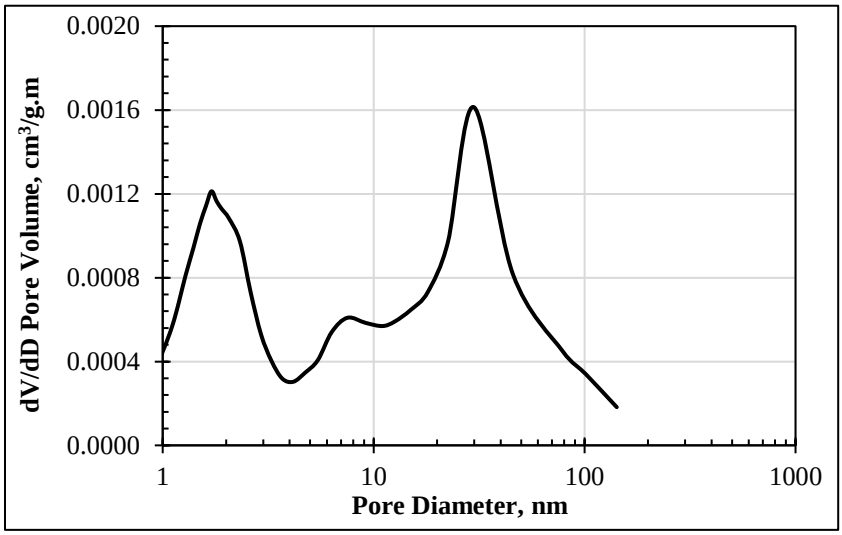

Figure 3.4: BJH pore size distribution plot for 20 wt% Ag – 4 wt% Mo/ZrO_2

The measured pore size distribution indicated the materials were mesoporous (2 – 50 nm) [90]. However, in the epoxidation reaction macropores were preferred as micropores and mesopores might cause ring opening reactions for the formed epoxides during the reaction [58, 59, 76].

The active surface Ag site concentration of unpromoted and 4 wt% Mo promoted 20 wt% Ag/ZrO_2 catalysts were summarized in Table 3.2. The H_2 uptake on the unpromoted 20 wt% Ag/ZrO_2 catalyst was significantly higher compared to the 4 wt% Mo promoted 20 wt% Ag/ZrO_2 catalyst. The MoO_3 might be covering the active surface Ag sites resulting in lower H_2 uptake. The 4 wt% Mo/ZrO_2 did not show any H_2 uptake during H_2 pulse titration. The chemisorption micrographs for H_2 uptake for these materials were shown in Figure 3.5.

Table 3.2: Chemisorption result summary of unpromoted and 4 wt% Mo modified Ag/ZrO_2 catalyst.

Sample	H_2 uptake, cm^3/g STP	Number of Ag active sites
20 wt% Ag/ZrO_2	1.19	3.18×10^{19}
20 wt% Ag - 4 wt% Mo/ZrO_2	0.08	2.07×10^{18}

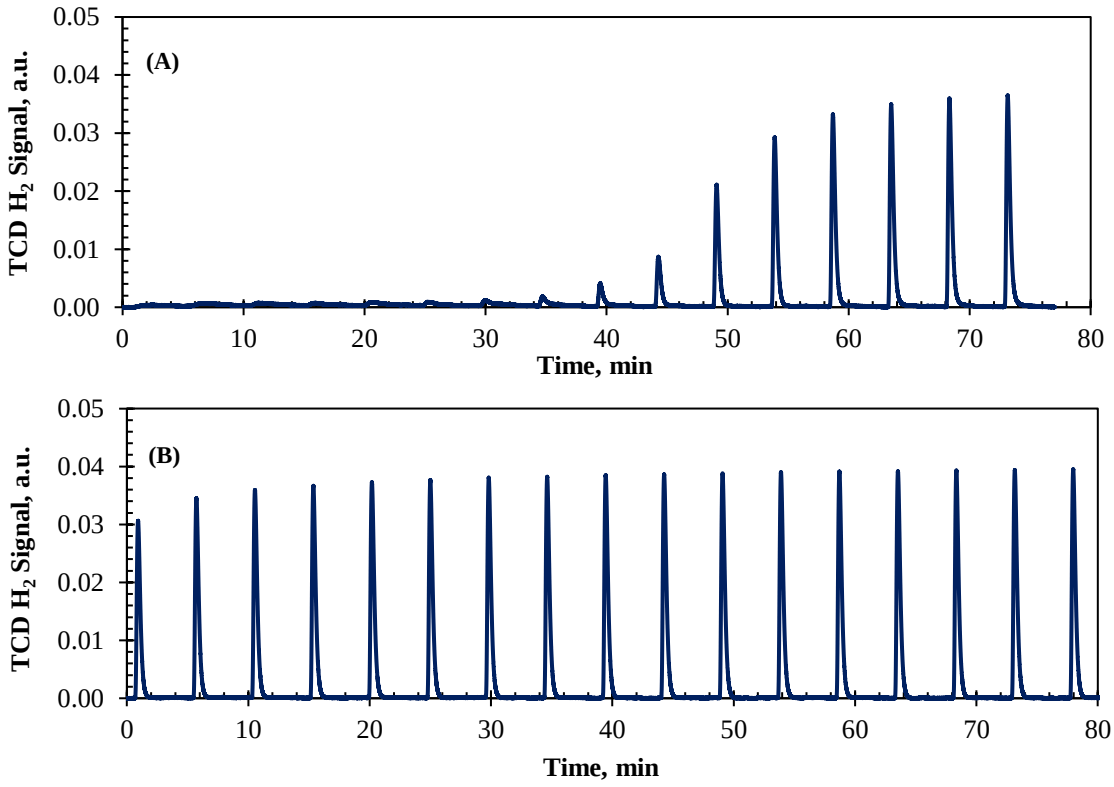

Figure 3.5: H_2 pulse titration on oxygen pre-covered surface, (A) 20 wt% Ag/ZrO_2; (B) 20 wt% Ag – 4 wt% Mo/ZrO_2.

Crystalline structures of unpromoted, 4 wt% Mo promoted 20 wt% Ag/ZrO_2 catalysts and ZrO_2 were examined by XRD analysis and shown in Figure 3.6. The unpromoted and 4 wt% Mo promoted catalyst showed characteristic diffraction peaks of Ag at 2θ = 38°, 44°, 64°, and 77° attributed to Ag (111), (200), (220), (311) facet, respectively (PDF#03-065-2871). Mo promoted catalyst showed MoO_3 diffraction peak at 2θ = 27°, 29, and 33° (PDF#98-000-0314). Both catalysts also showed a diffraction peak of tetragonal ZrO_2 at 2θ = 34° and 49° and a monoclinic ZrO_2 peak at 2θ = 28° and 31° [83, 84, 88].

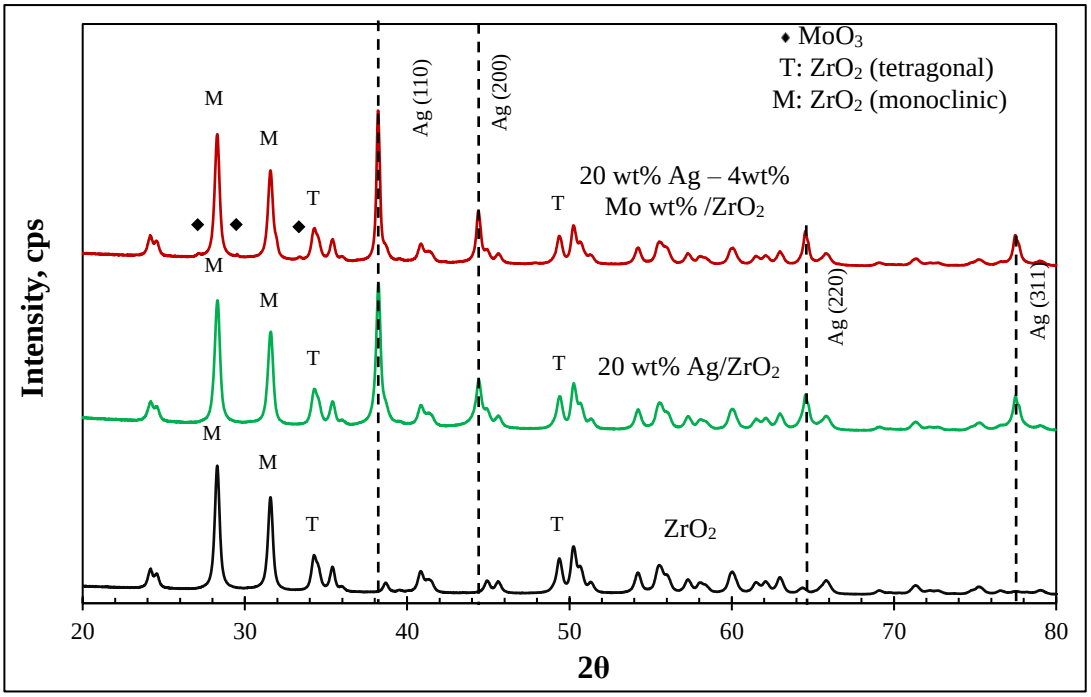

Figure 3.6: XRD patterns of ZrO_2, 20 wt% Ag/ZrO_2, and 20 wt% Ag – 4 wt% Mo/ZrO_2

Surface morphologies and metal distribution on the catalyst surface were investigated by SEM imaging and EDXS mapping. Figure 3.7 showed SEM images at different magnifications and EDXS mapping on a bulk particle of 20 wt% Ag – 4 wt% Mo/ZrO_2 catalyst. The SEM images showed a well distribution of different sized Ag particles. The EDXS mapping on a bulk particle showed uniform dispersion of Ag and

MoO_3 on ZrO_2 support. The SEM images also indicated that Ag has a wide range of particle size distribution.

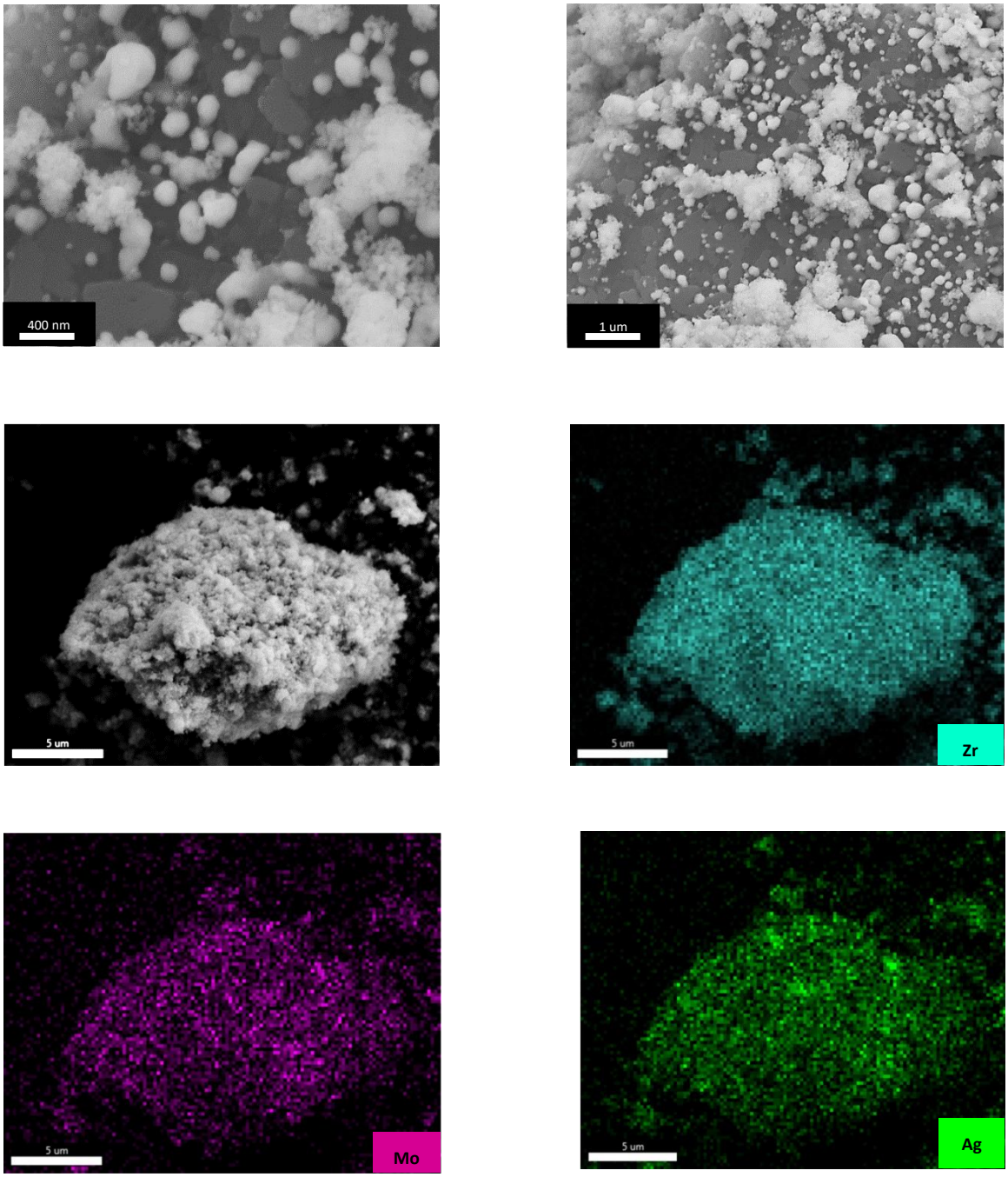

Figure 3.7: SEM and SEM-EDXS mapping images of 20 wt% Ag – 4 wt% Mo/ZrO_2 catalyst.

3.4.2 Support stability study

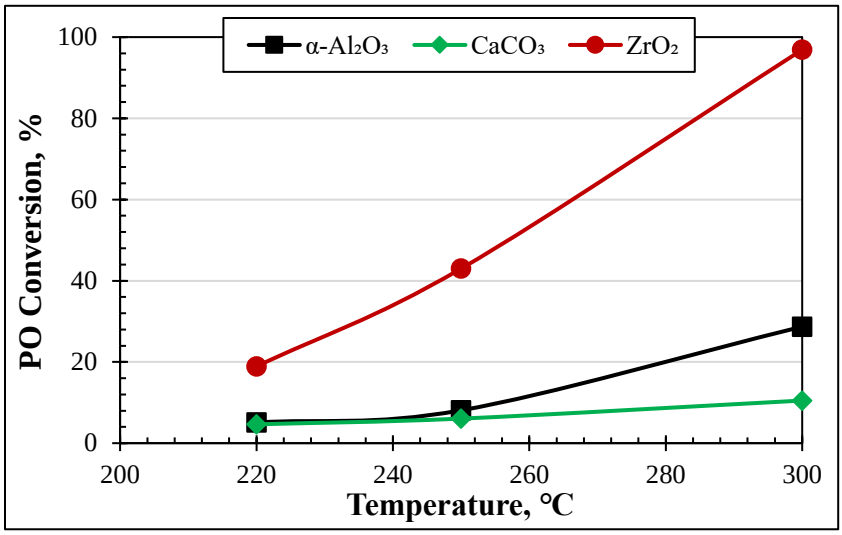

(A)

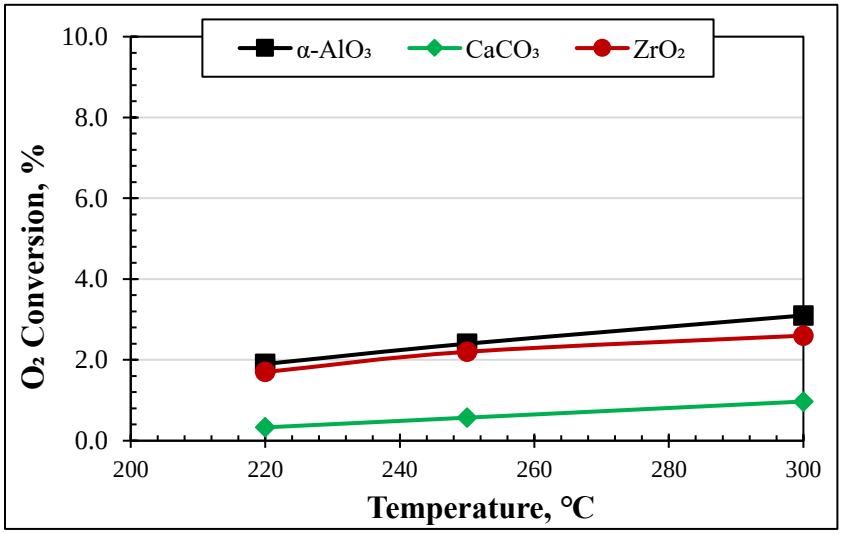

(B)

Figure 3.8: (A) PO conversion vs Temperature; (B) O_2 conversion vs Temperature plot, over α-Al_2O_3, $CaCO_3$ and ZrO_2.

For ethylene and 1,3 butadiene epoxidation low surface α-Al_2O_3 was used as support [14, 58, 59, 76]. ARCO used low surface area $CaCO_3$ as a support to achieve PO selectivity up to 60% at 3.2% conversion of C_3H_6 [50, 52, 78]. Comparatively higher surface area ZrO_2 (20 m^2/g) support was reported to achieve > 60% selectivity to PO at > 10% conversion of C_3H_6 [79, 85, 88]. In this study PO stability was tested over low surface area α-Al_2O_3,

$CaCO_3$ and ZrO_2 at three different temperatures (220°C, 250°C and 300°C) to examine any beneficial effects of using ZrO_2 over low surface area α-Al_2O_3 and $CaCO_3$. The results were shown in Figure 3.8. The experimental result showed PO converted into acetaldehyde, propionaldehyde, acetone and acrolein. This result was in line with our previous work [89]. The formation of acrolein was only observed at 300°C as it was an energy demanding process. At 300°C all the PO fed to the reactor was converted into isomer products of PO over the ZrO_2 support indicating PO was highly unstable even at 300°C on ZrO_2. In all three temperatures, PO conversion was found higher over ZrO_2 compared to low surface area α-Al_2O_3 and $CaCO_3$. $CaCO_3$ was the most effective to stabilize PO showing least PO conversion. For all cases, O_2 conversion was < 5.0% indicating PO was not oxidized and it was converted into its isomers. No beneficial effect was found for using ZrO_2 as a support for direct epoxidation of C_3H_6 instead of low surface area α-Al_2O_3 and $CaCO_3$.

3.4.3 Catalyst evaluation

A 20 wt% Ag/ZrO_2 was evaluated at 250°C temperature and 1 atm pressure using a standard feed. O_2 conversion was found close to 100% and total oxidation of C_3H_6 to CO_2/H_2O was recorded as the product. Selectivity to PO was < 1.0%. When a 20 wt% Ag – 4 wt% Mo/ZrO_2 catalyst was evaluated at 250°C, < 1.0% C_3H_6 conversion was obtained. The C_3H_6 conversion at 250°C over these two samples showed in agreement with the previous H_2 pulse titration experiment. The H_2 uptake for the 20 wt% Ag – 4 wt% Mo/ZrO_2 catalyst was significantly lower than 20 wt% Ag/ZrO_2 sample as MoO_3 covered most of the active surface Ag sites. Increasing the temperature up to 460°C, increased C_3H_6 conversion to 8.3% and acrolein was found to be the selective product. 55.2% selectivity to acrolein was obtained. Formation of CO_2/H_2O, CH_3CHO, acetone and a small amount

of propionaldehyde was also recorded. The catalytic evaluation result of 20 wt% Ag – 4 wt% Mo/ZrO_2 catalyst was shown in Figure 3.9. The result showed stable catalytic activity over 90 h time on stream (TOS) with a trivial sign of deactivation. The reactor outlet stream was analyzed using an FID. To confirm acrolein retention time (RT) a standard solution of 5000 ppmw acrolein balance CH_3OH was used supplied by Restek.

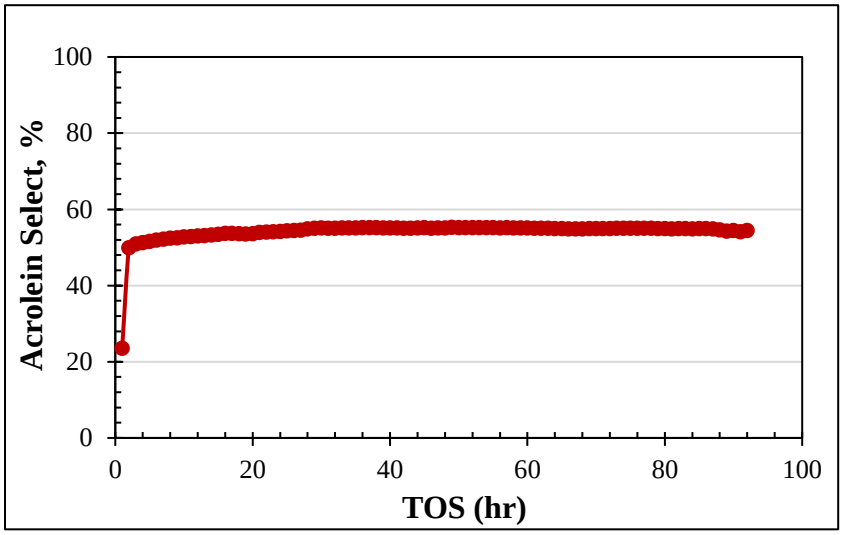

(A)

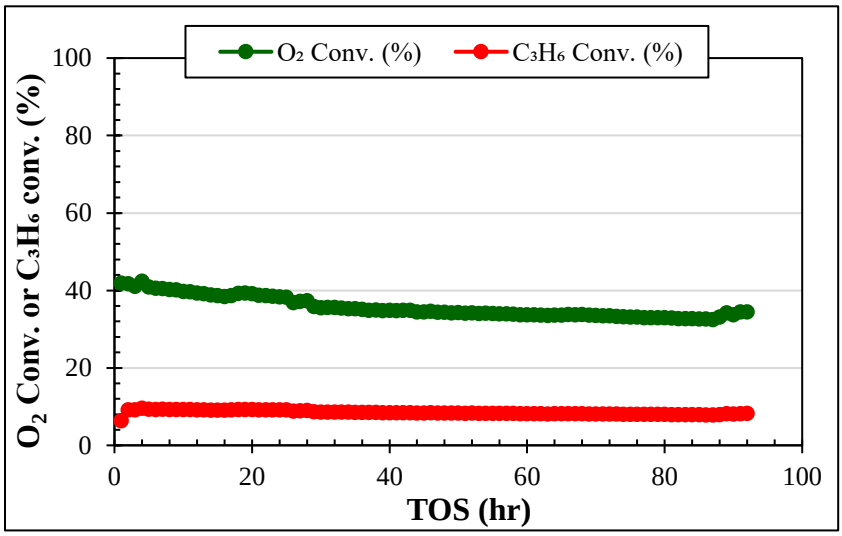

(B)

Figure 3.9: (A) Acrolein selectivity vs time on stream (TOS) plot; (B) O_2 conversion or C_3H_6 conversion vs TOS plot. Feed stream: 17% C_3H_6, 9% O_2 balance He, Temperature: 460°C, Pressure: 1 atm, sample mass: 0.3 g, GHSV: 12000 h^{-1}, sample: 20 wt% Ag – 4 wt% Mo/ZrO_2.

The GC chromatograph for standard 5000 ppmw acrolein balance CH_3OH, 1.0 vol.% PO balance He and actual reactor outlet stream analysis over a 20 wt% Ag – 4 wt% Mo/ZrO_2 sample were shown in Figure 3.10. The GC chromatograph with FID showed a clear peak separation between PO and acrolein with an RT difference of 0.5 min. In the reactor outlet stream, GC analysis of acrolein peak was found to be the selective component along with acetaldehyde, propionaldehyde, acetone and CO_2/H_2O when a 20 wt% Ag – 4 wt% Mo/ZrO_2 catalyst was evaluated for direct epoxidation of propylene at 460°C.

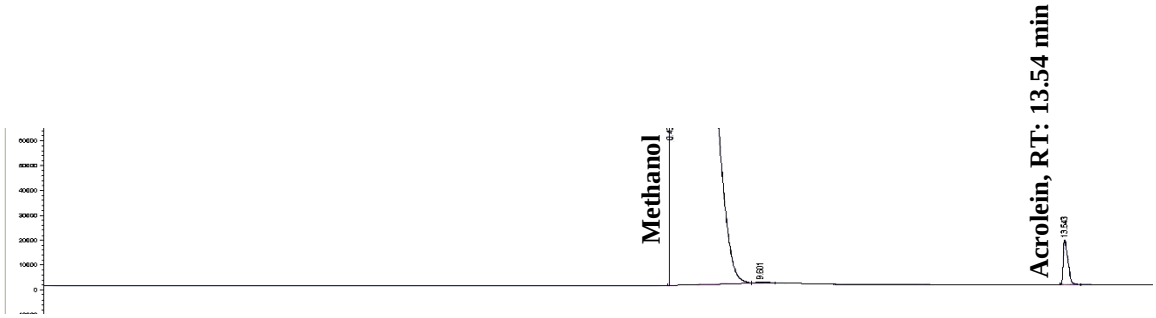

(A)

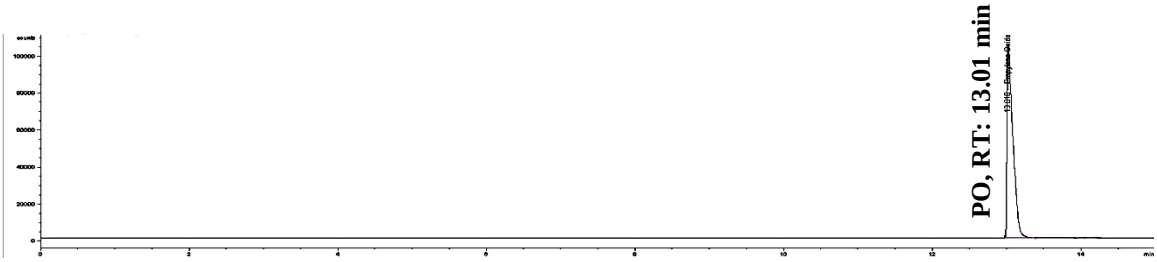

(B)

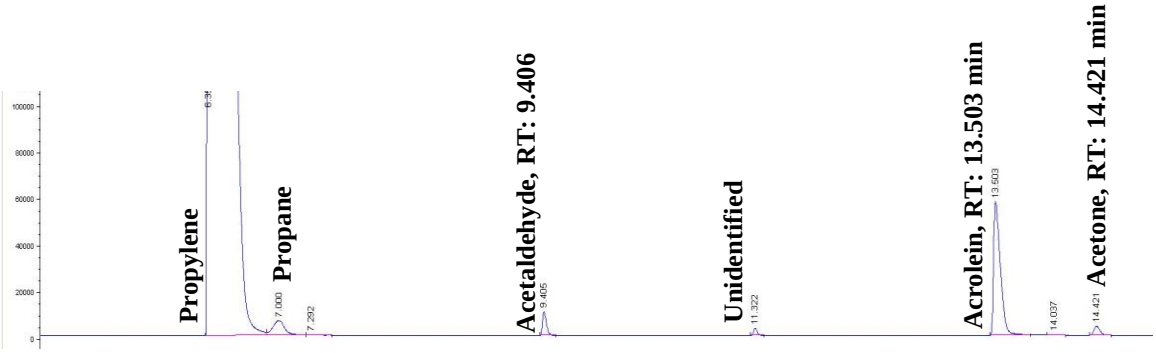

Figure 3.10: GC chromatographs using FID (A) 5000 ppmw Acrolein/Methanol, (B) 1.0 vol.% PO/He, (C) Reactor outlet stream analysis.

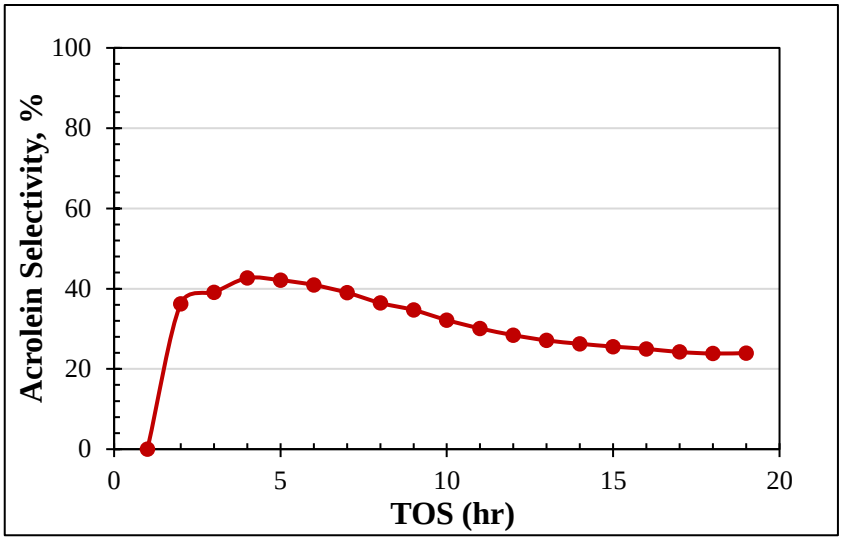

(A)

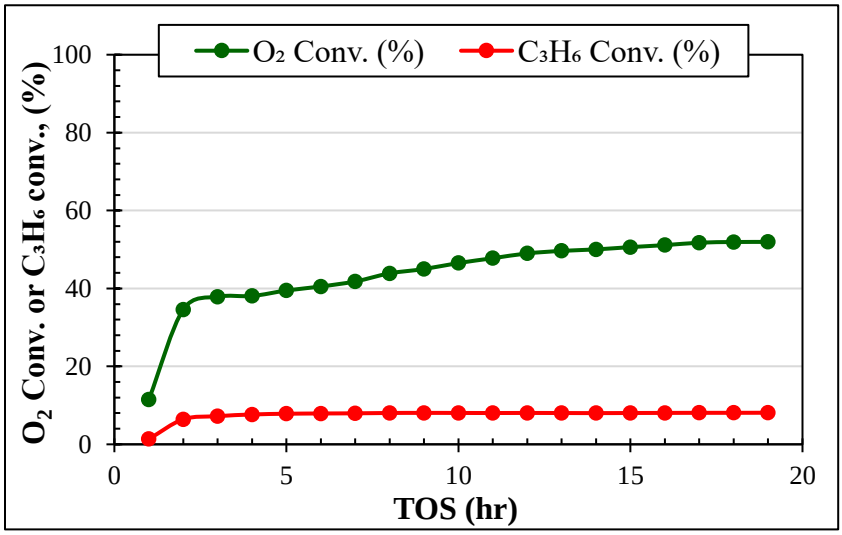

(B)

Figure 3.11: (A) Acrolein selectivity vs time on stream (TOS) plot; (B) O_2 conversion or C_3H_6 conversion vs TOS plot. Feed stream: 17% C_3H_6, 9% O_2 balance He, Temperature: 460°C, Pressure: 1 atm, sample mass: 0.3 g, GHSV: 12000 h^{-1}, sample: 4 wt% Mo/ZrO_2.

A 4 wt% Mo/ZrO_2 sample was tested using a standard feed at 460°C for direct epoxidation of propylene to understand the role of Mo and Ag. The results were shown in Figure 3.11 in terms of acrolein selectivity and O_2, C_3H_6 conversion. CO_2/H_2O was found to be the major product. The formation of acrolein was noticed along with a small amount of

acetaldehyde and acetone. The C_3H_6 conversion was comparable to (8.1%) 20 wt% Ag – 4 wt% Mo/ZrO_2. However, the reaction was stopped due to upstream pressure buildup after 15 h time on stream. Later unloading the catalyst coke formation was found on the 4 wt% Mo/ZrO_2 and catalyst bed (glass wool). The coke formation might be responsible for pressure buildup. The 20 wt% Ag – 4 wt% Mo/ZrO_2 catalyst over 90 h time one stream showed no sign of coke formation. The Ag might be assisting to inhibit coke formation over the 20 wt% Ag – 4 wt% Mo/ZrO_2 catalyst. The findings from this study concluded that for the formation of acrolein, the presence of Ag was not required.

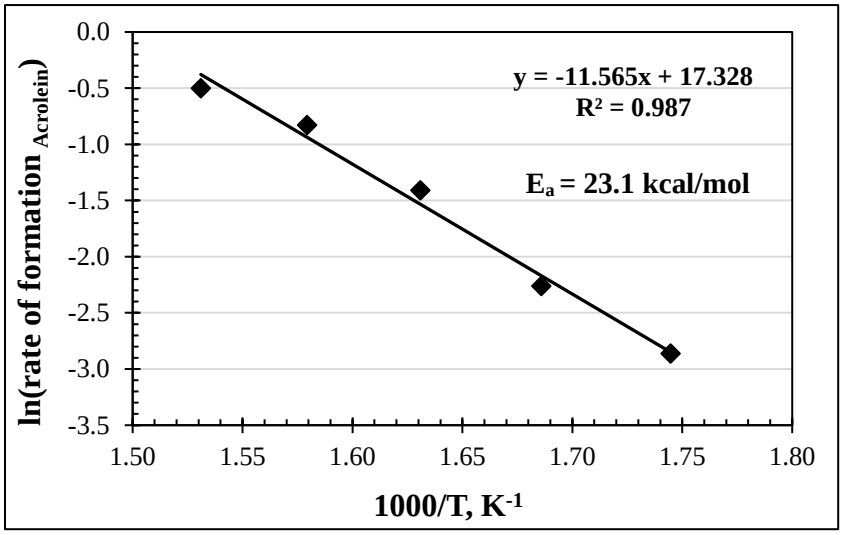

Figure 3.12: Arrhenius plot for propylene oxidation to acrolein over 20 wt% Ag – 4 wt% Mo/ZrO_2 catalyst. Feed stream: 17% C_3H_6, 9% O_2 balance He, Temperature: 300 - 380°C, Pressure: 1 atm.

Figure 3.12 showed the Arrhenius plot for propylene partial oxidation to acrolein over a 20 wt% Ag – 4 wt% Mo/ZrO_2 catalyst. The calculated activation energy was 23.1 kcal/mol. Q. Zhang *et al.* calculated the activation energy for propylene partial oxidation to acrolein over a series of Ag/MoO_3 catalysts where Ag weight loading was varied from 0.1% to 8.0%. The authors reported activation energy between 19.4 kcal/mol and 22.5 kcal/mol [91]. Z. Zhai *et al.* also reported activation energy for propylene to

acrolein formation of 18.8 kcal/mol over a Bi_2MoO_6 catalyst [92]. The activation energy measured in this study was in agreement with the literature reported value for propylene partial oxidation to form acrolein. Unfortunately, no activation energy was found in the literature for direct epoxidation of propylene to propylene oxide for comparison.

To check PO stability, a feed stream of 5.0 vol.% PO, 10.0 vol% O_2 balance He was fed over a 20 wt% Ag – 4 wt% Mo/ZrO_2 catalyst at 360°C and 1 atm pressure. The reactor outlet stream was analyzed using a GC equipped with FID and TC. All the PO fed was found to convert into CO_2/H_2O, propionaldehyde (EtCHO), acrolein, acetaldehyde (CH_3COH) and acetone. Table 3.3 summarized the product distribution of PO conversion.

Table 3.3: Product distribution of PO converted into, at 360°C over a 20 wt% Ag – 4 wt% Mo/ZrO_2 catalyst.

CO_2 (%)	**CH_3CHO (%)**	**EtCHO (%)**	**Acrolein (%)**	**Acetone (%)**
82.7	0.2	5.6	11.5	0.02

The result of this study showed PO was not stable at 360°C over a 20 wt% Ag – 4 wt% Mo/ZrO_2 catalyst and it should not also be stable at a higher temperature.

3.4.4 Discussion

Bi_2O_3.MoO_3 based catalyst has been used industrially to produce acrolein and acrylonitrile from partial oxidation of C_3H_6 at reaction temperature > 400°C [93-95]. In this process lattice oxygen from the catalyst takes part to oxidize C_3H_6 as a result, the catalyst itself was reduced and molecular O_2 re-oxidized the catalyst following Mars-Van Krevelen mechanism [95, 96]. In this study, over a 20 wt% Ag – 4 wt% Mo/ZrO_2 catalyst acrolein was produced selectively instead of PO. This finding directly contradicted results reported in the literature for selective PO formation over Mo, W promoted

20 wt% Ag/ZrO_2 catalyst [79-83, 85, 88]. The selective formation of acrolein on a high loading Mo (3 – 4 wt%) promoted 20 wt% Ag/ZrO_2 catalyst at reaction temperature > 400℃ imitated the reaction environment used for partial oxidation of C_3H_6 over $Bi_2O_3.MoO_3$ based catalysts to produce acrolein. Q. Zhang *et al.* also reported acrolein formation over silver molybdate – coated MoO_3 nanobelts at 350ºC temperature [91]. The investigation of PO stability study over a 20 wt% Ag – 4 wt% Mo/ZrO_2 catalyst showed PO was highly unstable and converted into CO_2/H_2O, propionaldehyde (EtCHO), acrolein, acetaldehyde (CH_3COH) and acetone even at 360℃. From the results of this study, it can be concluded that literature reporting selective formation of PO by direct epoxidation of C_3H_6 over Mo modified Ag/ZrO_2 catalyst at > 400℃ was misleading.

3.5 CONCLUSION

20 wt% Ag/ZrO_2 and 20 wt% Ag – 4 wt% Mo/ZrO_2 catalysts were prepared, characterized by ICP AES, H_2 pulse titration over oxygen pre-covered surface, XRD analysis and SEM imaging with EDXS and evaluated for direct epoxidation or partial oxidation of C_3H_6 over 250°C to 460°C temperature range at 1 atm pressure. XRD analysis on 20 wt% Ag – 4 wt% Mo/ZrO_2 catalyst showed the formation of Ag (111), (200), (220), (311) facets and MoO_3. H_2 pulse titration over oxygen pre-covered surface performed on both Mo promoted and unpromoted 20 wt% Ag/ZrO_2 catalyst showed a significant fraction of the surface Ag sites were covered by MoO_3. Isomerization study showed ZrO_2 has no beneficial effects on stabilizing PO. A 20 wt% Ag – 4 wt% Mo/ZrO_2 catalyst was evaluated for direct epoxidation of C_3H_6 reaction at 460°C temperature and 1 atm pressure. Acrolein was found to be the selective product instead of PO as claimed in the literature. PO was fed over a 20 wt% Ag – 4 wt% Mo/ZrO_2 catalyst at 360°C temperature, 1 atm pressure and

was found ~100% conversion of PO. The result indicated the instability of PO at high temperatures. Evaluating a 4 wt% Mo/ZrO_2 catalyst for partial oxidation of C_3H_6 showed the formation of acrolein at 460°C temperature confirming Ag was not required to form acrolein. However, the 4 wt% Mo/ZrO_2 catalyst showed upstream pressure build-up and deactivation over 15 h time on stream due to coke formation. It might be possible Ag inhibited coke formation as 20 wt% Ag – 4 wt% Mo/ZrO_2 catalyst showed trivial deactivation and no upstream pressure build-up in 92 h time on stream. The results of this study concluded that the literature reports of selective PO formation at > 400°C by epoxidation of C_3H_6 were misleading.

REFERENCES

[1] B.T. Egelske, Recent Advances in Catalytic Ethylene Epoxidation: Synthesis, Characterization, and Evaluation, in, University of South Carolina, 2021.

[2] W. Diao, C.D. DiGiulio, M.T. Schaal, S. Ma, J.R. Monnier, An investigation on the role of Re as a promoter in Ag-Cs-Re/α-Al_2O_3 high-selectivity, ethylene epoxidation catalysts, *Journal of Catalysis*, 322 (2015) 14-23.

[3] H. Baer, M. Bergamo, A. Forlin, L.H. Pottenger, J. Lindner, Propylene Oxide, In: Ullmann's Encyclopedia of Industrial Chemistry, 2012.

[4] T.A. Nijhuis, M. Makkee, J.A. Moulijn, B.M. Weckhuysen, The Production of Propene Oxide: Catalytic Processes and Recent Developments, *Industrial & Engineering Chemistry Research*, 45 (2006) 3447-3459.

[5] Propylene Oxide: from a gap of 467,000 tons to self-sufficiency is just around the corner, In: ECHEMI News, ECHEMI, 2021.

[6] M. Boronat, A. Pulido, P. Concepcion, A. Corma, Propene epoxidation with O_2 or H_2-O_2 mixtures over silver catalysts: theoretical insights into the role of the particle size, *Phys Chem*, 16 (2014) 26600-26612.

[7] J. Monnier, The selective epoxidation of conjugated olefins containing allylic substituents and epoxidation of propylene in the presence of butadiene, *Journal of Catalysis*, 225 (2004) 374-380.

[8] J.R. Monnier, The direct epoxidation of higher olefins using molecular oxygen, *Applied Catalysis A: General*, 221 (2001) 73-91.

[11] Y. Dai, Z. Chen, Y. Guo, G. Lu, Y. Zhao, H. Wang, P. Hu, Significant enhancement of the selectivity of propylene epoxidation for propylene oxide: a molecular oxygen mechanism, *Phys Chem*, 19 (2017) 25129-25139.

[12] J.R. Monnier, The selective epoxidation of non-allylic olefins over supported silver catalysts, *Studies in Surface Science and Catalysis*, 110 (1997) 135-149.

[13] A.M. Lauritzen, Ethylene oxide catalyst and process for preparing the catalyst, in, Shell Oil Company, United States, 1988.

[14] J. Monnier, J. Stavinohajr, R. Minga, Stability and distribution of cesium in Cs-promoted silver catalysts used for butadiene epoxidation, *Journal of Catalysis*, 226 (2004) 401-409.

[15] A.M.G. Andrew P. Kahn, Rangasamy Pitchai, Propylene oxide process using alkaline earth metal compound-supported silver catalysts, in, ARCO Chemical Technology, L.P., United States, 1998.

[16] A.M.G. Andrew P. Kahn, Propylene oxide process using alkaline earth metal compound-supported silver catalysts containing tungsten and potassium promoters, in, ARCO Chemical Technology, L.P., United States, 1999.

[17] A.P.K. Anne M. Gaffney, Rangasamy Pitchai, Propylene oxide process using mixed precious metal catalyst supported on alkaline earth metal carbonate, in, ARCO Chemical Technology, L.P., United States, 1997.

[18] A.M. Gaffney, Propylene oxide process using alkaline earth metal compound-supported silver catalysts containing rhenium and potassium promoters, in, Arco Chemical Technology, L.P., United States, 1999.

[19] A.P.K. Rangasamy Pitchai, Anne M. Gaffney, Vapor phase oxidation of propylene to propylene oxide, in, ARCO Chemical Technology, L.P., United States, 1997.

[20] A.P.K. Rangasamy Pitchai, Anne M. Gaffney, Vapor Phase Oxidation of Propylene to Propylene Oxide, in, ARCO Chemical Technology, L.P., United States, 1997.

[21] A.M.G. Bernard Cooker, Jennifer D. Jewson, Andrew P. Kahn, Rangasamy Pitchai, Epoxidation process using supported silver catalysts pretreated with organic chloride, in, ARCO Chemical Technology, L.P., United States, 1998.

[22] A.M.G. Bernard Cooker, Jennifer D. Jewson, Wilson H. Onimus, Propylene epoxidation using chloride-containing silver catalysts, in, ARCO Chemical Technology, L.P., United States, 1998.

[23] A.M.G. Bernard Cooker, Jennifer D. Jewson, Wilson H. Onimus, Chloride containing silver catalysts for propylene epoxidation, in, ARCO Chemical Technology, L.P., United States, 1999.

[24] P. Hayden, Production of Ethylene Oxide, in, Imperial Chemical Industries PLC, United States, 1989.

[25] R.W.C. Percy Hayden, John R. Ramforth, Alan F. G. Cope, Production of olefine oxides, in, Imperial Chemical Industries PLC, United States, 1995.

[26] T.M. Notermann, Catalytic System for Epoxidation of Alkenes, in: U.S.P. Office (Ed.), Union Carbide Chemicals and Plastics Company Inc., United States, 1991.

[27] D.E. Strohmayer, G.L. Geoffroy, M.A. Vannice, Measurement of silver surface area by the H_2 titration of chemisorbed oxygen, *Applied Catalysis*, 7 (1983) 189-198.

[28] G. te Velde, F.M. Bickelhaupt, E.J. Baerends, C. Fonseca Guerra, S.J.A. van Gisbergen, J.G. Snijders, T. Ziegler, Chemistry with ADF, *Journal of Computational Chemistry*, 22 (2001) 931-967.

[29] J.P. Perdew, K. Burke, M. Ernzerhof, Generalized Gradient Approximation Made Simple, *Physical Review Letters*, 77 (1996) 3865-3868.

[30] E. van Lenthe, E.J. Baerends, J.G. Snijders, Relativistic total energy using regular approximations, *The Journal of Chemical Physics*, 101 (1994) 9783-9792.

[31] Z. Luo, G.U. Gamboa, J.C. Smith, A.C. Reber, J.U. Reveles, S.N. Khanna, A.W. Castleman, Spin Accommodation and Reactivity of Silver Clusters with Oxygen: The Enhanced Stability of Ag_{13}, *Journal of the American Chemical Society*, 134 (2012) 18973-18978.

[32] M. Parizad, A.P. Wong, A.C. Reber, J.M.M. Tengco, S.G. Karakalos, S.N. Khanna, J.R. Regalbuto, J.R. Monnier, Stabilization of Catalytic Surfaces through Core–Shell Structures: Ag–Ir/Al_2O_3 Case Study, *ACS Catalysis*, 10 (2020) 13352-13363.

[33] W. Diao, C.D. DiGiulio, M.T. Schaal, S. Ma, J.R. Monnier, An investigation on the role of Re as a promoter in Ag Cs Re/α-Al_2O_3 high-selectivity, ethylene epoxidation catalysts, *Journal of Catalysis*, 322 (2015) 14-23.

[34] J. Monnier, Effects of chlorine and chlorine dynamics during silver-catalyzed epoxidation of butadiene, *Journal of Catalysis*, 226 (2004) 321-333.

[35] J.W. Harris, A. Bhan, Moderation of chlorine coverage and ethylene epoxidation kinetics via ethane oxychlorination over promoted Ag/α-Al_2O_3, *Journal of Catalysis*, 367 (2018) 62-71.

[36] F.W. Zemichael, A. Palermo, M.S. Tikhov, R.M. Lambert, Propene Epoxidation over K-Promoted Ag/CaCO3 Catalysts: The Effect of Metal Particle Size, *Catalysis Letters*, 80 (2002) 93-98.

[37] J.P. Dever, K.F. George, W.C. Hoffman, H. Soo, Ethylene Oxide, In: Kirk-Othmer Encyclopedia of Chemical Technology, 2000.

[38] S.E. Specht, S.P. Phivilay, A. Chieregato, S. Nagy, B.F.M. Kimmich, I. Hermans, Kinetics of the Ag/KNO_3/$CaCO_3$ Catalyzed Aerobic Propylene Epoxidation and Effects of CO_2, *ChemCat*, 12 (2020) 2522-2532.

[39] H.P. Percy Haden, Production of Ethylene Oxide and Catalysts Therefor, in: U.S.P. Office (Ed.), Imperial Chemical Industries PLC, United States, 1992.

[40] J. Müslehiddinoğlu, M.A. Vannice, Adsorption of NO on promoted Ag/α-Al_2O_3 catalysts, *Journal of Catalysis*, 217 (2003) 442-456.

[41] K.A. Bethke, H.H. Kung, Supported Ag Catalysts for the Lean Reduction of NO with C_3H_6, *Journal of Catalysis*, 172 (1997) 93-102.

[42] T.E. Lefort, Process for the production of ethylene oxide, In: US Patent No. 1998878, 1931.

[43] A.M. Lauritzen, Ethylene oxide catalyst and process for preparing the catalyst, In: US Patent No. 4761394, 1988.

[44] W. Shen-Wu, Oxidation of ethylene to ethylene oxide, *Industrial & engineering chemistry*, 45 (1953) 234-238.

[45] G.J. Millar, M. Collins, Industrial Production of Formaldehyde Using Polycrystalline Silver Catalyst, *Industrial & Engineering chemistry research*, 56 (2017) 9247-9265.

[46] K.H. Stefan Boeck, Rolf Fischer, Herbert Vogel and Martin Fischer Preparation of 3,4-epoxy-1-butene, in: US Patent No: 5,618,954, BASF Aktiengesellschaft, Germany, 1997.

[47] J.R. Monnier, The selective epoxidation of non-allylic olefins over supported silver catalysts, *3rd World Congress on Oxidation Catalysis*, 3 (1997) 135-149.

[48] A.M.G. Bernard Cooker, Jennifer D. Jweson, Andrew P. Kahn, Rangasamy Pitchai Epoxidation process using supported silver catalysts pretreated with organic chloride, In: US Patent No: 5,770,746, Arco Chemical Technology, 1998.

[49] R. Pitchai, A.P. Kahn, A.M. Gaffney, Vapor phase oxidation of propylene to propylene oxide, In: US Patent No: 5,686,380, Arco Chemical Technology, 1997.

[50] A.P.K. Anne M. Gaffney, Rangasamy Pitchai Propylene oxide process using mixed precious metal catalyst supported on alkaline earth metal carbonate, In: US Patent No: 5,703,254, Arco Chemical Technology, 1997.

[51] A.M.G. Bernard Cooker, Jennifer D. Jweson, Wilson H. Onimus, Propylene epoxidation using chloride containing silver catalysts, In: US Patent No: 5,780,657, Arco Chemical Technology, 1998.

[52] A.M.G. Andrew P. Kahn, Rangasamy Pitchai, Propylene oxide process using alkaline earth metal compound supported silver catalysts, In: US Patent No: 5,763,630, Arco Chemical Technology, 1998.

[53] A.M.G. Bernard Cooker, Jennifer D. Jweson, Andrew P. Kahn Epoxidation process using supported silver catalysts treated with carbon dioxide, In: US Patent No: 5,856,534, Arco Chemical Technology, 1999.

[54] A.M.G. Andrew P. Kahn, Propylene oxide process using alkaline earth metal compound supported silver catalysts containing tungsten and potassium promoters, In: US Patent 5,861,519, Arco Chemical Technology, 1999.

[55] P.A. Kilty, W.M.H. Sachtler, THE MECHANISM OF THE SELECTIVE OXIDATION OF ETHYLENE TO ETHYLENE OXIDE, *Catalysis Reviews*, 10 (1974) 1-16.

[56] W.E. Evans, J.M. Kobe, M. Matusz, Process for improving the selectivity of an EO catalyst, In: US Patent No: 9174928, 2015.

[57] N. Rizkalla, A. Rokieki, Method for making a highly selective ethylene oxide catalyst, In: US Patent No. 8883675, 2014.

[58] J.R. Lockemeyer, R.C. Yeates, D. Reinalda, Method for improving the selectivity of a catalyst and the process for the epoxidation of an olefin, In: US Patent No. 8148555, 2012.

[59] J.R. Lockemeyer, R.C. Yeates, D. Reinalda, Method for improving the selectivity of a catalyst and process for the epoxidation of an olefin, In: US Patent No. 7485597, 2009.

[60] H.V. Milligen, B. VanderWilp, G.J. Wells, Enhancements in the ethylene oxide/ethylene glycol manufacturing technology, In: Whitepaper, Shell Global Solutions, 2016.

[61] D.E. Strohmayer, G.L. Geoffroy, M.A. Vannice, Measurement of silver surface area by H_2 titration of chemisorbed oxygen, *Applied Catalysis*, 7 (1983) 189-198.

[62] A.W. Czanderna, The adsorption of oxygen on silver, *The Journal of Physical Chemistry* 68 (1964).

[63] J.V. Sengers, J.T.R. Watson, Improved International Formulations for the Viscosity and Thermal Conductivity of Water Substance, *J. Phys. Chem.*, (1986) 1291.

[64] E. Vogel, B. Jager, R. Hellmann, E. Bich, *Ab initio* Pair Potential Energy Curve for the Argon Atom Pair and Thermophysical Properties for the Dilute Argon Gass. II. Thermophysical Properties for Low-Density Argon, *Mol. Phys.*, (2010).

[65] J.R. Anderson, Structure of metallic catalysts, Academic Press, New York, NY, 1975.

[66] M.V. Badani, M.A. Vannice, Effects of cesium chloride and oxygen adsorption on promoted Ag/α-Al_2O_3 catalysts, *Applied Catalysis A: General*, 204 (1999) 129-142.

[67] F. Pargar, D. Koleva, Polarization Behaviour of Silver in Model Solutions, Int. J. Structural and Civil Eng. Res. , 6 (2017).

[68] T.B. Reed, Free Energy of Formation of Binary Compounds, MIT Press, Cambridge, MA, 1971.

[69] A. Jain, G. Hautier, S.P. Ong, C.J. Moore, C.C. Fischer, K.A. Persson, G. Ceder, Formation enthalpies by mixing GGA and GGA + ***U*** calculations, *PHYSICAL REVIEW B*, 84 (2011).

[70] G. Milazzo, S. Caroli, V.K. Sharma, Tables of Standard Electrode Potentials Wiley London, 1978.

[71] R. Schrebler, C.S. P. Cury, E. Munoz, F. Vera, R. Cordova, H. Gomez, J.R. Ramos-Barrado, D. Leinen, E.A. Dalchiele, Study of the electrodeposition of rhenium thin films by electrochemical quartz microbalance and X-ray photoelectron spectroscopy, *Thin Sol. Films*, 483 (2005).

[72] E.H. Swift, E.A. Butler, Quantitative Measurements and Chemical Equilibria, Freeman Publ. New York, 1972.

[73] J.R. Monnier, J.L. Stavinoha, R.L. Minga, Stability and distribution of cesium in Cs-promoted silver catalysts used for butadiene epoxidation, *Journal of Catalysis*, 226 (2004).

[74] S. Rebsdat, D. Mayer, Ullmann's Encylopedia of Industrial Chemistry VCH, New York, 1998.

[75] N. Rizkalla, PROMOTED SILVER CATALYST, in, Scientific Design Company, Inc., 1997.

[76] A.M. Lauritzen, ETHYLENE OXIDE CATALYST AND PROCESS FOR PREPARING THE CATALYST, in, Shell Oil Company, 1988.

[77] J.A. Dean, N.A. Lange, Lange's handbook of chemistry, 15 ed., 1999.

[78] A.M. Gaffney, Propylene oxide process using alkaline earth metal compound supported silver catalysts containing rhenium and potassium promoters, In: US Patent No: 5,864,047, Arco Chemical Technology, 1999.

[79] G. Jin, G. Lu, Y. Guo, Y. Guo, J. Wang, X. Liu, W. Kong, X. Lui, Modification of Ag-MoO_3/ZrO_2 Catalyst with Metallic Chloride for Propylene Epoxidation by Molecular Oxygen, *Catalysis Letters*, 97 (2004) 191-196.

[80] G. Jin, G. Lu, Y. Guo, J. Wang, X. Liu, Epoxidation of Propylene by Molecular Oxygen over Modified Ag-MoO_3 Catalyst, *Catalysis Letters*, 87 (2003) 249-252.

[81] G. Jin, G. Lu, Y. Guo, Y. Guo, J. Wang, W. Kong, X. Liu, Effect of preparation condition on performance of Ag-MoO_3/ZrO_2 catalyst for direct epoxidation of propylene by molecular oxygen, *Journal of Molecular Catalysis A: Chemical*, 232 (2005) 165-172.

[82] G. Jin, G. Lu, Y. Guo, Y. Guo, J. Wang, X. Liu, Direct epoxidation of propylene with molecular oxygen over Ag-MoO_3/ZrO_2 catalyst, *Catalysis Today*, 93-95 (2004) 173-182.

[83] E.J. Lee, J. Lee, Y.-J. Seo, J.W. Lee, Y. Ro, J. Yi, I.K. Song, Direct Epoxidation of Propylene to Propylene Oxide Over Ag-W/ZrO_2 Catalysts: Effect of Tungsten (W) Addition, *Journal of Nanoscience and Nanotechnology*, 17 (2017) 8219-8225.

[84] E.J. Lee, J.W. Lee, H.K. Min, J. Yi, I.K. Song, D.H. Kim, Ag-(Mo-W)/ZrO_2 Catalysts for the Production of Propylene Oxide: Effect of pH in the Preparation of ZrO_2 Support, *Catalysis Communications*, 89 (2017) 156-160.

[85] E.J. Lee, J.W. Lee, J. Lee, H.K. Min, J. Yi, I.K. Song, D.H. Kim, Ag-(Mo-W)/ZrO2 catalysts for the production of propylene oxide: Effect of pH in the preparation of ZrO2 support, *Catalysis Communications*, 111 (2018) 80-83.

[86] C. Bolivar, H. Charcosset, R. Frety, M. Primet, L. Tournayan, Platinum-Rhenium-Alumina catalysts II. Study of the metallic phase after reduction, *Journal of Catalysis*, 45 (1975) 163-178.

[87] J.R. Monnier, J.L. Stavinoha, G.W. Hartley, Effects of chlorine and chlorine dynamics during silver-catalyzed epoxidation of butadiene, *Journal of Catalysis*, 226 (2004) 321-333.

[88] E.J. Lee, J. Lee, Y.J. Seo, J.W. Lee, Y. Ro, J. Yi, I.K. Song, Direct epoxidation of propylene to propylene oxide with molecular oxygen over Ag-Mo-W/ZrO_2 catalysts. , *Catalysis Communications*, 89 (2017) 156-160.

[89] M.B. Burkholder, M.M. Rahman, A.C. Reber, A.M. Gaffney, B.F. Gupton, J.R. Monnier, New perspectives and insights into direct epoxidation of propylene using O2 and silver-based catalysts, *Applied Catalysis A: General*, 650 (2023).

[90] U. Ciesla, F. Schüth, Ordered mesoporous materials, *Microporous and Mesoporous Materials*, 27 (1999) 131-149.

[91] Q. Zhang, A. Goldbach, N. Ta, W. Shen, Selective Oxidation of Propylene to Acrolein over Silver Molybdate Coated MoO_3 Nanobelts, *ACS Applied Nano Materials* 5(2022) 7187-7197.

[92] Z. Zhai, M. Wutschert, R.B. Licht, A.T. Bell, Effects of catalyst crystal structure on the oxidation of propene to acrolein, *Catalysis Today*, 261 (2016) 146-153.

[93] J.D. Idol, Jr., S. Heights, PROCESS FOR THE MANUFACTURE OF ACRYLONITRILE in, The Standard Oil Company, 1959.

[94] J.L. Callahan, Bedford, R.W. Foreman, Cleveland, F. Veatch, Lyndhurst, ATTRITION RESISTANT OXIDATION CATALYSTS, in, The Standard Oil Company, 1962.